



Collision Avoidance Function Concept

Avoiding collisions with cyclists located in the blind spot of the driver during right turn scenarios

ELINOR JERNHEDEN

DANIEL ÖSTERGREN BERNDTSON

MASTER'S THESIS 2020

Collision Avoidance Function Concept

Avoiding collisions with cyclists located in the blind spot of the driver during right turn scenarios

Elinor Jernheden
Daniel Östergren Berndtson



CHALMERS
UNIVERSITY OF TECHNOLOGY

Department of Electrical Engineering
Division of Systems and Control
CHALMERS UNIVERSITY OF TECHNOLOGY
Gothenburg, Sweden 2020

Collision Avoidance Function Concept
Avoiding collisions with cyclists located in the blind spot of the driver during right
turn scenarios
ELINOR JERNHEDEN
DANIEL ÖSTERGREN BERNDTSON

© ELINOR JERNHEDEN, 2020.
© DANIEL ÖSTERGREN BERNDTSON, 2020.

Supervisor: Faisal Mahmood Ahmed, Volvo Car Corporation
Examiner: Jonas Sjöberg, Electrical Engineering

Master's Thesis 2020
Department of Electrical Engineering
Division of Systems and Control
Chalmers University of Technology
SE-412 96 Gothenburg
Telephone +46 31 772 1000

Cover: Visualization of car and cyclist approaching intersection where driver of the
car might turn right, resulting in the cyclist hitting the side of the car. Image created
using IPG CarMaker.

Typeset in L^AT_EX
Printed by Chalmers Reproservice
Gothenburg, Sweden 2020

Collision Avoidance Function Concept

Avoiding collisions with cyclists located in the blind spot of the driver during right turn scenarios

ELINOR JERNHEDEN

DANIEL ÖSTERGREN BERNDTSON

Department of Electrical Engineering

Chalmers University of Technology

Abstract

A large number of road traffic accidents occur every year, with serious injuries or death as an outcome. Driver error, distraction and driving under the influence constitutes a majority of these accidents. To help mitigate or avoid collisions, the automotive industry have introduced passive and active safety features in vehicles. In this thesis, a collision avoidance function concept for passenger vehicles is developed with the purpose of avoiding collisions with cyclists located in the blind spot of the driver, using radars placed in the rear bumper of the host vehicle. Data is collected both in a simulation environment and at a proving ground. The function concept consists of object detection, path prediction and threat assessment. The object detection is part of a sensor setup in current Volvo Car Corporation vehicles. Its accuracy and limitations regarding sensor placement are evaluated on cyclists. This thesis also presents and evaluates models for path prediction for both the host vehicle and the cyclist. Furthermore, methods for threat assessment via estimated steering, acceleration or braking required to avoid a collision are applied and evaluated. The results presented in this thesis shows that the function concept detects collisions with cyclists and indicates the severity of the avoidance maneuver required to avoid them.

Keywords: Active safety, Collision avoidance (CA), Path prediction, Threat assessment (TA), Vulnerable Road Users (VRU), Autonomous Emergency Braking (AEB), Advanced driver-assistance systems (ADAS), Cyclist.

Acknowledgements

First we would like to thank our supervisor Faisal Mahmood Ahmed from Volvo Car Corporation for his guidance throughout this project. The experience and support from him and the rest of his team have been greatly helpful. We would also like to thank the members of the Virtual Car Team for providing us with simulation tools and for answering all our questions whenever we had any. Furthermore we would like to thank the team working at Hällered proving ground for making us a slot at the test track, and for technical support during the tests. We also wish to thank the members of the Radar Team for help with preparing the test vehicle. Lastly, we would like to thank our supervisor Jonas Sjöberg from Chalmers University of Technology for his guidance on writing this thesis.

Elinor Jernheden, Gothenburg, August 2020
Daniel Östergren Berndtson, Gothenburg, August 2020

Contents

Glossary	xi
Acronyms	xiii
List of Figures	xv
List of Tables	xvii
1 Introduction	1
1.1 Background	1
1.2 Scope of thesis	2
1.3 Method	4
1.4 Contributions	6
1.5 Outline	6
2 Sensors and data collection	7
2.1 Available sensors and sensor data	7
2.2 Recreating the scenario in simulation	8
2.2.1 Simulation environment	8
2.2.2 Scenario design	9
2.3 Data collection in vehicle on proving ground	11
2.4 Positioning accuracy in data collected on the proving ground	12
3 Initial scenario analysis	15
3.1 TTI estimation with parallel and oncoming objects	15
3.2 Window of action for the collision avoidance function	16
3.3 Radar sensor FOV in relation to the window of action for the collision avoidance function	17
4 Path prediction	19
4.1 Coordinate system	19
4.2 Host vehicle prediction	20
4.3 Object prediction	23
4.4 Calculation of intersection and TTI	24
4.5 Simulation results	26
4.5.1 General behaviour of object prediction	26
4.5.2 Predicted object position	27

4.5.3	Predicted object heading	28
4.5.4	Predicted TTI between the host vehicle and the object	29
4.5.5	Predicted curvature of the host vehicle at TTI	31
5	Threat Assessment	33
5.1	Threat assessment metrics	33
5.2	Required steering to avoid a collision	33
5.3	Required acceleration/braking to avoid a collision	34
5.4	Simulation results	35
6	Proving ground results	39
6.1	Object size	39
6.2	Object predictions	40
6.3	Threat assessment	41
7	Discussion	45
7.1	Findings and implementation	45
7.2	Difficulties of execution	47
8	Conclusions and Future work	49
8.1	Conclusions	49
8.2	Future work	50
	Bibliography	51
A	Detection accuracy in proving ground data	I
B	Predicted TTI, simulation results	IX
C	Required braking/acceleration, simulation results	XIII
D	Required steering, simulation results	XIX
E	Predicted TTI, proving ground results	XXV
F	Required braking/acceleration, proving ground results	XXXI
G	Required steering, proving ground results	XLIII

Glossary

curvature The curvature describes the sharpness of a curve and is defined as $\frac{1}{R}$, where R is the radius of the curve. The unit is $\frac{1}{m}$.

curvature rate The curvature rate describes the rate of change of the curvature and is defined as $\frac{\frac{1}{R}}{t}$, where R is the radius of the curve and t is time. The unit is $\frac{1}{ms}$.

host vehicle The passenger vehicle hosting the collision avoidance system.

object Any road user apart from the host vehicle.

Acronyms

FOV Field Of View.

GPS Global Positioning System.

IMU Inertial Measurement Unit.

TTI Time To Intersection.

TTR Time To React.

VRU Vulnerable Road User.

List of Figures

1.1	Illustration of potential scenarios.	2
1.2	Flowchart illustrating the steps taken to decide whether a driver needs assistance in order to avoid a collision.	3
1.3	In every collision case, there is a critical time beyond which the driver cannot avoid the collision.	3
1.4	General structure of the collision avoidance function concept.	4
1.5	Sensor data used as input to the collision avoidance function.	5
2.1	Radar sensor placement and approximate FOV.	8
2.2	The parameters used to recreate the scenario in simulation.	10
2.3	Simulation of collision case.	10
2.4	True and measured object position in scenario on test track.	14
3.1	Two vehicles travelling in the opposite direction.	15
3.2	Two vehicles travelling in the same direction.	16
3.3	The host vehicle and the object are said to collide when their bounding boxes starts to overlap.	16
3.4	Illustration of how the limited radar FOV affects the possibility to detect the object under certain circumstances.	17
4.1	The coordinate system used in the predictions.	19
4.2	Bicycle model.	20
4.3	A clothoid curve.	22
4.4	The object's path prediction is recalculated every Δt seconds, based on the most recent measurement.	23
4.5	Transformation from predictions of the host vehicle's rear axle to the host vehicle's front right corner.	25
4.6	The intersection point between the host vehicle's and the object's paths.	25
4.7	Object prediction when the host vehicle travels straight.	26
4.8	Radar measurements when the host vehicle is travelling straight vs in a curve.	27
4.9	Object prediction when the host vehicle turns.	27
4.10	Evaluation of predicted object position.	28
4.11	Evaluation of predicted object heading.	29
4.12	The TTI vs time in a simulated collision case.	30
4.13	How different lateral distance to the object affects the host vehicle curvature at TTI.	31

5.1	The edges of the object that needs to be avoided by steering.	34
5.2	Avoiding an object by braking.	35
5.3	The required braking/acceleration to avoid all edges of the object at each sample of a simulated collision case.	36
5.4	Predicted TTI in a simulated collision case.	37
5.5	The required steering to avoid all edges of the object at each sample of a simulated collision case.	37
5.6	The host vehicle and the object are side by side as long as there is an overlap in the longitudinal direction.	38
6.1	Size of the object in reality vs measured by the radar setup.	39
6.2	The influence of measurement noise on the object predictions.	40
6.3	The measured lateral acceleration of an object travelling straight is non-zero due to the curved path of the host vehicle.	41
6.4	Predicted TTI in a scenario based on proving ground data.	42
6.5	The required braking/acceleration to avoid all edges of the object at each sample of a collision case based on proving ground data.	43
6.6	The required steering to avoid all edges of the object at each sample of a collision case based on proving ground data.	44

List of Tables

2.1	Detection error in proving ground data.	13
3.1	Summary of the time in curvature for the simulated scenarios.	17
4.1	Parameters used in bicycle model.	21
4.2	Maximum curvature and curvature rate in simulation data.	22
4.3	Maximum curvature and curvature rate in proving ground data.	23
4.4	Accuracy of the predicted position.	28
4.5	Accuracy of the predicted heading.	29
4.6	Accuracy of the predicted TTI.	30
4.7	Accuracy of the predicted curvature.	31

1

Introduction

Road traffic accidents result in about 1.35 million deaths worldwide annually [1]. This number is a result of many factors such as unused seat belts, distracted drivers and driving under the influence. A wide range of methods are therefore applicable in the aim to reduce the number of accidents and their severity. VRU's such as pedestrians, cyclists and motorcyclists are over-represented and constitute more than half of all fatalities in road traffic accidents [1]. Therefore, it is important to continue the development of safety features which not only protect the occupants of the host vehicle, but also the VRU's. These passive safety features aim at reducing the injuries inflicted on the VRU in the case of a collision. The other type is active safety features, which are aimed at avoiding a collision before it becomes inevitable or mitigate the damages by autonomously reducing the velocity of the vehicle before the impact occurs [2]. This is done through features which can aid the driver in the driving task by issuing warnings or performing interventions if the driver is inattentive or impaired. Such systems continuously monitor the vehicle surroundings and aim at detecting plausible dangers that the driver might be unaware of. Driver support systems are especially interesting, since statistics show that driver errors are contributory factors in a majority of all road traffic incidents [3], [4], [5].

Early innovations within active safety were mainly focused on enhancing the drivers ability to maintain control of the vehicle under difficult circumstances. Such innovations included, e.g., Anti-lock Braking Systems (ABS) and Electronic Stability Control (ESC) [6]. The innovations have since shifted towards a more preventative focus, with development of warning systems and aids to reduce the overall number of incidents. Systems which can detect VRU's, like pedestrians and cyclists, are common in new vehicles and are often used to autonomously initiate emergency braking if a collision is imminent [7]. Systems on the market include, e.g., Volvo Cars Pedestrian detection with full auto brake, BMW's Pedestrian Warning with City Braking Activation and Audi's pre sense front/city.

1.1 Background

This thesis was carried out at Volvo Car Corporation (VCC) at the department of Active Safety, in the collision avoidance domain. VCC aim to be leading in both passive and active safety, with the goal of reducing fatal or severe accidents to zero by 2020. Hence, it is important to identify accident scenarios which result in severe

injuries, e.g., accidents involving VRU's. Once a high risk scenario has been identified, there arise a need for an active safety function to handle the situation. There is also a large possibility that a function concept similar to the one proposed will be included in future vehicle safety rating systems and governmental legislations.

1.2 Scope of thesis

The scope of this thesis covers the development of a collision avoidance function concept. The function concept is to be installed in a passenger vehicle and used to assist the driver in avoiding certain type of collisions with cyclists. The studied scenario is illustrated in Figure 1.1, where the host vehicle is about to make a right turn in the upcoming intersection. Next to the host vehicle, on the bike path or on the road edge, is a cyclist who travels straight ahead through the intersection. A radar sensor placed in the rear bumper of the host vehicle is used to detect the cyclist. The radar setup is further described in Section 2.1.

Figure 1.1a illustrates a collision case, where the host vehicle and the cyclist will enter the intersection at the same time and collide, if they continue along their predicted paths. In Figure 1.1b and 1.1c, the host vehicle and the cyclist will not enter the intersection at the same time, i.e., they will not collide if they continue along their predicted paths. This implies that in the cases **(b)** and **(c)**, the driver of the host vehicle can handle the situation solely, as there is no risk of collision. However, in case **(a)**, there will be a collision if the host vehicle and the cyclist continues along their predicted paths. Hence, the driver may need assistance to avoid the collision. Deciding whether a situation is case **(a)** or case **(b)/(c)** corresponds to answering the leftmost question in the flowchart shown in Figure 1.2. Situations corresponding to case **(a)** are referred to as collision cases, while cases corresponding to **(b)/(c)** are referred to as no collision cases.

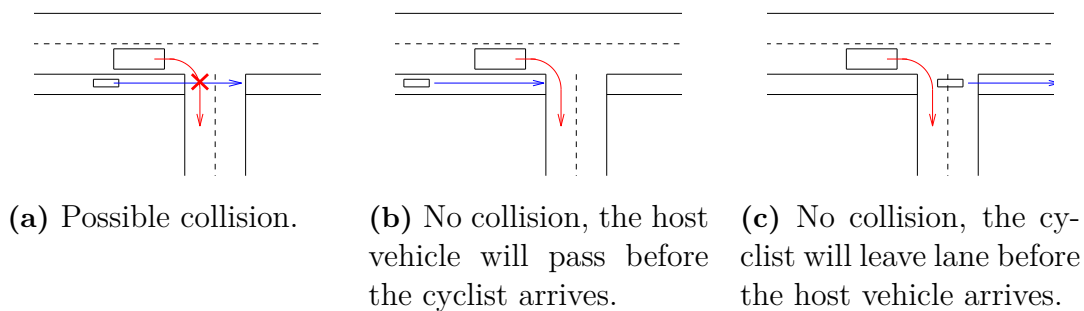


Figure 1.1: Illustration of potential scenarios.

Definition 1.1. Collision case: A collision case is a situation where the host vehicle and the cyclist will collide if they continue along their predicted paths.

Definition 1.2. No collision case: A no collision case is a situation where the host vehicle and the cyclist will not collide if they continue along their predicted paths.

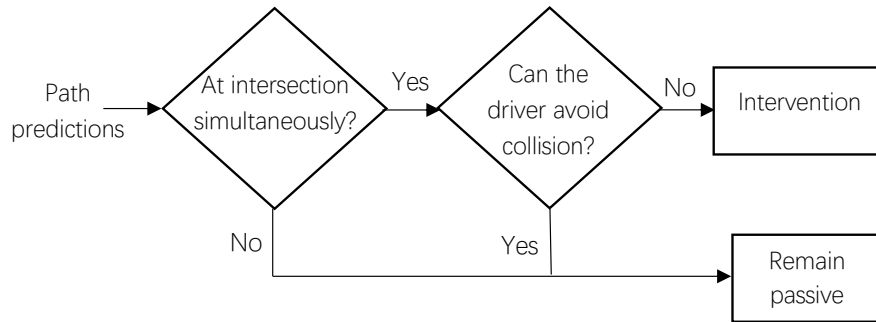


Figure 1.2: Flowchart illustrating the steps taken to decide whether a driver needs assistance in order to avoid a collision.

Given that the situation is a collision case, the function concept needs to evaluate if the driver can avoid the collision. This corresponds to answering the second question in the flowchart in Figure 1.2. If both the host vehicle and the cyclist continue traveling along their predicted paths, they will enter the red collision area, seen in Figure 1.3, at the same time and collide. However, at time t_0 in the figure, there is still enough time left until the host vehicle enters the collision area for the driver to react and avoid the collision through, e.g., braking. If the driver does not react to the situation, there is a critical time where the time left to the collision is too short for the driver to avoid the collision. The time left until the critical time is reached is referred to as the Time To React (TTR) [8]. The critical time and the TTR are affected by multiple factors, e.g., driver reaction time and tire to road friction. This is further described in Section 5.1. By choosing the critical time conservatively, it is possible to intervene only when the driver no longer can avoid the collision. This reduces the number of unnecessary interventions, where the driver actually is in control of the vehicle. Otherwise, the intervening function could be a nuisance to the driver and possibly cause a collision by acting unexpectedly. The goal is to intervene to completely avoid a collision. In cases where a complete avoidance is not possible, the function may still mitigate the impact of the collision by reducing the velocity of the host vehicle before the collision. From now on, the concept is referred to as collision avoidance, regardless of whether a complete avoidance can be achieved or not.

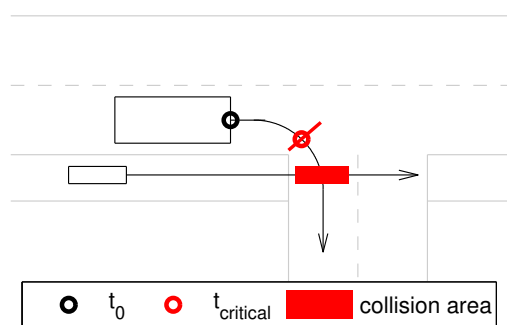


Figure 1.3: In every collision case, there is a critical time beyond which the driver cannot avoid the collision.

1.3 Method

As explained in Section 1.2, the purpose of the function concept is to detect if the host vehicle is in a collision case and perform an intervention only if the driver no longer can avoid the collision. This problem can be divided into several subproblems as illustrated in Figure 1.4. Green markings indicate areas that were developed and worked on in this thesis. The function concept is made to run in real time in the host vehicle. Hence, all of the steps are repeated with an interval of Δt seconds.

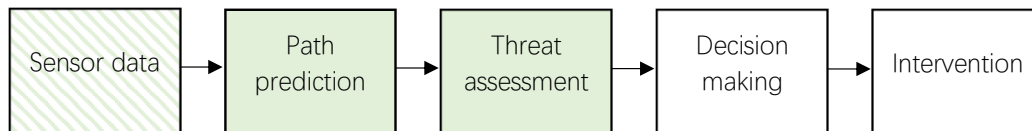


Figure 1.4: General structure of the collision avoidance function concept.

The purpose of the threat assessment part is to provide the information required to decide if the driver still can avoid the collision or not. The method applied in this thesis was suggested by Brännström et al. in their paper *Model-Based Threat Assessment for Avoiding Arbitrary Vehicle Collisions* [9]. Their method assesses how much steering, acceleration or braking the driver has to apply to avoid colliding with an object. These three measures are then used together to decide if the critical time, described in Figure 1.3, yet has been reached. To make the decision based on required steering, acceleration and braking is beneficial, as it may be too late for the driver to brake to avoid a collision but still possible to steer away from the collision. In such a case, the driver may be in control and intends to steer away from the object, i.e., no emergency braking should be initiated. In this thesis, the object is considered being passive. Hence, no calculations are made on which maneuvers that are available to the object in order to avoid a collision.

The amount of required steering, braking or acceleration to avoid collision with an object is calculated based on the host vehicle's and the object's predicted paths. The predicted paths also provides the Time To Intersection (TTI) between the host vehicle and the object. Both the paths and the TTI are calculated based on current information, which means that if an intervention is initiated, it will affect the path predictions and the TTI during the future times. This means that during an intervention, the object may have time to leave the collision area described in Figure 1.3 before the host vehicle arrives, which is a disadvantage of this method. However, at the low velocities studied in this thesis, further described in Section 2.2.2, the duration of an active intervention is short, which reduces this effect.

The path predictions for the host vehicle and the object are calculated based on data that is available through the sensors in the host vehicle. An overview of the sensor data can be seen in Figure 1.5. The path predictions are performed in two parts: the predictions of the host vehicle, which uses driver inputs and vehicle sensors; and the predictions of the object, which uses the radar setup's object detections and

positioning. Only the most recent sensor data is used in the path predictions. As the path prediction of the object rely only on the measurements provided by the radar setup, the accuracy of the object detections and positioning directly affects the accuracy of the predictions. Hence, the radar setup's detection and positioning accuracy were evaluated on cyclists, which is further described in Section 2.4.

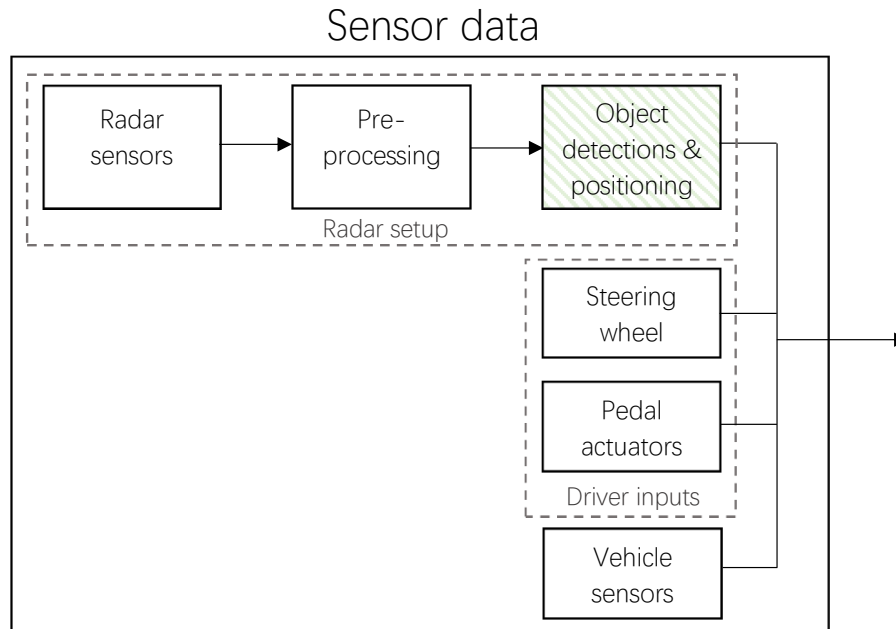


Figure 1.5: Sensor data used as input to the collision avoidance function.

In order to develop the different parts of the function concept, sensor data of the form described above is required. Apart from the sensor data, there is additional data required for evaluation of the function concept. This additional data is referred to as development data, with the additional parts being:

- The true position, velocity and acceleration of the host vehicle and the object (or ideal radar measurements) at all times during the scenario.
- Ideal measurements of host vehicle yaw and yaw rate.

Two different data sets were designed and created for the purpose of data collection, both containing collision cases. The first data set was collected in a simulation environment, consisting of ideal signals; the second data set was collected in a test vehicle, consisting of non-ideal signals.

1.4 Contributions

The contributions of this thesis are:

- Evaluation of the accuracy with which cyclists can be detected and positioned using current VCC radar setup.
- Analysis of the traffic scenario described in Section 1.2, highlighting the differences compared to situations with oncoming objects.
- A proposed method for the host vehicle's path prediction, evaluated on both data sets.
- A proposed method for the object's path prediction, evaluated on both data sets.
- Evaluation of how threat assessment, through the principles suggested by Brännström et al. in [9], behaves in the scenario described in Section 1.2.

The contributions are all subject to the following limitations:

- Hardware setups different to the one used in current VCC vehicles have not been considered.
- Scenarios where the radar setup output is unusable due to disturbing reflections from the surroundings or to weather conditions such as precipitation, have not been considered.
- Traffic signs or road markings have not been used to assess whether it is necessary to intervene or not. The host vehicle should try to avoid collisions regardless of who have the legal right of way.

1.5 Outline

This thesis is structured as follows. Chapter 2 describes the sensors and data collection. It includes descriptions on simulation software and an accuracy analysis of data collected in a test vehicle. Chapter 3 presents limitations and inherent difficulties related to the right turn scenario and the limitations of the radar setup. Chapter 4 presents the methods of path prediction for both the host vehicle and the object. Results from when these methods are applied to ideal data are also included. Chapter 5 explains the methods used for threat assessment. It includes results from when the threat assessment methods are applied to ideal data. Chapter 6 demonstrates how the path prediction and threat assessment are affected by noise and inaccuracies present in data collected in a test vehicle. Chapter 7 contains the discussion and Chapter 8 presents conclusions and suggestions for future work.

2

Sensors and data collection

This chapter describes the sensor data to the function concept and the sensors used to collect it. It also describes how data is collected both in the simulation environment and on the proving ground. Finally, it includes an evaluation of how accurately the cyclist is detected and positioned using the radar setup in the host vehicle.

2.1 Available sensors and sensor data

As stated in Section 1.2, the collision avoidance function is to be implemented in the host vehicle. Hence, it is restricted to use data which is available from the sensors in the vehicle. The sensor data can be divided into three parts, as illustrated in Figure 1.5. The three parts consist of the following signals:

- Object detections & positioning
 - Object position, lateral¹ and longitudinal² direction - relative to the host vehicle
 - Object velocity, lateral and longitudinal direction - over ground
 - Object acceleration, lateral and longitudinal direction - over ground
 - Object size
- Driver inputs
 - Steering wheel angle
 - Steering wheel angle rate
 - Requested acceleration
 - Requested deceleration
- Vehicle sensors
 - Host vehicle velocity - over ground
 - Host vehicle acceleration - over ground
 - Host vehicle yaw rate - over ground

¹Orthogonal to the host vehicle

²Parallel to the host vehicle

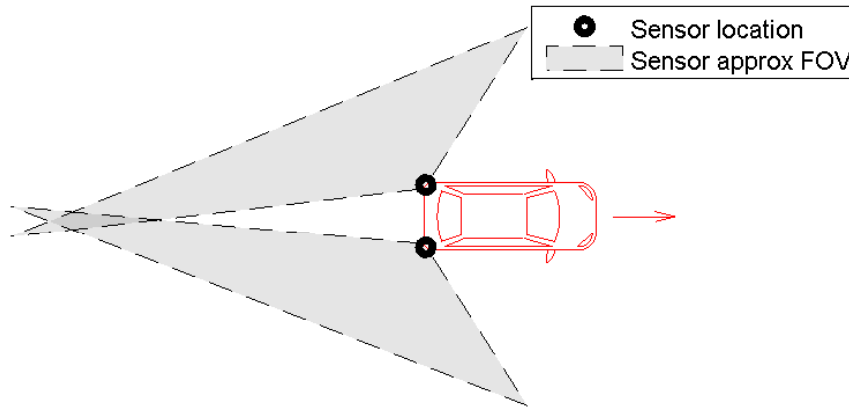


Figure 2.1: Radar sensor placement and approximate FOV.

The first part, object detections and positioning, focuses on the detection of objects in the host vehicle's surroundings. These signals are provided by a predefined radar setup, one that is currently used in VCC vehicles for detecting other motor vehicles. The current area of use is mainly the driver support function *Blind Spot Information System, BLIS*. In this function, the radar setup is used to detect objects travelling on the road. Hence, its focus has been larger vehicles such as motorcycles, cars and trucks. There are two radar sensors located in the rear bumper of the host vehicle, facing backwards as illustrated in Figure 2.1. The setup also includes the associated preprocessing unit from the supplier, which clusters the sensor data into objects and supplies information on position, velocity and acceleration. The position is reported as a single point, representing the center of the object. The radar setup also provide some information about the size of the object, which is further discussed in Section 2.4.

The second and third parts, driver inputs and vehicle sensors, are information regarding the host vehicle. The driver inputs are directly measured. Vehicle sensors consists of wheel speed sensors measuring the velocity and an IMU, measuring the acceleration and yaw.

2.2 Recreating the scenario in simulation

The scenario for which the function concept is developed was introduced in Section 1.2. In order to collect sensor data and development data, the scenario was recreated in a simulation environment which is described below.

2.2.1 Simulation environment

The simulation environment used was created by VCC and designed for active safety applications. The environment uses a 7-DOF vehicle model for the host vehicle. This model includes longitudinal, lateral and yaw motion of the chassis and the rotational

axis of the four wheels, i.e., no pitch, roll or suspension movements are considered. The accuracy of the 7-DOF vehicle model has been validated for levels of lateral and longitudinal acceleration that are not exceeded by simulating variations of the scenario described in Section 1.2. The 7-DOF vehicle model is implemented in MATLAB/Simulink, where also the surroundings, driver, actuators and control systems can be modeled. A 0-DOF model was used for the object, i.e., no vehicle dynamics are considered, only allowing translational movement in 3 dimensions.

2.2.2 Scenario design

In reality, there are multiple different factors which can be varied and still create a scenario which fits the description in Section 1.2. However, if too many factors are taken into account, the number of different combinations will increase rapidly. To limit the amount of different test cases, the scenario was simplified using a few assumptions. The host vehicle and the object are both represented by rectangular bounding boxes. The bounding boxes are set to 4.7×1.9 meters for the host vehicle and 1.8×0.5 meters for the object. The host vehicle is placed stationary 15 meters before the curve entry and once it starts moving, it will accelerate to the desired velocity and maintain it for the rest of the simulation. This illustrates the case where the host vehicle stops at a red light and then starts moving again. The velocity of the host vehicle varies with the radius of the curve as;

- Radius 6 meters \rightarrow host vehicle velocity 10 kph
- Radius 9 meters \rightarrow host vehicle velocity 15 kph
- Radius 12 meters \rightarrow host vehicle velocity 25 kph

where 6 meters corresponds to a sharp curve generally found in urban environments [10]. The object keeps a constant velocity of 8, 13, 18 or 23 kph throughout the simulation. Both the host vehicle and the object are assumed to travel straight ahead until the host vehicle makes the right turn. This implies that the object does not sway when passing the host vehicle and possible lane changes of the host vehicle are not represented. The lateral distance between the host vehicle and the object, center to center, is varied from 1.8 to 3.3 meters in steps of 0.5 meters. The smaller distances corresponds to when the object travels on the shoulder of the road, while the larger distances corresponds to when the object travels on a separate bike path further away. The parameters used to create the scenario in simulation are illustrated in Figure 2.2.

The relative placement of the host vehicle and the object is important, due to the limited field of view of the radar sensor and because it affects the type of collision that will take place. An early collision will imply that the object hits the side of the host vehicle. This may be considered a more likely scenario, since the object is harder to detect if it is further back. A later collision implies that the front of the host vehicle hits the object.

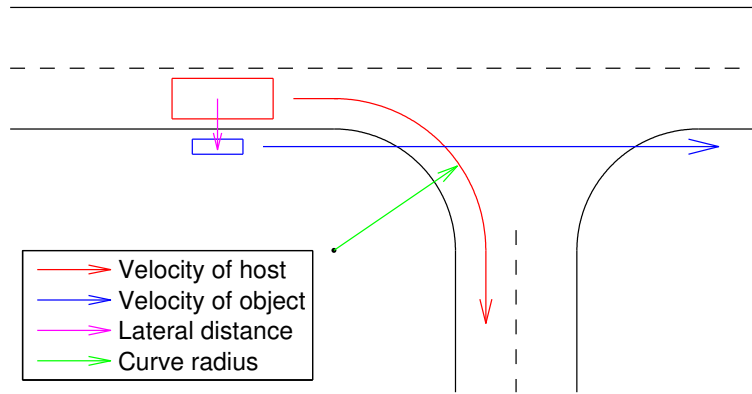


Figure 2.2: The parameters used to recreate the scenario in simulation.

The timeline of the scenarios is illustrated in Figure 2.3. Figure 2.3a shows how the host vehicle is stationary while the object approaches from behind. When the object comes close enough to the intersection, the host vehicle starts moving, see Figure 2.3b. The host vehicle and the object continue along their paths until the collision occurs, see Figure 2.3c and 2.3d.

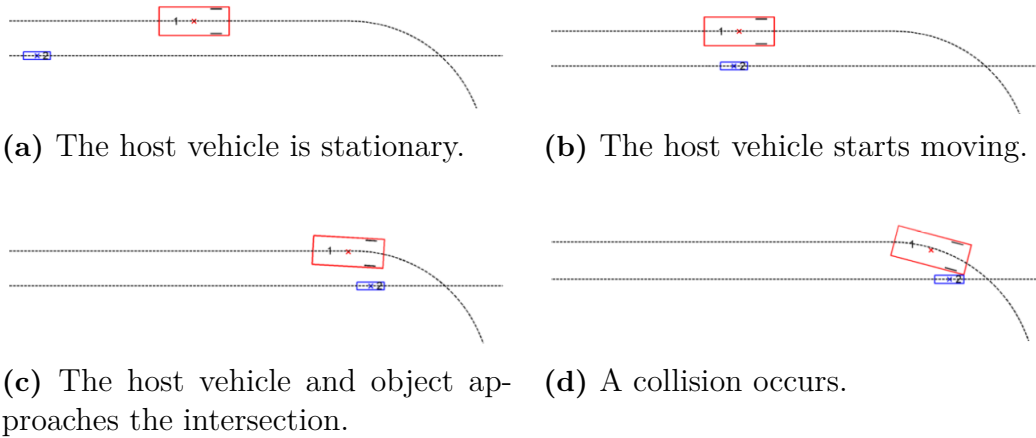


Figure 2.3: Simulation of collision case.

The simulation environment creates a file containing both sensor data and development data. The sensor data is of the form described in Section 2.1, with all signals being ideal and noise free. This sensor data is referred to as simulation data and the results based on the simulation data are referred to as simulation results. As this sensor data is ideal, the measured length and width of the object will also be reported without error.

Definition 2.1. Simulation data: Sensor data collected in a simulation environment, with ideal and noise free signals.

Definition 2.2. Simulation results: Results derived from tests, where simulation data was used as input.

2.3 Data collection in vehicle on proving ground

A set of test runs were carried out using a vehicle on a test track. The vehicle used was a Volvo XC40, which was fitted with the following equipment:

- A steering robot
- A pedal robot
- An IMU
- A high precision GPS
- A computer

The steering robot was attached to the steering wheel and the vehicle chassis, to enable the required torque to turn the steering wheel. The pedal robot is attached to the vehicle chassis and have two rods, which are used to control the accelerator and brake pedals respectively. The IMU monitors the state of the vehicle and the GPS connects to a local antenna on the proving ground to provide high precision measurements. The computer enables the four systems installed in the test vehicle to communicate with each other. It also allows for wireless communication with a third robot located outside the vehicle. This third robot has the form of a low platform with wheels and is powered by electrical motors so that it can move on its own. A Euro NCAP bicyclist and bike target is fitted to this platform and used as the object in the scenarios.

Predefined paths can be inputted to the system. The system can steer both the host vehicle and the object such that they follow their paths with high precision. This means that paths like the ones created in the simulation environment can be used as input to the proving ground setup. The test scenarios have three differences relative to the simulation data described in Section 2.2. First, the host vehicle held constant velocity throughout the scenarios. This was a necessary change in order to achieve repetitiveness between different runs of the same case. Without the constant velocity, the hit-point between the host vehicle and the object would differ between runs of the same case. Second, the velocities of the host vehicle and the object were changed to ensure that the object was within the radar sensor's FOV at critical times in all runs. Third, the lateral distance between the host vehicle and the object was either 2 or 3.3 meters in most of the cases to limit the number of runs.

The data collected on the proving ground consists of sensor data of the type described in Section 2.1. There is also development data created by the robot setup, which reports highly accurate measurements of position, velocity and acceleration of both the host vehicle and the object. For extra support during the analysis, the host vehicle was also fitted with cameras directed backwards through the window of the right rear door and the trunk lid. The sensor data collected in the test vehicle is referred to as proving ground data, and the results based on this data is referred to as proving ground results. The measurements provided by the robots, the IMU

and the GPS are considered as ground truth when evaluating the detection- and positioning accuracy of the radar setup in Section 2.4.

Definition 2.3. Proving ground data: Sensor data collected in a test vehicle on a proving ground.

Definition 2.4. Proving ground results: Results derived from tests, where proving ground data was used as input.

The area used for the tests was flat and empty to minimize radar disturbances and detections of other objects. During the entirety of the data collection on the test track, the weather was sunny to slightly overcast with temperatures ranging from 10 to 15 degrees Celsius and calm to light winds.

2.4 Positioning accuracy in data collected on the proving ground

The positioning accuracy in the data collected by the host vehicle highly affects the possibilities to predict if a collision will occur. If objects are reported far from where their actual position is, the function could make an incorrect decision to stay passive in a collision case, and vice versa. The radar measurements of position, velocity and acceleration can together be used to predict the future path of the object. Hence, the accuracy of these are evaluated below. Another aspect is how well the object can be identified in terms of size and shape. In order to avoid collision with a cyclist, it is necessary to avoid the entire cyclist, not only the reported midpoint.

The evaluation was performed by comparing the host vehicle's radar measurements to the development data reported by the robot setup described in Section 2.3. The accuracy of the measured position of the object during one of the runs at the proving ground is shown in Figure 2.4. The host vehicle travels at 10 kph and the object at 13 kph, the lateral distance between them is 2.8 meters. It can be seen in the figure that the lateral error increases when the object approaches the host vehicle. This is a general behaviour observed in most of the proving ground data, irrespective of the true lateral distance. The average errors, calculated over a set of tests, are shown in Table 2.1. Lateral velocity and acceleration was not evaluated due to lack of a reliable ground truth. Additional evaluations like the one presented in Figure 2.4, can be viewed in Appendix A.

The size of the objects detected by the radar setup is processed during the setup's preprocessing steps, resulting in a classification of *small*, *medium* or *large* object. This is the only classification of size that is available for use in the function. On this scale, the cyclist is presented as a *medium* object, which is the same category as cars and motorcycles etc. Hence, object size is reported as too large for a cyclist based on assumptions of average car size. To be able to use more accurate estimations of

	Average lateral error	Average longitudinal error
Position [m]	0.49	-0.35
Velocity [m/s]	-	0.06
Acceleration [m/s ²]	-	0.08

Table 2.1: Detection error in proving ground data.

object size, the function will have to rely on other quantities such as object velocity to make assumptions on the object type, e.g., car, cyclist, pedestrian etc.

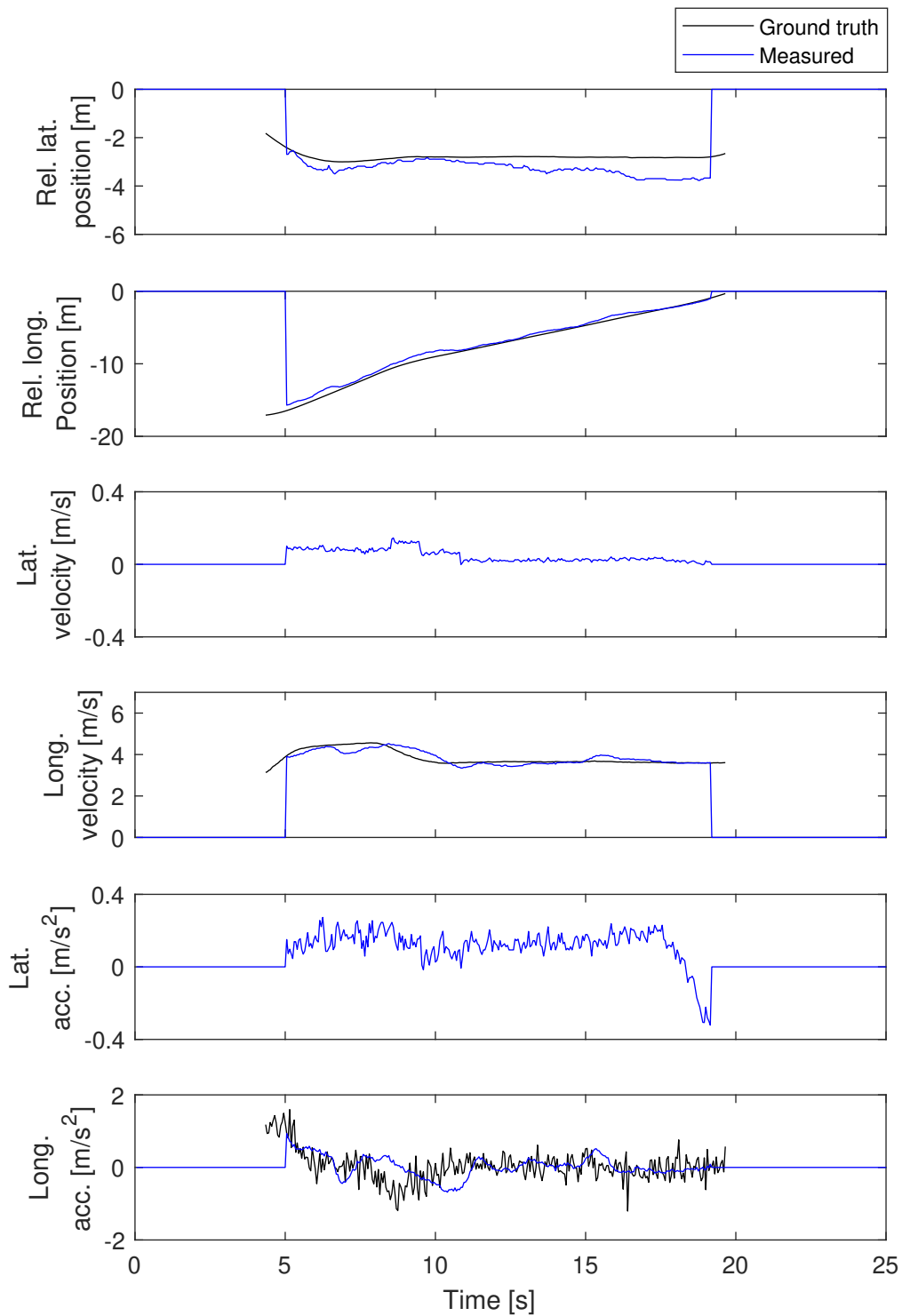


Figure 2.4: True and measured object position in scenario on test track.

3

Initial scenario analysis

This chapter discusses the inherent difficulties of the scenario for which the function concept was developed. It also describes some of the function concept's limitations due to the placement of the radar sensors on the host vehicle.

3.1 TTI estimation with parallel and oncoming objects

One of the challenges with scenarios in which the object travels the same direction as the host vehicle, is that the TTI is unknown until the host vehicle or the object starts turning. Figure 3.1 shows a scenario where two vehicles travel in the opposite direction. In this case, the TTI can be estimated based on the distance, relative velocity and relative acceleration between the two vehicles. The critical moments take place at the time when the two vehicles meet longitudinally. The time for when this happens can be approximated even before the driver of the red vehicle starts turning. All calculations on how to avoid the collision can then be concentrated to this point in time. Figure 3.2 shows a scenario where two vehicles travel in the same direction. In this case there is no information about the critical time, i.e., the time of intersection, until the driver of the red car starts turning. Both of the vehicles may continue side by side for an arbitrary amount of time.

This means that the calculation of TTI has to rely on a more complex model than a pure calculation of relative velocity, relative acceleration and longitudinal distance.

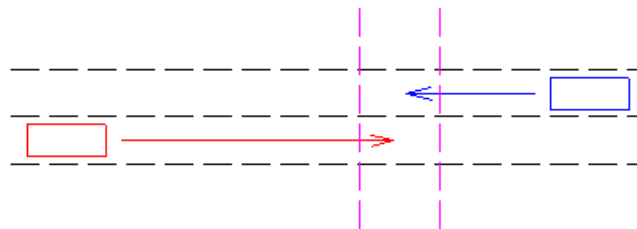


Figure 3.1: Two vehicles travelling in the opposite direction.

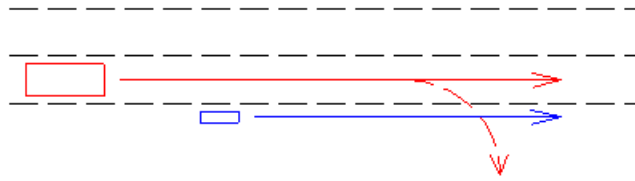


Figure 3.2: Two vehicles travelling in the same direction.

3.2 Window of action for the collision avoidance function

As outlined in Section 3.1, the moment at which the host vehicle starts turning is highly important in the context of estimating when and where a collision can or will take place. Hence, it is interesting to examine the simulated scenarios and define the possible window of action, from the point where the host vehicle starts turning to the point where the collision occurs. This defines the time window in which the host vehicle must be able to detect the imminent collision and intervene in order to avoid it. This time window is referred to as the time in curvature.

Definition 3.1. Time in curvature: The time in curvature is the duration in seconds from the point where the driver of the host vehicle starts turning the steering wheel, to the point where the host vehicle collides with the object.

The time of collision is defined as the time instance where the bounding boxes of the host vehicle and the object start to overlap, as illustrated in Figure 3.3. The time in curvature depends on the curve radius, the velocity of the host vehicle and the object and the lateral distance between them. Hence, the time is different in all of the simulated scenarios. A summary of the times are shown in Table 3.1. The longest, the shortest and the mean time in curvature are presented for each of the host vehicle's velocities, i.e., each curve radius was only subject to one host vehicle velocity.

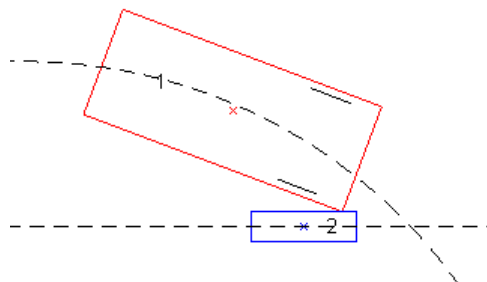


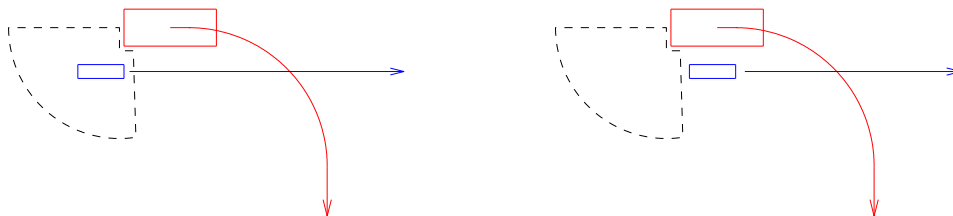
Figure 3.3: The host vehicle and the object are said to collide when their bounding boxes starts to overlap.

Host vehicle velocity, curve radius	Min time [s]	Max time [s]	Mean time [s]
10 kph, 6 m	1.30	2.25	1.80
15 kph, 9 m	1.13	2.00	1.59
25 kph, 12 m	0.73	1.39	1.06

Table 3.1: Summary of the time in curvature for the simulated scenarios.

3.3 Radar sensor FOV in relation to the window of action for the collision avoidance function

As stated in Section 3.1, the window of action for the collision avoidance function starts when the driver of the host vehicle starts turning. This factor, together with the radar sensors FOV, limits the possibility to detect objects under certain conditions. Figure 3.4a shows a situation where the host vehicle has started turning while the object is still within the FOV of the radar. In this case, it is possible to predict that the paths of the host vehicle and the object are going to intersect. Hence, there are also prerequisites for predicting if they are going to collide. In Figure 3.4b, there is a similar situation. However, the timing is different such that the object is outside FOV at the time when the host vehicle starts turning. A collision could still occur, but it is not possible to predict that a collision will occur because the host vehicle is not aware of the object's existence.



(a) Object within radar FOV.

(b) Object outside radar FOV.

Figure 3.4: Illustration of how the limited radar FOV affects the possibility to detect the object under certain circumstances.

3. Initial scenario analysis

4

Path prediction

This chapter describes how path predictions for both the host vehicle and the object are made. It also describes the calculation of intersection and TTI. The predictions are evaluated on simulation data.

4.1 Coordinate system

The coordinate system used in the path predictions is illustrated in Figure 4.1. It is a ground fixed coordinate system and the origin is placed at the rear axle of the host vehicle, with the x-axis pointing in the direction of travel. The y-axis is pointing towards the left side of the host vehicle and the z-axis is pointing upwards. The x- and y-axis are referred to as the longitudinal and the lateral direction respectively. This selection of coordinate system implies that when, e.g., the vehicle turns left, it results in a positive curvature and a positive curve radius. Likewise, when the vehicle turns right, the corresponding values are negative. All measurements and predictions of the object's position and heading are presented relative to the host vehicle, in the same coordinate system.

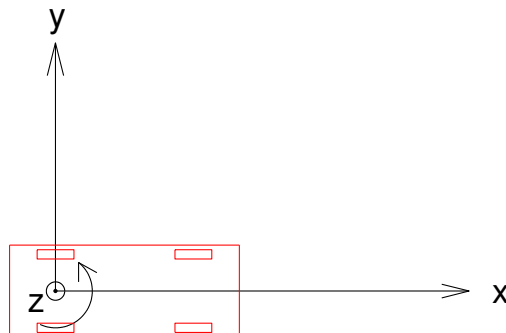


Figure 4.1: The coordinate system used in the predictions.

4.2 Host vehicle prediction

As stated in Section 1.2, the path predictions are used as a basis for the threat assessment. Hence, this host vehicle prediction is mainly created to provide the estimates needed in later calculations and have two main purposes:

- Predict the TTI with the object's path.
- Predict the curvature that the host vehicle will follow, i.e., in the beginning of a curve, it is desirable to predict the radius that the host vehicle will follow through the rest of the curve.

Furthermore, this initial path prediction can be used to omit further calculations in situations when the host vehicle and the object are far from each other throughout the entire prediction horizon.

The input to the path prediction are the signals described in Section 2.1. The steering wheel signals are converted to curvature and curvature rate using a linear bicycle model [11] and host vehicle parameters. A detailed derivation of curvature and curvature rate is presented below, derived from [11].

The calculation for curvature and curvature rate are identical, with the outcome depending on whether the steering wheel angle or the steering wheel angle rate are selected as input to the calculation. Therefore, the following equations will only show the derivation of the curvature. The host vehicle velocity and vehicle specific parameters, such as cornering stiffness, mass and wheelbase measurements, together with steering wheel angle/angle rate constitutes the input to the calculations. The abbreviations listed in Table 4.1, relating to the host vehicle, are used in the equations below. A simple bicycle model is illustrated in Figure 4.2.

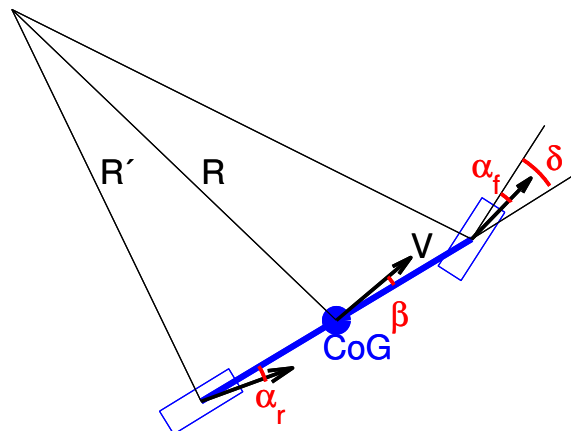


Figure 4.2: Bicycle model.

L_f	Distance from center of gravity to the front axle
L_r	Distance from center of gravity to the rear axle
$L_w = L_f + L_r$	The wheelbase
R	Curvature radius at center of gravity
R'	Curvature radius at rear axle
M	Mass
v	Velocity
C_f	Cornering stiffness, front
C_r	Cornering stiffness, rear
θ	Steering wheel angle
$\dot{\theta}$	Steering wheel angle rate
n	Steering ratio
δ	Wheel angle
$\dot{\delta}$	Wheel angle rate
α_f	Front tire slip angle
α_r	Rear tire slip angle
c	Curvature at center of gravity
\dot{c}	Curvature rate at center of gravity

Table 4.1: Parameters used in bicycle model.

First, the wheel angle is derived from the steering wheel angle and the steering ratio as

$$\delta = \frac{\theta}{n} . \quad (4.1)$$

The front tire slip angle α_f , can be expressed as

$$\alpha_f = \frac{ML_r v^2}{L_w C_f R} = c \frac{L_r}{L_w C_f} M v^2 \quad (4.2)$$

and the rear tire slip angle α_r can be expressed as

$$\alpha_r = \frac{ML_f v^2}{L_w C_r R} = c \frac{L_f}{L_w C_r} M v^2 . \quad (4.3)$$

The wheel angle δ is related to the front and rear tire slip angles through

$$\delta = L_w c + \alpha_f - \alpha_r = c \left(L_w + M v^2 \left(\frac{L_r}{L_w C_f} - \frac{L_f}{L_w C_r} \right) \right) . \quad (4.4)$$

Solving this equation for the curvature c results in

$$c = \frac{\delta}{L_w + M v^2 \left(\frac{L_r}{L_w C_f} - \frac{L_f}{L_w C_r} \right)} , \quad (4.5)$$

where δ is found through Equation (4.1), the velocity v is measured and the rest of the parameters are vehicle specific and thus known. Respectively, the curvature rate \dot{c} is given as

$$\dot{c} = \frac{\dot{\delta}}{L_w + M v^2 \left(\frac{L_r}{L_w C_f} - \frac{L_f}{L_w C_r} \right)} . \quad (4.6)$$

The host vehicle's path is predicted under the assumption of constant curvature rate and constant acceleration. It is common that vehicles that travel through a curve follow a clothoid [12]. A clothoid curve is illustrated in Figure 4.3. It can be described as being comprised of three segments. The curve entry is a constant curvature rate part, the middle of the curve is a constant curvature (radius) part and the transition back to straight road is a constant curvature rate part. As stated in Section 3.2, the time from the curve entry to the collision is short, usually less than 2.25 seconds. Hence, it is reasonable to predict constant curvature rate in this type of situations. Based on this data, the prediction horizon was set to 3 seconds. Constant acceleration is based on the assumption that drivers often change their velocity when making a sharp turn. The acceleration may therefore improve the prediction of the position in many cases.

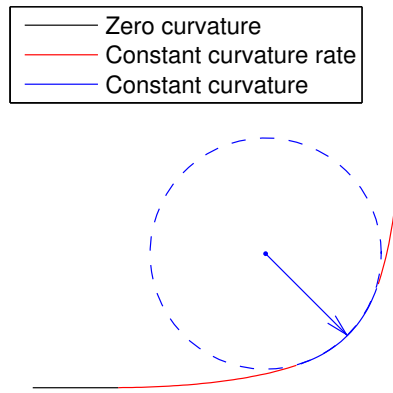


Figure 4.3: A clothoid curve.

To ensure that the path prediction outputs reasonable values that complies with the physical limitations of the host vehicle, the predicted curvature and curvature rate values are bounded. The maximum curvature and curvature rate values found in the simulation data are shown in Table 4.2. The corresponding values from the proving ground data are shown in Table 4.3. It should be noted that the on track runs were terminated just before a collision occurred. Hence, the vehicle did not follow through the entire turn. This is supposedly the reason for why the proving ground data provides lower values than the simulation data, for the same scenario. The limits are set to the maximum values found in testing with an additional 20% margin to allow for some variations, resulting in: $Curvature_{Limit} = \pm 0.1668[1/m]$ and $CurvatureRate_{Limit} = \pm 0.1032[1/ms]$. These limits could also be viewed as tuning parameters and be adjusted at a later stage to improve performance.

Host vehicle velocity, curve radius	Max Curvature $\left[\frac{1}{m}\right]$	Max Curvature Rate $\left[\frac{1}{ms}\right]$
10 kph, 6 m	-0.139	-0.079
15 kph, 9 m	-0.095	-0.065
25 kph, 12 m	-0.07	-0.086

Table 4.2: Maximum curvature and curvature rate in simulation data.

Host vehicle velocity, curve radius	Max Curvature $\left[\frac{1}{m}\right]$	Max Curvature Rate $\left[\frac{1}{ms}\right]$
10 kph, 6 m	-0.084	-0.065
15 kph, 9 m	-0.080	-0.054
25 kph, 12 m	-	-

Table 4.3: Maximum curvature and curvature rate in proving ground data.

4.3 Object prediction

As stated in Section 2.1, the object is detected and positioned using radar sensors. The available information includes position, velocity and acceleration in lateral and longitudinal direction. The main purposes of the object prediction are to:

- Predict the position of the object.
- Predict the heading of the object.

As stated in Section 1.3, all steps of the collision avoidance function concept are repeated with a delay of Δt . This is illustrated in Figure 4.4. The object's position at time t is marked in blue. Based on this position and the measurements available at this time, a path prediction is performed with the result also illustrated in blue. The predicted positions are numbered from $k = 1$ up to the length of the prediction horizon. The time between two positions in the predicted path is called Δt_p . The object moves, new measurements are collected and all the calculations are performed again. At time $t + \Delta t$, the object has the position marked in magenta in the figure. A new path prediction is performed and this prediction is illustrated in magenta in the figure. The calculations are repeated with an interval of Δt as long as the function concept is running.

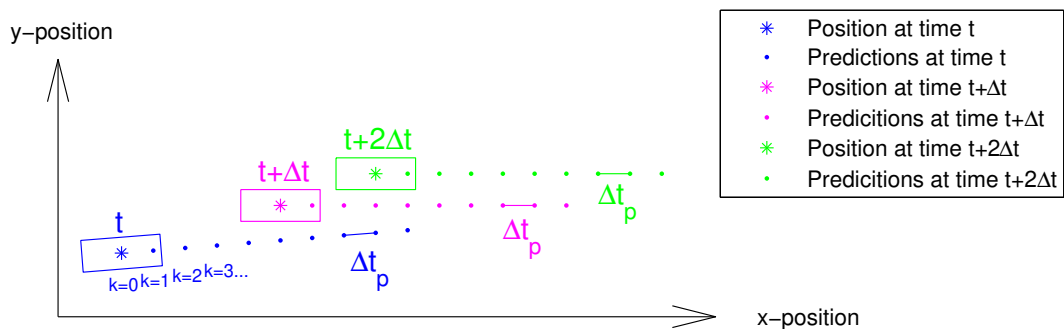


Figure 4.4: The object's path prediction is recalculated every Δt seconds, based on the most recent measurement.

The measurements of the object at time t are denoted as (x_t^0, y_t^0) for position, $(\dot{x}_t^0, \dot{y}_t^0)$ for velocity and $(\ddot{x}_t^0, \ddot{y}_t^0)$ for acceleration. The path of the object is predicted under the assumption of constant acceleration and the lateral and longitudinal directions

are handled separately. The predicted path at time t is achieved by iteratively applying

$$\begin{bmatrix} x_t^{k+1} \\ y_t^{k+1} \\ \dot{x}_t^{k+1} \\ \dot{y}_t^{k+1} \\ \ddot{x}_t^{k+1} \\ \ddot{y}_t^{k+1} \end{bmatrix} = \begin{bmatrix} 1 & 0 & \Delta t_p & 0 & \Delta t_p^2/2 & 0 \\ 0 & 1 & 0 & \Delta t_p & 0 & \Delta t_p^2/2 \\ 0 & 0 & 1 & 0 & \Delta t_p & 0 \\ 0 & 0 & 0 & 1 & 0 & \Delta t_p \\ 0 & 0 & 0 & 0 & 1 & 0 \\ 0 & 0 & 0 & 0 & 0 & 1 \end{bmatrix} \begin{bmatrix} x_t^k \\ y_t^k \\ \dot{x}_t^k \\ \dot{y}_t^k \\ \ddot{x}_t^k \\ \ddot{y}_t^k \end{bmatrix} \quad (4.7)$$

until $k + 1$ reaches the length of the prediction horizon. The two top rows of the equation defines the predicted position at the next sample as the current position, plus the distance traveled during the time Δt_p . The two middle rows of the equation ensures that non-zero acceleration will change the predicted velocity at the next sample. The two bottom rows of the equation enforces that the measured acceleration of the object remains the same from one sample to another, i.e., constant over the prediction horizon. The prediction horizon for the object was set to 3 seconds, same as for the host vehicle.

The heading of the object is used in the threat assessment to place the edges of the object's bounding box correctly. As the heading is not measured by the radar setup, it is instead calculated based on the longitudinal and lateral velocity according to

$$\theta_t^k = \tan^{-1} \left(\frac{\dot{y}_t^k}{\dot{x}_t^k} \right). \quad (4.8)$$

4.4 Calculation of intersection and TTI

Once the host vehicle's and the object's predicted paths are available, it is possible to evaluate if they are going to intersect. As explained in Section 4.1, all predictions are presented relative to the center of the host vehicle's rear axle. Hence, calculations based on these predictions would result in a very late intersection point. Instead, the predictions of the host vehicle's rear axle is converted to predictions of the host vehicle's front right corner. That is the first part of the host vehicle that will cross the object's path and therefore provide a more reasonable intersection point and TTI. The width of the object is neglected since the bounding box of the cyclist is very narrow. The original predictions of the host vehicle's path at time t are labeled (x_t^k, y_t^k) . These are converted to predictions of the host vehicle's front right corner, $(\tilde{x}_t^k, \tilde{y}_t^k)$, using

$$\tilde{x}_t^k = x_t^k + d_{RearAxleToFront} \cos(\phi_t^k) + \frac{W_{Host}}{2} \sin(\phi_t^k), \quad k \in [1, Pred.Horizon] \quad (4.9)$$

and

$$\tilde{y}_t^k = y_t^k + d_{RearAxleToFront} \sin(\phi_t^k) - \frac{W_{Host}}{2} \cos(\phi_t^k), \quad k \in [1, Pred.Horizon] \quad (4.10)$$

where ϕ is the predicted heading angle of the host vehicle. The parameters labeled $d_{RearAxleToFront}$ and W_{Host} are vehicle specific and represents the distance from the rear axle to the front of the host vehicle, and the width of the host vehicle respectively. The result of the transformation is illustrated in Figure 4.5.

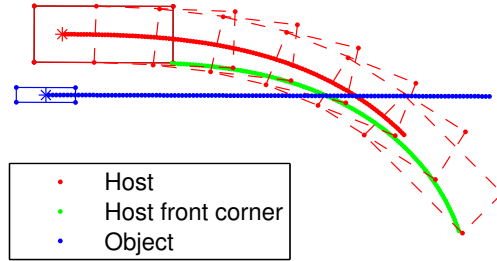


Figure 4.5: Transformation from predictions of the host vehicle's rear axle to the host vehicle's front right corner.

The point of intersection is then calculated based on the host vehicle's front right corner, as illustrated in Figure 4.6. The calculations are performed in three steps:

- Check if the predictions are parallel (or very close to).
- Find the minimal lateral distance between the paths.
- Decide if the paths are close enough to consider it an intersection.

In the first step, the algorithm finds the minimal and the maximal lateral distance between the two paths. If these values are close enough to each other, the paths are considered parallel and the time to intersection is set to $TTI_{default} = 3$ seconds. This is needed to avoid an incorrect TTI estimation when the host vehicle and the object travel very close to each other, but on parallel paths. The algorithm then finds the minimal lateral distance between the two paths. If this distance is below $d_{lat,threshold}$, the paths are considered close enough to be treated as an intersection of the paths. The time it will take for the host vehicle to reach this point is then set as the TTI. The value of $d_{lat,threshold}$ is a tuning parameter and was set to half of the width of the host vehicle, $w_{host}/2 = 0.93$ meters for a Volvo XC40.

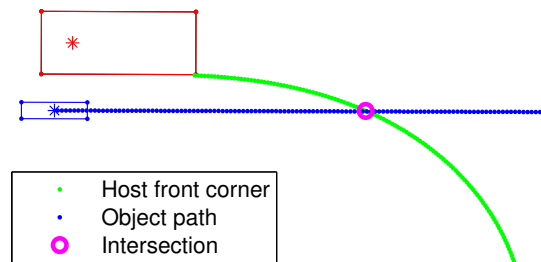


Figure 4.6: The intersection point between the host vehicle's and the object's paths.

4.5 Simulation results

As both the host vehicle's and the object's predictions together are used to find the point of intersection, both of their uncertainties affects the end result. The predictions were therefore evaluated in several ways to single out the pros and cons of each of the prediction methods.

4.5.1 General behaviour of object prediction

As the constant acceleration model used for the object was evaluated on simulation data, one drawback was singled out. That is the problem of measuring and/or interpreting the lateral distance, velocity and acceleration of the object in a correct way.

Figure 4.7 shows the behaviour of the path prediction while the host vehicle travels straight ahead, parallel to the object. During this period, the measurements are performed as illustrated in Figure 4.8a. Hence, the object has zero lateral velocity and 8-23 kph longitudinal velocity, which explains the accurate prediction seen in Figure 4.7. The problem arise when the host vehicle reaches the curve. At the moment shown in Figure 4.8b, it is clearly visible that the host vehicle is getting closer to the object. However, this is because the figure shows the entire perimeter of the host vehicle, where the front of the host vehicle has moved significantly closer to the object. However, the radar sensor is placed in the rear bumper of the host vehicle and has not yet moved much closer to the object. Instead, the geometry of the situation becomes such that the lateral distance rather seems to increase as the measurements are taken orthogonal to the host vehicle. This results in the behaviour seen in Figure 4.9, where the object's path is influenced by the host vehicle's heading direction.

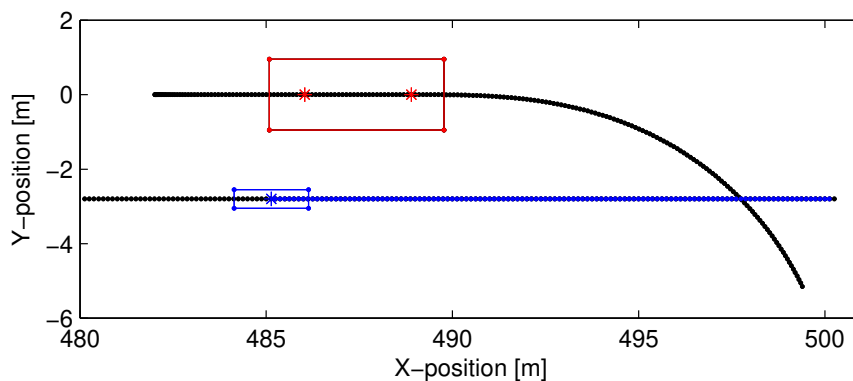


Figure 4.7: Object prediction when the host vehicle travels straight.

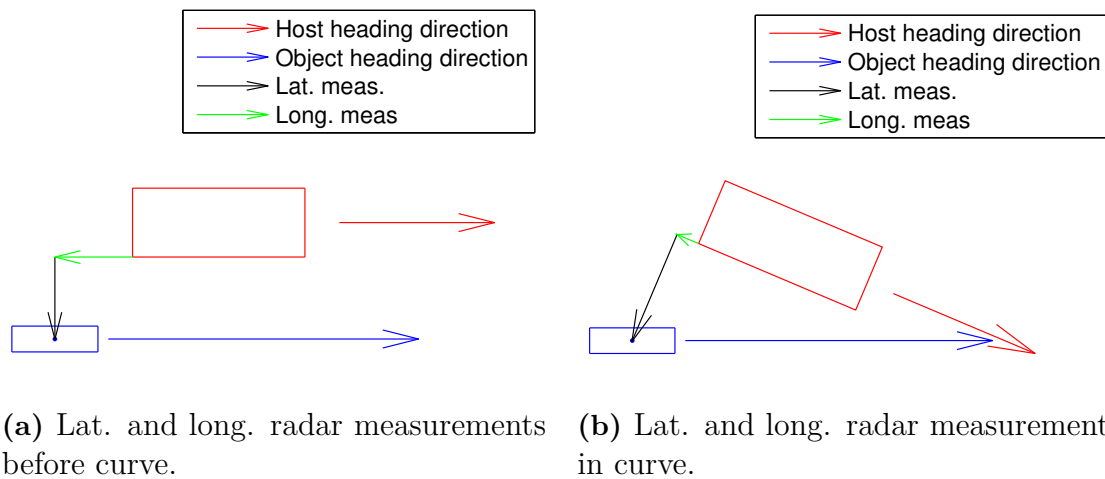


Figure 4.8: Radar measurements when the host vehicle is travelling straight vs in a curve.

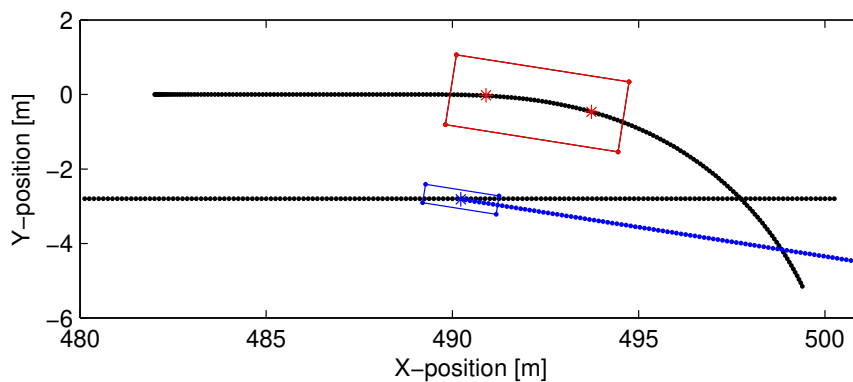


Figure 4.9: Object prediction when the host vehicle turns.

4.5.2 Predicted object position

The evaluation of the object's predicted position was performed by converting the positions to the global coordinate system and calculating the error relative to the true path. The true path being the path defined in the simulation environment. The evaluation was performed when the true TTI is 1 second, considering the error at the time of intersection as illustrated in Figure 4.10. The simulation results are shown in Table 4.4. To avoid the possibility of the object being outside the FOV of the radar, the cases were picked such that the object had higher (or similar) velocity than the host vehicle.

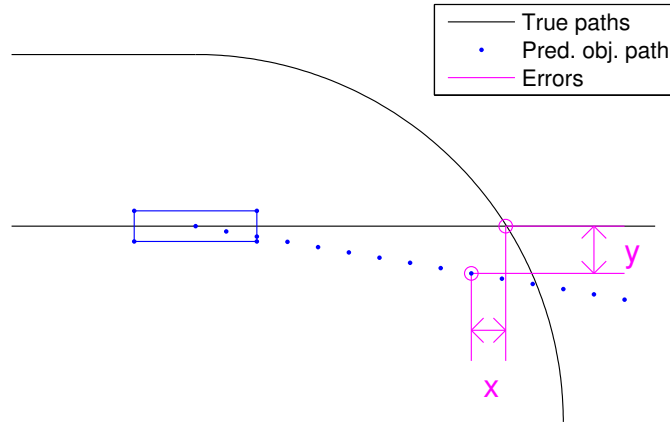


Figure 4.10: Evaluation of predicted object position.

Host vehicle velocity, curve radius	Lateral distance [m]	Error x [m]	Error y [m]
10 kph, 6 m	1.8	-0.07	-0.35
	2.3	0.86	-0.37
	2.8	-0.06	-0.5
	3.3	-0.10	-0.94
15 kph, 9 m	1.8	0.82	-0.03
	2.3	-1.17	-0.16
	2.8	-0.32	-0.11
	3.3	-0.25	-0.44
25 kph, 12 m	1.8	-	-
	2.3	-	-
	2.8	-0.37	0.23
	3.3	-0.43	0.16

Table 4.4: Accuracy of the predicted position.

4.5.3 Predicted object heading

The predicted object heading is directly related to the predicted lateral and longitudinal velocities through (4.8), as stated in Section 4.3. This implies that the error in predicted object position also gives an intuition about the error in predicted heading angle. However, the accuracy of the heading was also evaluated separately, with simulation results shown in Table 4.5. The true values were taken as the ones calculated by the simulation environment. The evaluation was performed when the true TTI is 1 second and the point of interest is the true time of intersection, see Figure 4.11. The values are specified in the global coordinate system, hence the true heading of the object is always zero.

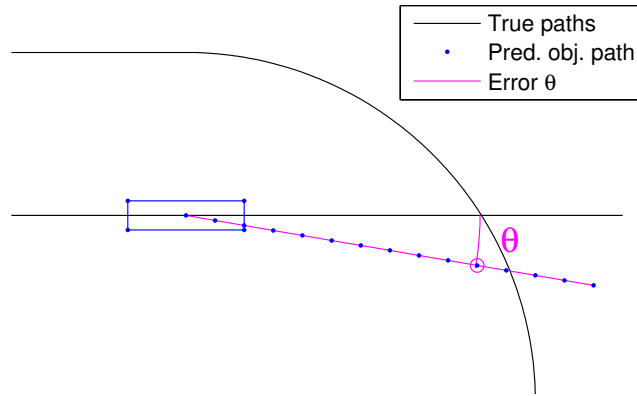


Figure 4.11: Evaluation of predicted object heading.

Host vehicle velocity, curve radius	Lateral distance [m]	Pred. heading [deg]	True heading [deg]
10 kph, 6 m	1.8	-0.98	0
	2.3	-3.39	0
	2.8	-6.58	0
	3.3	-10.39	0
15 kph, 9 m	1.8	-0.32	0
	2.3	-1.66	0
	2.8	-3.55	0
	3.3	-6.56	0
25 kph, 12 m	1.8	-	0
	2.3	-	0
	2.8	-0.19	0
	3.3	-0.92	0

Table 4.5: Accuracy of the predicted heading.

4.5.4 Predicted TTI between the host vehicle and the object

As stated in Section 4.4, the TTI is defined as the time left until the host vehicle intersects the object's path. These calculations were evaluated in two ways. The first evaluation was performed by checking the accuracy of the predicted TTI at 1 second before the true time of intersection. The true values being the times calculated by the simulation environment. This was due to the very short time in curvature in several of the scenarios, see Section 3.2. Simulation results are presented in Table 4.6.

Host vehicle velocity, curve radius	Lateral distance [m]	Pred. TTI [s]	True TTI [s]
10 kph, 6 m	1.8	1.23	1
	2.3	1.15	1
	2.8	1.25	1
	3.3	1.33	1
15 kph, 9 m	1.8	1.13	1
	2.3	1.05	1
	2.8	1.03	1
	3.3	1.13	1
25 kph, 12 m	1.8	-	1
	2.3	-	1
	2.8	1.15	1
	3.3	0.98	1

Table 4.6: Accuracy of the predicted TTI.

The second evaluation was performed by inspecting how the TTI value changed during a collision case. Figure 4.12 shows the predicted TTI in a test run based on simulation data. In this scenario the curve radius is 6 meters, the host vehicle travels at 10 kph, the object travels at 18 kph and the lateral distance between them is 1.8 meters. The blue area in the graph marks the time during which the object is outside the radar's FOV. At approximately 0.3 seconds, the radar setup starts detecting the object. The host vehicle and the object travel parallel for about 9 seconds, which is the area marked in red. The host vehicle starts turning at 9.5 seconds, and the paths of the host vehicle and the object starts to intersect. This results in the decreasing TTI marked in green. This far, the TTI calculations performs as expected. The problem occur in the yellow area of the graph where the TTI stops decreasing (or decreases slowly). Note that the dashed red line marks the time of the collision, thus the TTI should reach zero by this time. This inaccuracy is the result of the behaviour described in Section 4.5.1. As the predicted path of the object tends to stay parallel to the host vehicle, the point of intersection is moved forward. Hence, the TTI becomes overestimated when the host vehicle reaches further into the curve. TTI-graphs from additional collision cases based on simulation data can be viewed in Appendix B.

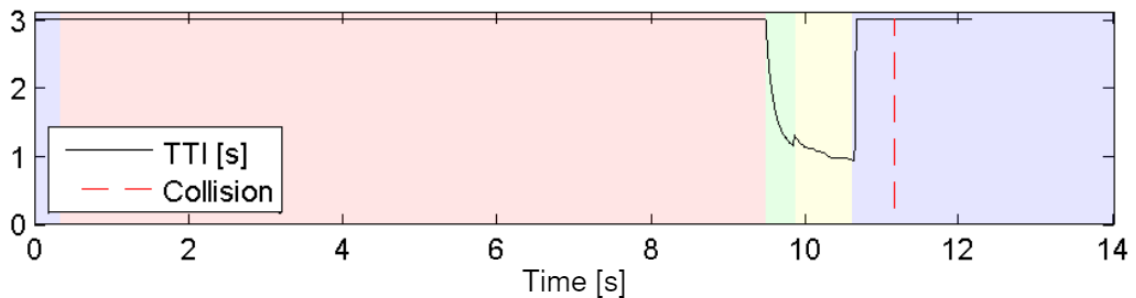


Figure 4.12: The TTI vs time in a simulated collision case.

4.5.5 Predicted curvature of the host vehicle at TTI

The evaluation of the predicted curvature of the host vehicle was performed by comparing the true and the predicted curvature at TTI. The true curvature being the curvature in the path used in the simulation environment. The comparison was made at the point when the real TTI is 1 second. The simulation results are presented in Table 4.7. Lateral distance refers to the lateral distance between the host vehicle and the object, as described in Section 2.2. This distance affects how far into the curve the host vehicle can travel before a collision occurs. The effect of different lateral distances on the curvature at TTI is illustrated in Figure 4.13. The host vehicle follows the same trajectory in both cases but reaches the object's path at different points.

Note that the true curvature is not strictly equal to $1/R$. This stems from the driver model in the simulation environment, which replicates typical driver behaviour by deviating from the center of the lane in curves.

Host vehicle velocity, curve radius	Lateral distance [m]	Pred. curvature $[\frac{1}{m}]$	True curvature $[\frac{1}{m}]$
10 kph, 6 m	1.8	-0.11	-0.12
	2.3	-0.14	-0.13
	2.8	-0.16	-0.14
	3.3	-0.17	-0.15
15 kph, 9 m	1.8	-0.06	-0.08
	2.3	-0.09	-0.10
	2.8	-0.11	-0.11
	3.3	-0.09	-0.11
25 kph, 12 m	1.8	-	-
	2.3	-	-
	2.8	-0.06	-0.09
	3.3	-0.09	-0.09

Table 4.7: Accuracy of the predicted curvature.

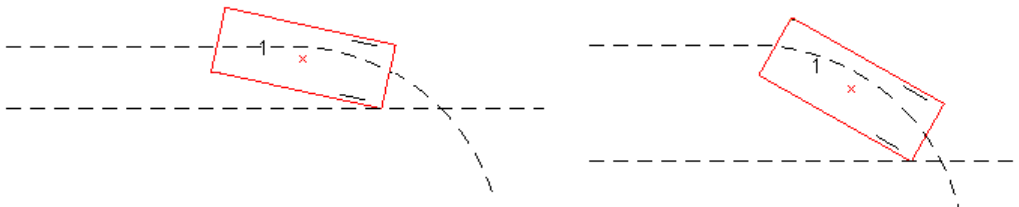


Figure 4.13: How different lateral distance to the object affects the host vehicle curvature at TTI.

5

Threat Assessment

This chapter explains the threat assessment. It describes which quantities that are taken into account, and states the results that are produced when applying the calculations to simulation data.

5.1 Threat assessment metrics

As stated in Section 1.2, there is a critical time in every collision case, after which the driver no longer can avoid the collision. This critical time depends on several factors. It depends on delays, such as the driver's reaction time and delays in the brake system. It also depends on the tire to road friction and the current curvature of the host vehicle, as these affect how much the driver can steer, brake or accelerate to avoid the object. However, these factors are not incorporated in the function concept, since the decision making process is not a part of this thesis.

As stated in Section 1.3, the threat assessment was performed through calculations of the estimated steering or acceleration/braking required to avoid a collision, as described by Brännström et al. in [9]. The steering or acceleration/braking required to avoid a collision are calculated separately and the method does not consider any combined use of them.

5.2 Required steering to avoid a collision

The first part in the work presented by Brännström et al. [9] is to calculate the steering required for the entire host vehicle to avoid the entire perimeter of the object. Hence, the first step to implement this algorithm in the situation of interest was to find the edges of the object. The calculations are performed based on the positions of both the host vehicle and the object at the predicted TTI. To make room for small errors in the predicted TTI, ten time instances are picked out around the TTI.

For each of the ten time instances, the corners of the object are calculated based on object heading and size. These are illustrated in Figure 5.1. Only three of the object's corners are needed since the host vehicle is going to collide with one of the

two closest edges first. As illustrated in the figure, the edges of the object's predicted positions are wider than the actual width of the object. This is due to an added safety margin of 0.5 meters around the object. The safety margin adds additional space between the host vehicle and the object, such that there is some distance left to the object when the host vehicle have performed a successful avoidance maneuver. Since the added safety margin directly affects the initiating of the AEB, and that a sufficient distance left between the host vehicle and the object after an intervention is arbitrary, the safety margin is considered a tunable parameter.

Once the positions of the object's edges are known, Brännström et al. [9] proceeds to calculate the curvature c_1 required for the host vehicle to pass with the complete vehicle entirely to the left of each object edge. The process is repeated for all time instances i in the prediction horizon and all object edges m . Once completed, the requirement for passing to the left of the object is to apply enough steering wheel angle to satisfy

$$c_1 \geq \max_{i,m} \{c_{1,i,m}\} . \quad (5.1)$$

The calculations are then repeated in a similar manner to calculate curvature required to pass on the right side of the object.

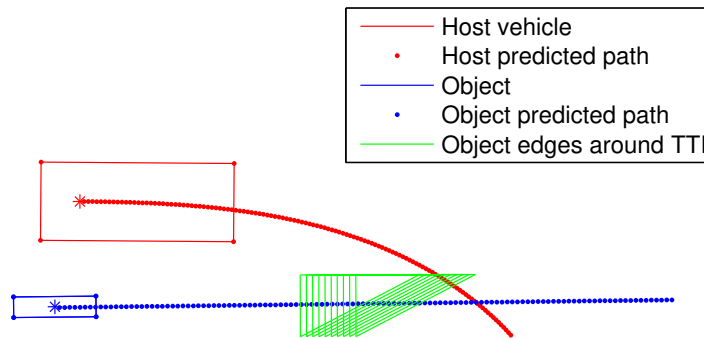


Figure 5.1: The edges of the object that needs to be avoided by steering.

5.3 Required acceleration/braking to avoid a collision

The basis in the calculations of required braking/acceleration is very similar to the steering case. Brännström et al. [9] calculates the values such that the entire host vehicle avoids the entire object. These calculations are performed under the assumption of constant curvature throughout the braking/acceleration. The curvature value used in these calculations was chosen as the value calculated by the host vehicle predictions at TTI. The current curvature of the host vehicle is going to be a poor representation of the rest of the curve, as the host vehicle may just have entered the curve when the threat assessment is performed.

The predicted position of the object was used to calculate the position of the object's

corners at every time instant during the prediction horizon. Then, Brännström et al. [9] finds the critical parts of the object as the points which are inside the width of the host vehicle's path, as can be seen in Figure 5.2. These are the points which have to be avoided to avoid a collision with the object. The required braking j_r is then calculated as the amount of deceleration needed to keep each of the critical points ahead of the host vehicle. In the same way, the required acceleration j_r is calculated such that the entire host vehicle will pass in front of each of the critical points. The calculations are repeated for all time instances i in the prediction horizon and all edges m . The required braking to avoid a collision should then be picked such that

$$j_r \leq \min_{i,m} \{j_{r,i,m}\} \quad (5.2)$$

is fulfilled. In the same manner, the required acceleration should be picked such that

$$j_r \geq \max_{i,m} \{j_{r,i,m}\} \quad (5.3)$$

is fulfilled.

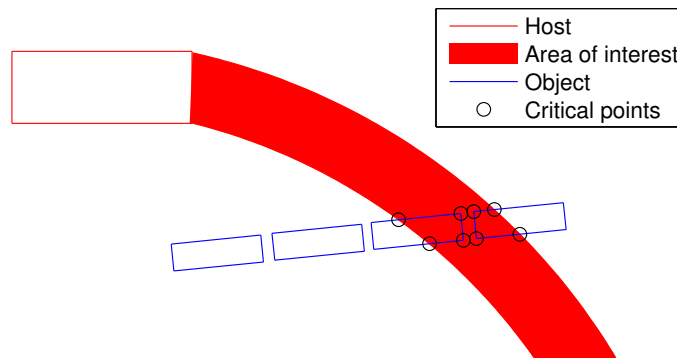


Figure 5.2: Avoiding an object by braking.

5.4 Simulation results

The threat assessment was evaluated in simulation by running a set of collision cases. The results of one of the simulation data cases are illustrated in Figure 5.3. In this case the curve radius is 6 meters, the host vehicle travels at 10 kph, the object travels at 18 kph and the lateral distance between them is 1.8 meters. Figure 5.3 shows the required braking, acceleration, positive- and negative jerk required to avoid the collision. The required braking to avoid a collision reaches about -3.5 m/s^2 . This value is a result of the low velocity of the host vehicle, but it was also affected by the inaccuracy in predicted TTI discussed in Section 4.5.4. The graph of the estimated TTI for this scenario is shown in Figure 5.4 for reference. As the TTI approaches zero, the required braking would increase towards infinity. The same principle holds for the required acceleration to avoid a collision. The value increases as the host vehicle and the object approaches the collision, but not towards infinity. The signals provide a clear indication that a collision is imminent, but the values do not represent the full severity of the situation. Results from additional simulated scenarios can be viewed in Appendix C.

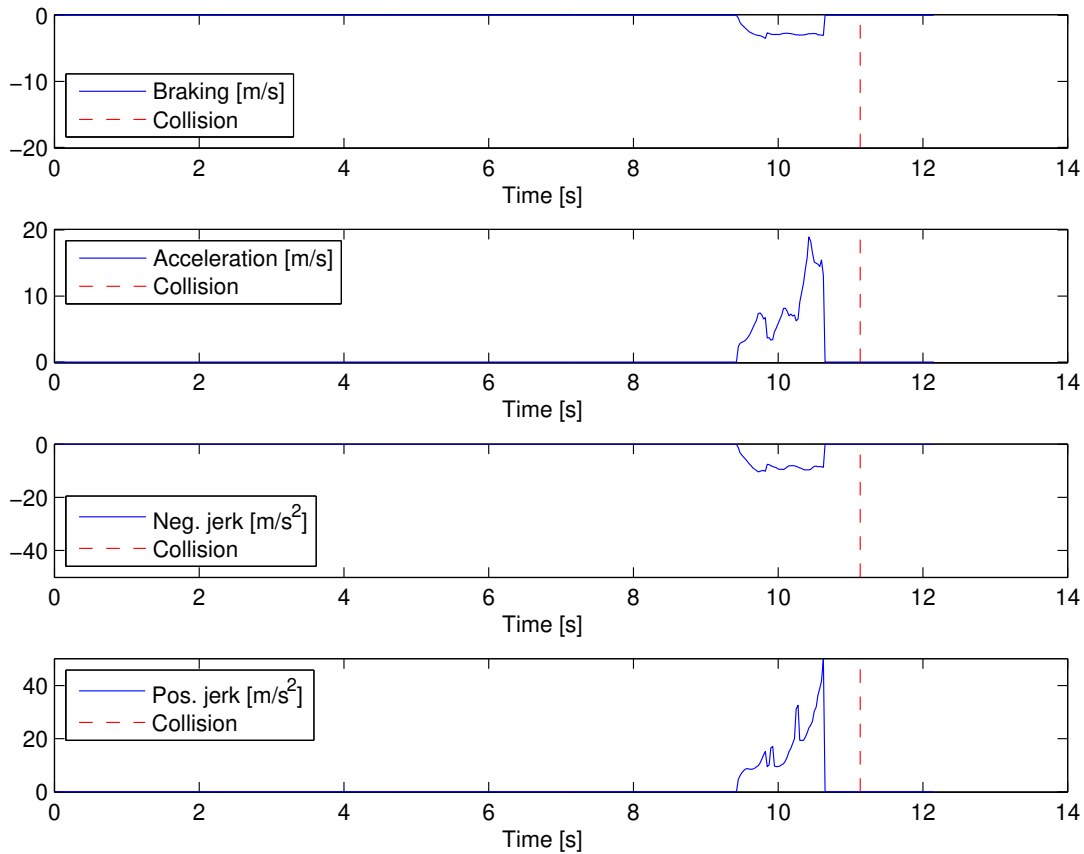


Figure 5.3: The required braking/acceleration to avoid all edges of the object at each sample of a simulated collision case.

Figure 5.5 shows the required steering to avoid a collision in the test case described above. As the object is located on the right side of the host vehicle, less curvature is required to avoid the collision by passing the object on the left side. The curvature required to pass on the left side of the object indicates that a steering intervention is needed to avoid a collision. However, it is likely that this value is an underestimation of the steering required due to the overestimation of the TTI. The curvature required to pass on the right side looks very different due to the placement of the object. This graph has two distinct bumps. The reason for the first bump is that while the host vehicle and the object are travelling straight ahead, the object is predicted to pass the host vehicle. During the time they are side by side it would take zero steering to pass to the left of the object, but much more steering to pass to the right of the object. Figure 5.6 illustrates this phenomenon. From the point shown in Figure 5.6a to the point shown in Figure 5.6b, the host vehicle would have to travel around the rear edge of the object to pass on the right side of it. The second bump in the signal is associated with the intersection. The value shows that it would be very difficult for the driver to steer enough to pass the object on the right side. Results from additional simulated scenarios can be viewed in Appendix D.

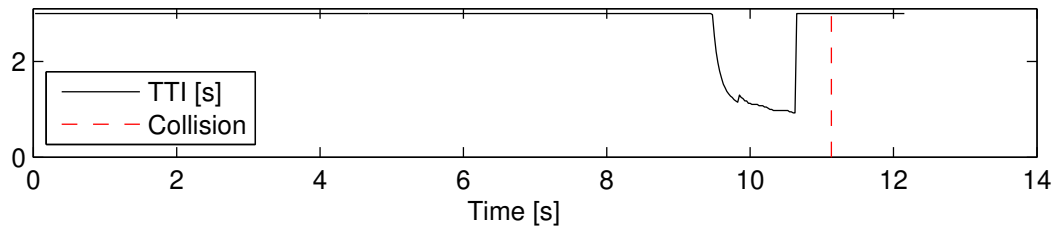


Figure 5.4: Predicted TTI in a simulated collision case.

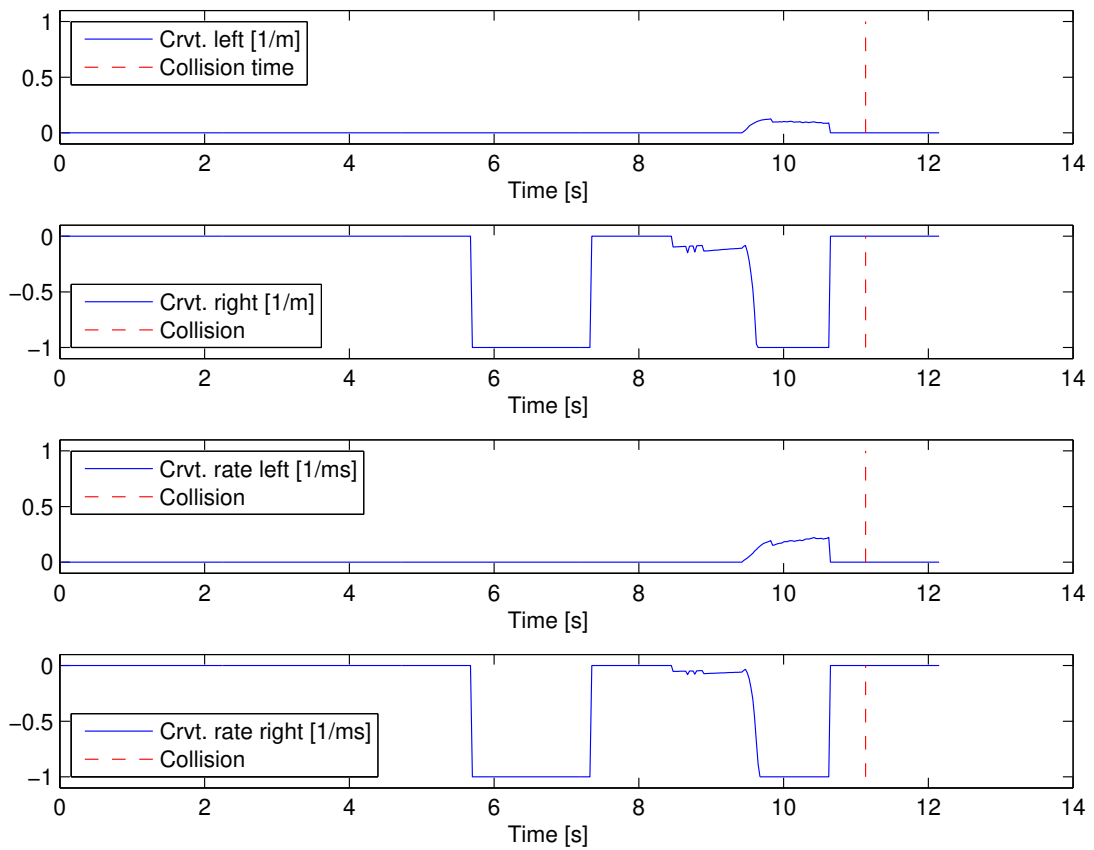


Figure 5.5: The required steering to avoid all edges of the object at each sample of a simulated collision case.

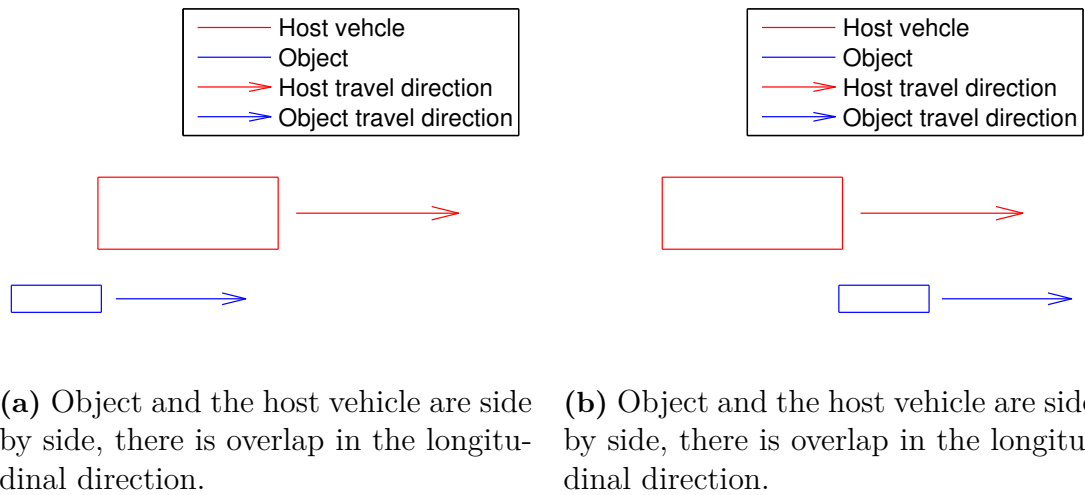


Figure 5.6: The host vehicle and the object are side by side as long as there is an overlap in the longitudinal direction.

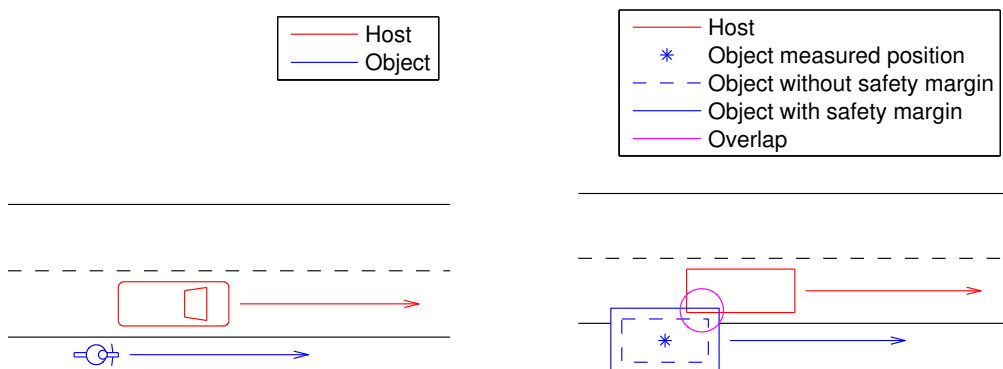
6

Proving ground results

This chapter presents results from when the path predictions and the threat assessment are evaluated on proving ground data. Some of the effects of measurement noise and measurement inaccuracies are highlighted.

6.1 Object size

As stated in Section 2.4, the radar setup reports a cyclist as a *medium*-size object. Hence, it is defaulted to the size of an average car. This is a limitation in the radar setup, which causes problems when performing calculations based on the proving ground data. As the Euro NCAP bicyclist and bike target used on the test track is only 0.5 meters wide [13], it can run at a lateral distance of 2 meters from the host vehicle without making contact, as illustrated in Figure 6.1a. This also implies that the measured position of the object can be very close to the host vehicle. However, when detected by the host vehicle, the size of the object is defaulted to the size of an average car. Hence, the situation is interpreted as illustrated in Figure 6.1b. This is a problem since the host vehicle and the object will seem to overlap/collide, although they do not make contact with each other in reality. This phenomenon causes strange and faulty outputs from the threat assessment.



(a) True size and shape of the host vehicle and the object. (b) Measured/assumed size and shape of the host vehicle and the object.

Figure 6.1: Size of the object in reality vs measured by the radar setup.

To avoid this problem, the size of the object must be changed. Instead of using the measurements reported by the sensor, the length and the width are altered to reflect the true size of the object. The length is set to 1.9 meters and the width to 0.5 meters, which are the measurements of the Euro NCAP bicyclist and bike target [13].

6.2 Object predictions

The accuracy of the proving ground data was evaluated in Section 2.4. Hence, this section will only present two examples based on proving ground data. One example of the effects of the measurement noise and one example of the problem of interpreting the lateral measurements. As can be seen in Section 2.4, the lateral acceleration was generally not measured to be zero, despite that the object traveled straight and parallel to the host vehicle. Figure 6.2 shows a snapshot from a test run based on proving ground data. The non-zero lateral acceleration results in a curved object prediction.

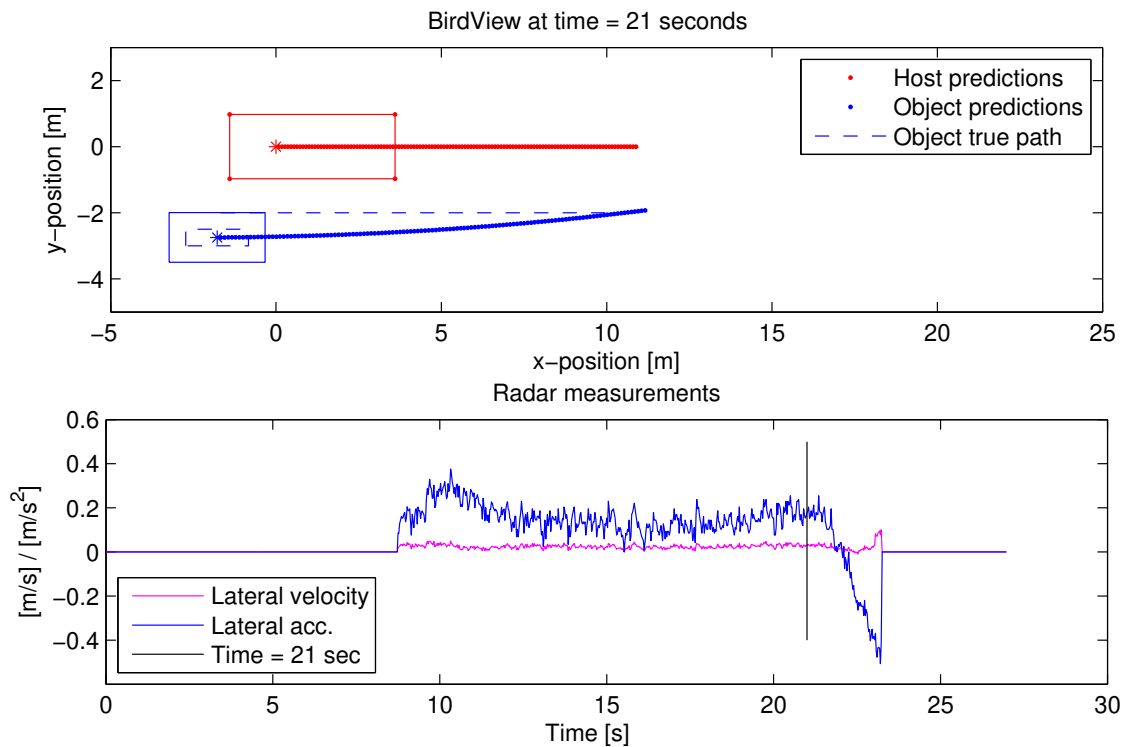


Figure 6.2: The influence of measurement noise on the object predictions.

Figure 6.3 shows an example of the problem discussed in Section 4.5.1. At around 21 seconds in to this scenario, the host vehicle starts turning, which results in the measured lateral acceleration shown in the bottom graph. This lateral acceleration affects the object predictions, making them bend away from the host vehicle. This behaviour is consistent with what can be seen in the simulation data. However, it seems to affect the object predictions mainly through lateral acceleration in the prov-

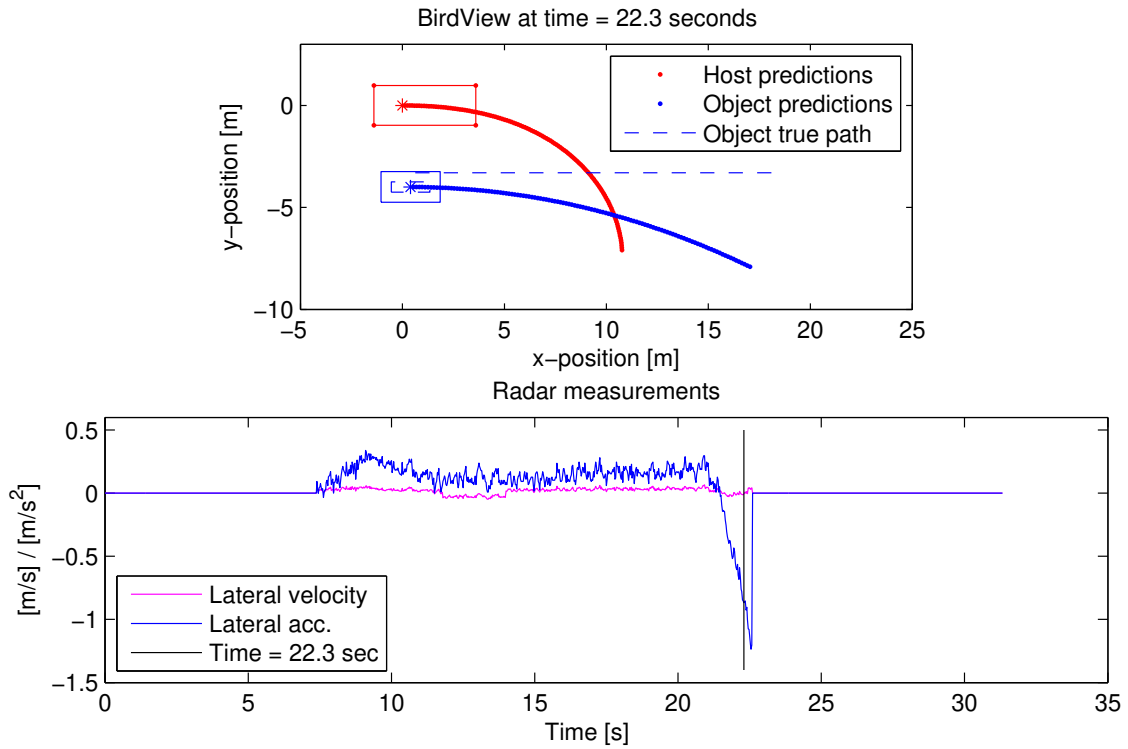


Figure 6.3: The measured lateral acceleration of an object travelling straight is non-zero due to the curved path of the host vehicle.

ing ground data. This results in an overestimation of the TTI, as the host vehicle's and the object's paths appear to intersect later than they actually would.

6.3 Threat assessment

The predicted TTI for a test run based on proving ground data is shown in Figure 6.4. In this run, the curve radius is 6 meters, the host vehicle travels at 13 kph, the object travels at 16 kph and the lateral distance between them is 3.3 meters. The run starts with that both the host vehicle and the object are travelling straight and parallel to each other. Around 5-10 seconds into the test, the host vehicle makes some adjustments to ensure that the lateral distance is correct. At about 22.5 seconds the host vehicle starts turning, which results in an intersection between the predicted paths, with the TTI decreasing until the object leaves the radar's FOV. The magenta colored line indicates the point where the test run was terminated by braking to avoid a collision with the object. This was performed solely to spare the test vehicle and the test object from damage. The green line is an approximation of the time at which the collision would have occurred, if the test was not terminated early. This time can not be measured, as the test was terminated before this time. The value was instead approximated using simulation data. However, this line indicates the point at which the TTI should reach zero.

The problem of interpreting the lateral measurements discussed in Section 4.5.1 and Figure 6.2 does exist in the proving ground data as well. When the object predictions are studied, it can be seen that the TTI is generally overestimated due to inaccurate object predictions. It is not as clearly visible in the TTI graphs made from proving ground data, as it is in the TTI graphs made from simulation data. However, the problem is present. By examining the TTI graph, it can be noticed that the decreasing value would probably not reach zero by the approximated collision time. The small bump in the TTI that occurs around 8 seconds into the simulation is a result of the position adjustment that the host vehicle does at the same time. TTI graphs from additional test cases can be viewed in Appendix E.

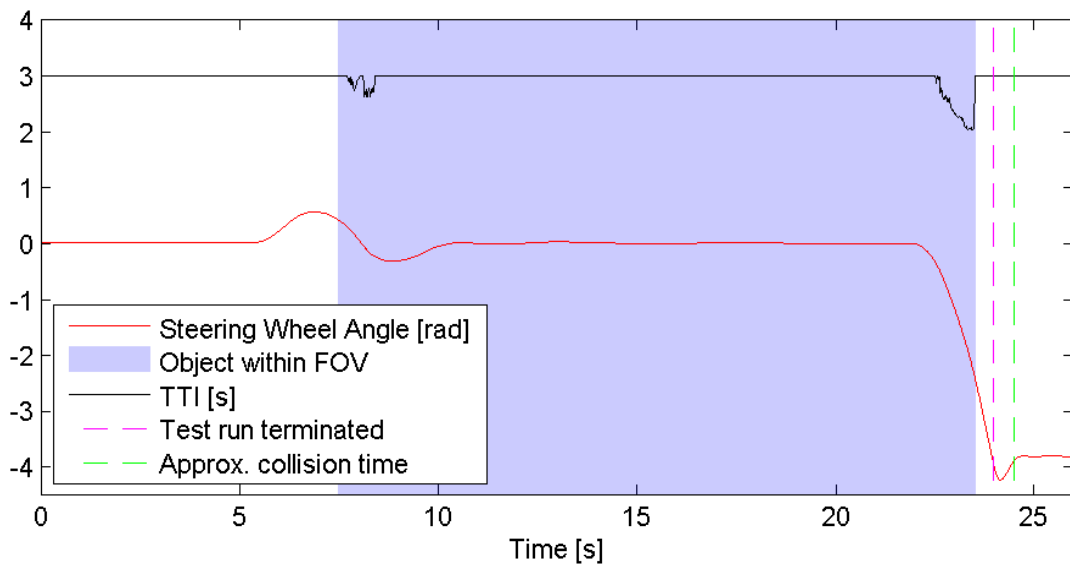


Figure 6.4: Predicted TTI in a scenario based on proving ground data.

The threat assessment outputs from the same test run are shown in Figure 6.5 and 6.6. The values of braking or acceleration required to avoid a collision gives a clear indication that a collision is imminent around 23-24 seconds into the run. This seems correct, given the approximated collision time. The required braking reaches about -2 m/s^2 , while the required acceleration reaches about $+6.7 \text{ m/s}^2$. The magnitude of these values are reasonable given the low velocity of the host vehicle, 13 kph, and the time that is left to the collision, 1-2 seconds. However, the overestimation of the TTI affects these values, which results in a moderate underestimation of the braking/acceleration required to avoid a collision.

The values of the steering required to avoid the collision are less intuitive. The curvature required to pass to the left of the object, has a small indication around 23-24 seconds. This is consistent with the indications of the required braking and acceleration signals, as expected. The values show that it is generally easier to avoid the object by passing on the left side, which is expected since the object travels to the right of the host vehicle. The curvature required to pass to the right of the object is difficult to interpret. The indications start around 17 seconds, which is the point where the predictions start to indicate that the host vehicle and the object

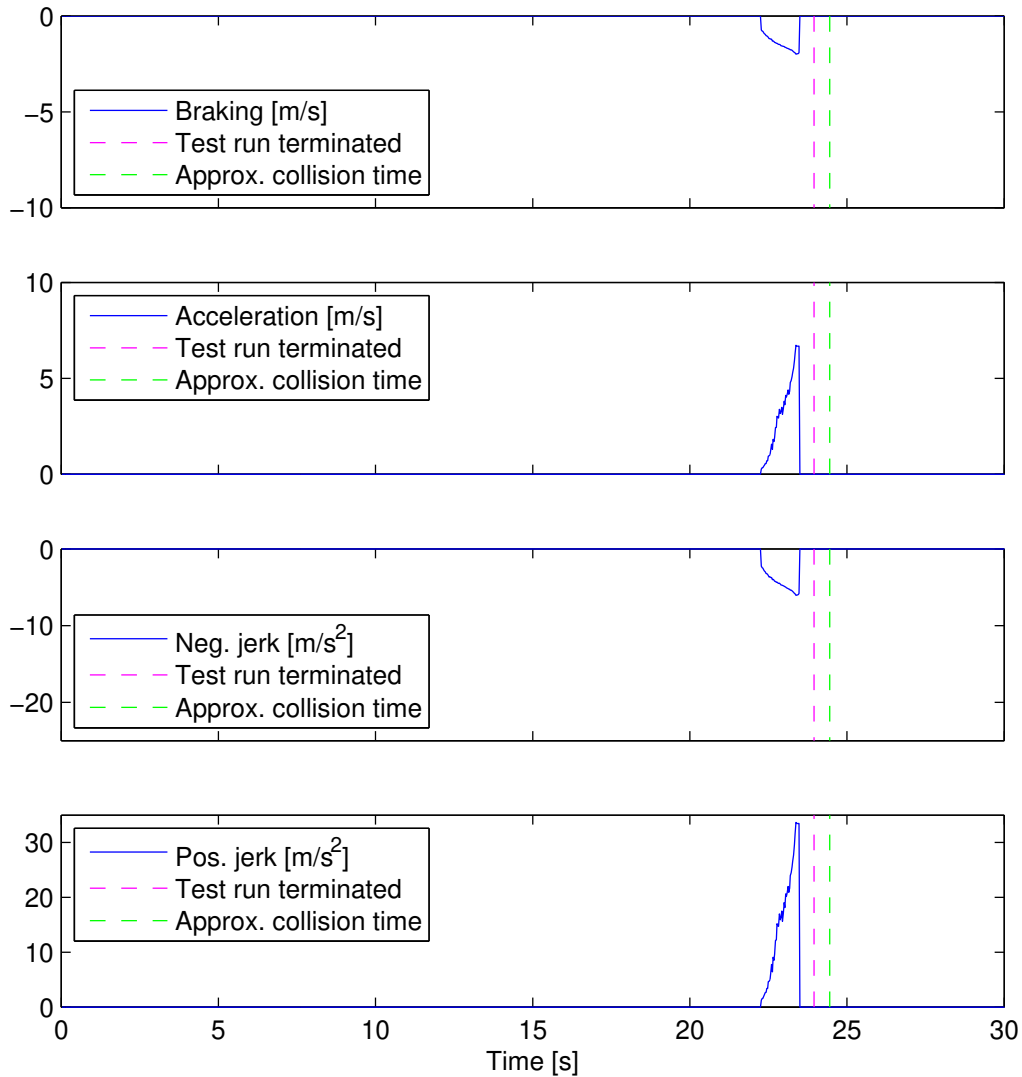


Figure 6.5: The required braking/acceleration to avoid all edges of the object at each sample of a collision case based on proving ground data.

will be side by side. This phenomenon was explained in Section 5.4. The difference is that these object predictions are made from non-ideal measurements, causing the fluctuations. At 23-24 seconds, the signal decreases as a result of the imminent collision. This is expected as the collision becomes more difficult to avoid as the object gets closer. The values, both in left- and right direction, are affected by the overestimation of TTI, just as the braking/acceleration required to avoid a collision. This causes a moderate underestimation of the steering required to avoid a collision. Threat assessment outputs from additional scenarios can be viewed in Appendix F and G.

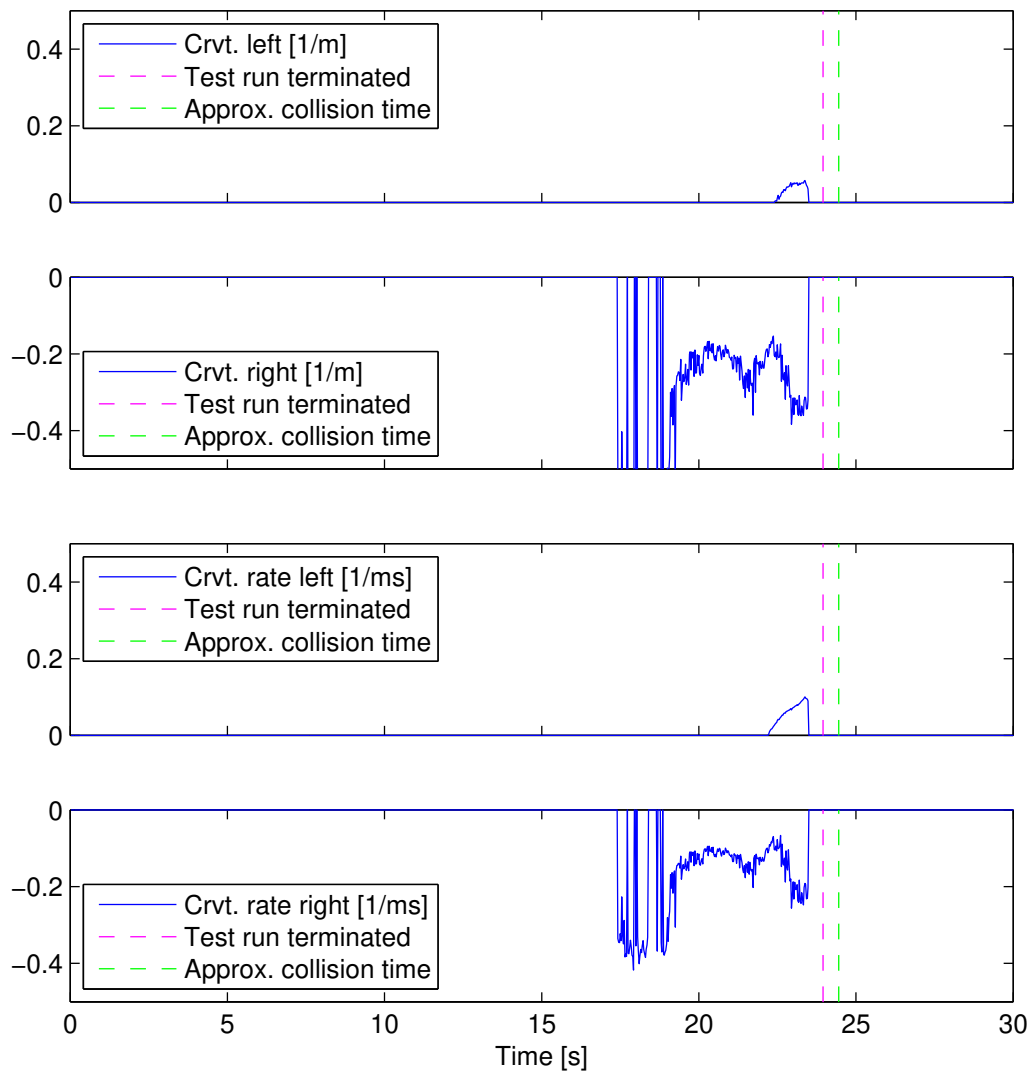


Figure 6.6: The required steering to avoid all edges of the object at each sample of a collision case based on proving ground data.

7

Discussion

Results from previous chapters constitutes a basis for answering how applicable the function concept could be. This chapter discusses the outcome of the evaluation and the difficulties of the execution.

7.1 Findings and implementation

The results presented in this thesis indicates that the function concept may be a suitable way to find and avoid collisions with cyclists in the scenario of interest. The concept clearly indicates when a collision is imminent, as seen by the substantial changes in the TTI and threat assessment output graphs in Section 5.4 and Chapter 6. The TTI graphs shows that the concept finds the time period, during which the paths of the host vehicle and the object are intersecting. Based on this information, the concept provides values of steering, acceleration and braking required to avoid the collision. These values gives an indication of how difficult the collision is to avoid, and also indicates whether steering, braking or accelerating is the easiest way to avoid it. Two major improvements are required on the function concept: find a solution on selecting the object size and to improve the accuracy of the threat assessment outputs.

As explained in Section 2.4, the current radar setup does not provide an accurate size estimate for the object, which results in the problems described in Section 6.1. To utilize the function concept, it is essential that the size of the object can be determined accurately. If not, the threat assessment may interpret that the host vehicle and the object overlaps in situations where they do not. The signals used in the radar setup to produce rear object size, i.e., length and width, are only accessible to the supplier of the radar setup. This makes it hard to determine whether the current radar sensor could provide better estimates of size with different software or not. If these signals were accessible, an easy way to solve the problem might be to change the software to classify objects into additional categories based on size. Otherwise, the problem would have to be solved by either altering the hardware, i.e., different sensors, or by changing the software, i.e., interpreting signals differently. Hardware alterations could be to change to more accurate or different sensors. Software changes could include classifying objects based on other properties,

e.g., their velocity, or performing sensor fusion with other already existing sensors. These could be, e.g., the parking camera or ultrasonic proximity sensors. Using sensor fusion to merge the rear radar sensors with the parking camera and/or the ultrasonic sensors, could possibly be enough to gain a basic ability to classify objects. The problem with using the parking camera and ultrasonic sensors, currently in the host vehicle, is that they are configured for close range applications. This makes it hard to detect and classify approaching objects, until they are very close to the host vehicle.

The accuracy of the threat assessment outputs are affected by the deficiency in the object predictions. The geometry of the scenario generates measurements of lateral velocity/acceleration of the object away from the host vehicle as it turns, as shown in Sections 4.5.1 and 6.2. This results in object predictions which are projected away from the host vehicle, although the host vehicle and the object are actually getting closer to each other. This could possibly be solved by altering the placement of the radar sensor. A different approach to solve the same problem could be to change the software, by interpreting the measurements differently. As the problem occurs while the host vehicle is turning, it may be possible to use the steering wheel angle to compensate for the geometry of the scenario. Another possible performance gain derived from altering the placement of the radar sensor could be a solution to the problem mentioned in Section 4.5.1. That is, the host vehicle can be quite far into the curve without decreasing the measured lateral distance to the object. This is because the radar sensor is located in the rear bumper of the host vehicle, which does not move much laterally during the moments leading up to the collision. A placement of the radar sensor longitudinally moved forwards on the host vehicle could decrease this measurement error, since the front of the host vehicle will have lateral movement earlier. One thing to take into consideration with a placement of the sensor longitudinally moved forwards, would be that objects travelling behind the host vehicle could be harder to detect. Hence, the solution could rather be to increase the number of sensors to be able to cover both aspects.

To further improve the performance of the concept, it would be of interest to ensure that objects cannot end up outside the radar's FOV at critical moments. With the current setup, the object may disappear outside the FOV of the sensor before the host vehicle starts turning, but still be close enough to collide with the host vehicle as it turns. There are mainly two possible solutions to this insufficiency. The first option is to increase the radar's FOV by changing to a different sensor, or adding more sensors. The second option is to experiment with artificially increasing the sensors FOV, by adding memory to the function and enable remembering of objects for a certain time after they have disappeared. However, this introduces uncertainty, as the function would have to make assumptions on the object's behaviour during the time that the object is kept in memory.

7.2 Difficulties of execution

Several aspects complicated the gathering of both the simulation data and the proving ground data during the course of the thesis work. Getting the scenarios to work in the simulation environment involved sorting out several bugs that were discovered. The reason being that the environment had not been used to simulate this kind of scenarios before, i.e., the bugs were present earlier but not affecting scenarios most commonly run in other tests. For the proving ground data, most issues relates to preparing the test vehicle and making sure that all relevant signals were available for logging. For the proving ground tests to be useful, the scenarios also had to be modified as mentioned in Section 2.3. On top of this, the current coronavirus pandemic greatly postponed the testing at the proving ground.

8

Conclusions and Future work

This chapter concludes the final outcome of the thesis and proposes possible directions for future work/research.

8.1 Conclusions

This thesis investigated a proof of concept for a collision avoidance function. The function concept consists of several parts, including path prediction of both the host vehicle and the object, TTI calculations and threat assessment. All parts were evaluated separately on both simulated data and on proving ground data. The data sets were designed based on a scenario specification given by VCC, where the simulated data was created in a simulation environment, and the proving ground data was collected in a test vehicle. Altogether, the function concept shows positive indications of identifying collision situations with cyclists in scenarios of the type described in Section 1.2. Furthermore, the function concept outputs sensible values of steering and/or braking/acceleration required in order to avoid the imminent collision.

Two major findings affecting the performance of the function concept have been identified during the course of the thesis. First, the performance of the TTI calculations correlates strongly with the performance of the object predictions. The object's position is measured relative to the placement of the radar sensor on the host vehicle, with the sensor being located in the rear bumper. This location works fine when the host vehicle and the object travel parallel to each other. However, when the host vehicle starts turning, the movement of the host vehicle generates measurements of lateral velocity/acceleration of the object, away from the host vehicle. This affects the object prediction such that it appears to diverge from the host vehicle, when they actually are approaching each other. In turn, this affects the calculated TTI such that it levels out close to the intersection point, instead of approaching zero. Second, the host vehicle could possibly start to turn with the object being outside the radar sensor's FOV, while the position of the object still entails a collision with the host vehicle. In this case, a collision will take place, since no path prediction can be performed on the object.

8.2 Future work

Apart from previously mentioned suggestions on how to solve several shortcomings of the current function concept, two more possible directions for future work are discussed in this section. First, this function concept was only tested with one object. It is reasonable to assume that there could be several objects, travelling close to each other. In that case, a method must exist for prioritizing the objects. This could be to perform threat assessment on all objects, selecting the object with the highest values of steering, acceleration or braking required to avoid a collision, as a primary object. The object could also be prioritized based on velocity or a combination of measurable parameters. This would have to be further investigated, in order to determine which alternative provides the best result. Second, the threat assessment calculations of braking/acceleration required to avoid a collision is now calculated for the entire prediction horizon. However, the steering required to avoid a collision is only calculated at ten time instances around the predicted TTI. A decrease in computational complexity could possibly be achieved if the same approach would be applied to the calculation of braking/acceleration required. Further research is required to determine if this approach also increases negative performance. When implementing the decision making part of the function concept, the estimation of the critical time could benefit from incorporating factors such as tire to road friction, driver behaviour and current curvature of the host vehicle.

Bibliography

- [1] World Health Organization, *Global status report on road safety*, 2018.
- [2] J. Jansson, *Collision Avoidance Theory with Application to Automotive Collision Mitigation*, 2005.
- [3] National Highway Traffic Safety Administration (NHTSA), Critical Reasons for Crashes Investigated in the National Motor Vehicle Crash Causation Survey, A Brief Statistical Summary February 2015.
- [4] European Commission, *Intelligent transport systems*. Accessed on: Feb. 13, 2020. Available: https://ec.europa.eu/transport/themes/its/road_en
- [5] V. L. Neale, T. A. Dingus, S. G. Klauer, J. Sudweeks, M. Goodman, *An overview of the 100-car naturalistic study and findings*, 2005.
- [6] European Automobile Manufacturers Association, *Active safety systems: what are they and how do they work?*. Accessed on: Feb. 13, 2020. Available: <https://roadsafetyfacts.eu/active-safety-systems-what-are-they-and-how-do-they-work/>
- [7] Euro NCAP, *AEB Pedestrian*. Accessed on: Feb. 13, 2020. Available: <https://www.euroncap.com/en/vehicle-safety/the-ratings-explained/vulnerable-road-user-vru-protection/aeb-pedestrian/>
- [8] J. Hillenbrand, A. M. Spieker, K. Kroschel *A Multilevel Collision Mitigation Approach—Its Situation Assessment, Decision Making, and Performance Trade-offs*, 2006.
- [9] M. Brännström, E. Coelingh, J. Sjöberg, *Model-Based Threat Assessment for Avoiding Arbitrary Vehicle Collisions*, 2010.
- [10] National Association of City Transportation Officials, *Urban Street Design Guide*, 2013.
- [11] T.D. Gillespie, *Fundamentals of Vehicle Dynamics*, Warrendale, PA, SAE, 1992.

- [12] R. Johansson, L. Linderholm, J. Moberg, *Vägar och gators utformning, Stöd-
jande kunskap - Linjeföring - Övergångskurvor*, Borlänge, Sweden, Swedish
Transport Administration, Publ. 2016:083, 2016.

- [13] Euro NCAP, *Test Protocol - AEB VRU systems v.3.0.3*, June, 2020.

A

Detection accuracy in proving ground data

Section 2.4 of the report discusses the detection and positioning accuracy of the radar sensors. That section presents an example of how the position, velocity and acceleration of the object is measured by the sensors on the host vehicle. The measurements are compared to the true values which are collected by the robot-setup used on the proving ground and described in Section 2.3. This appendix provides additional figures showing the same quantities but for 7 additional test scenarios. The parameters used in each scenario are listed in the caption of each figure.

A. Detection accuracy in proving ground data

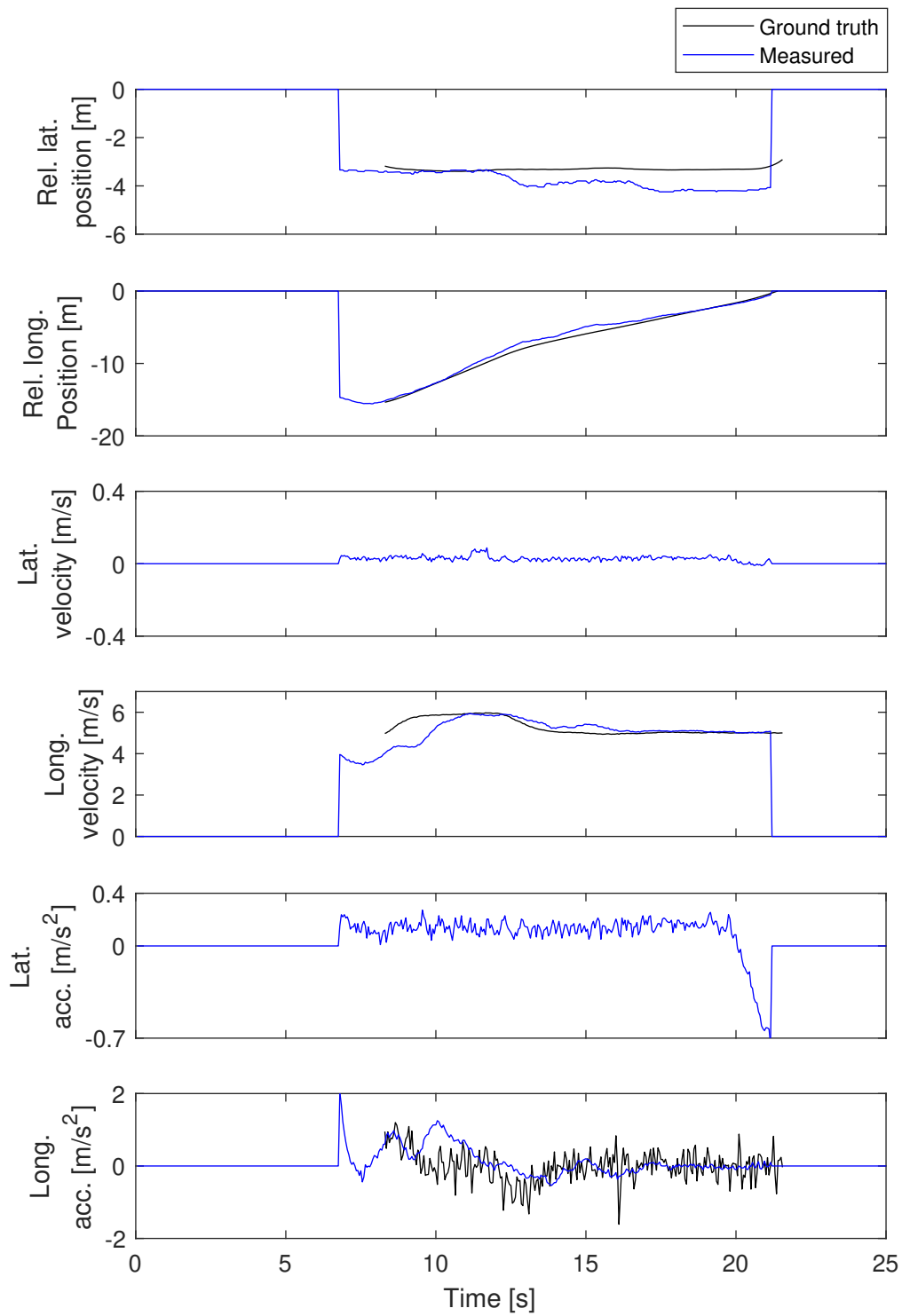


Figure A.1: Curve radius 9 m, host vehicle velocity 15 kph, object velocity 18 kph, lateral distance 3.3 m.

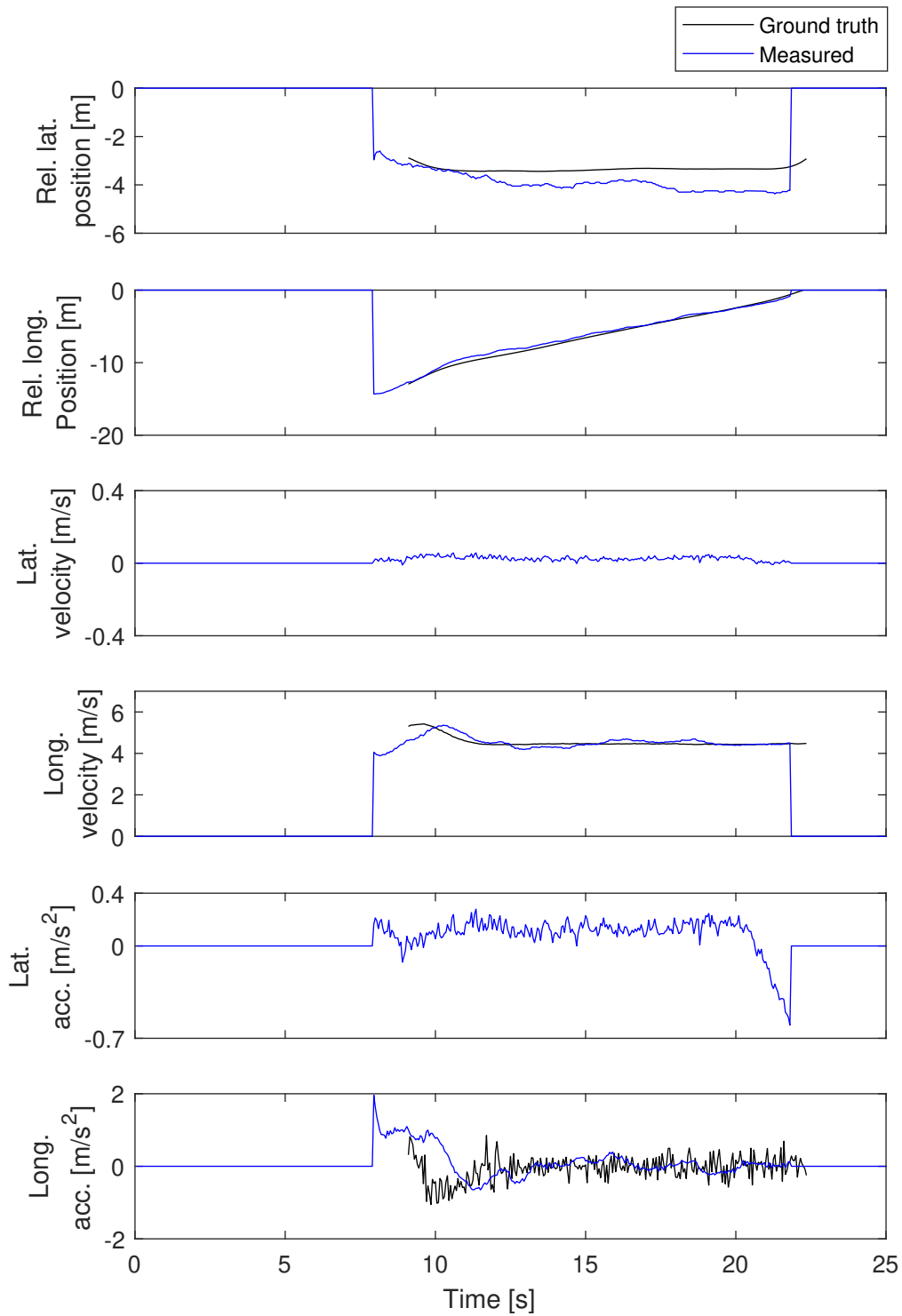


Figure A.2: Curve radius 9 m, host vehicle velocity 13 kph, object velocity 16 kph, lateral distance 3.3 m.

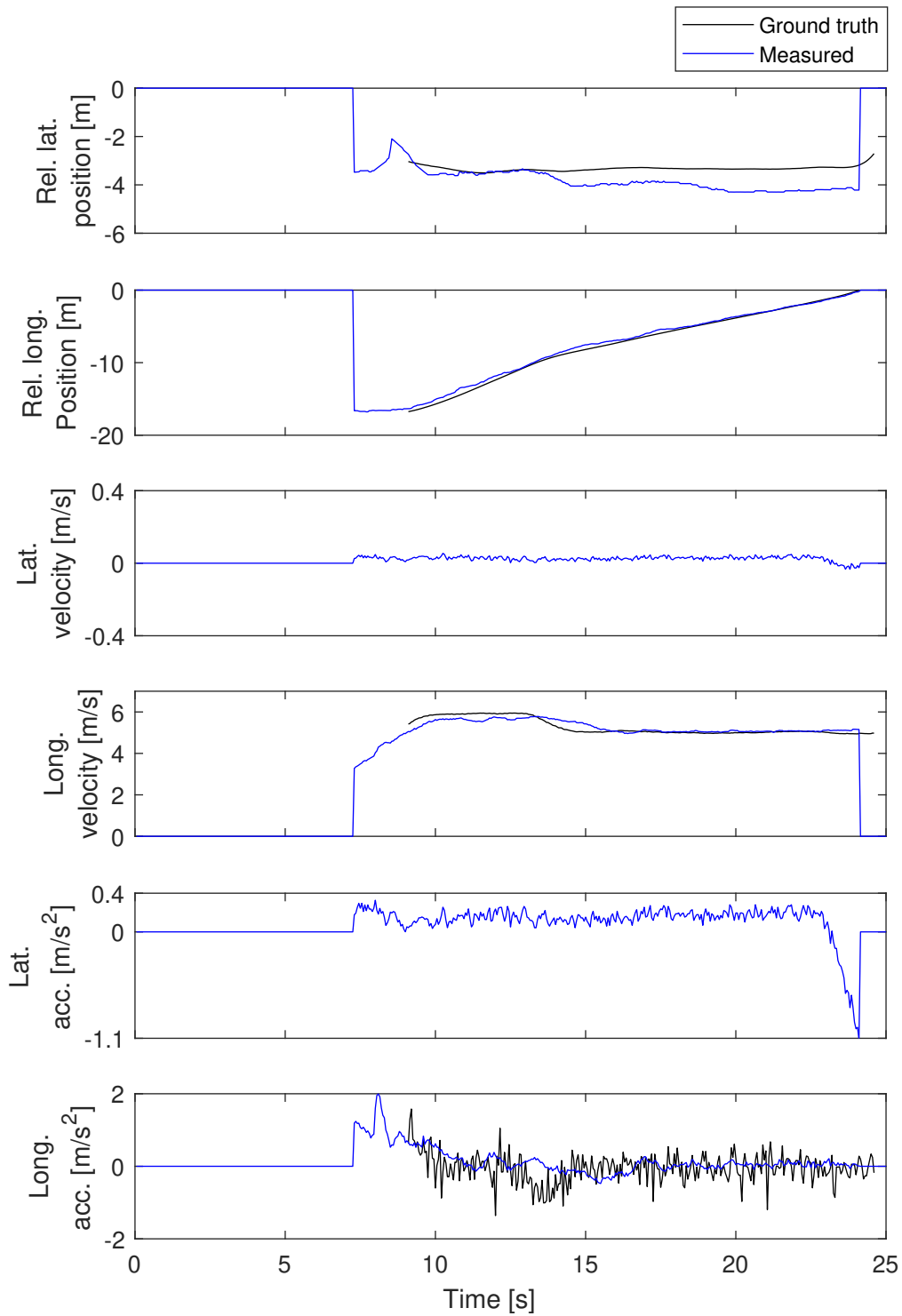


Figure A.3: Curve radius 6 m, host vehicle velocity 15 kph, object velocity 18 kph, lateral distance 3.3 m.

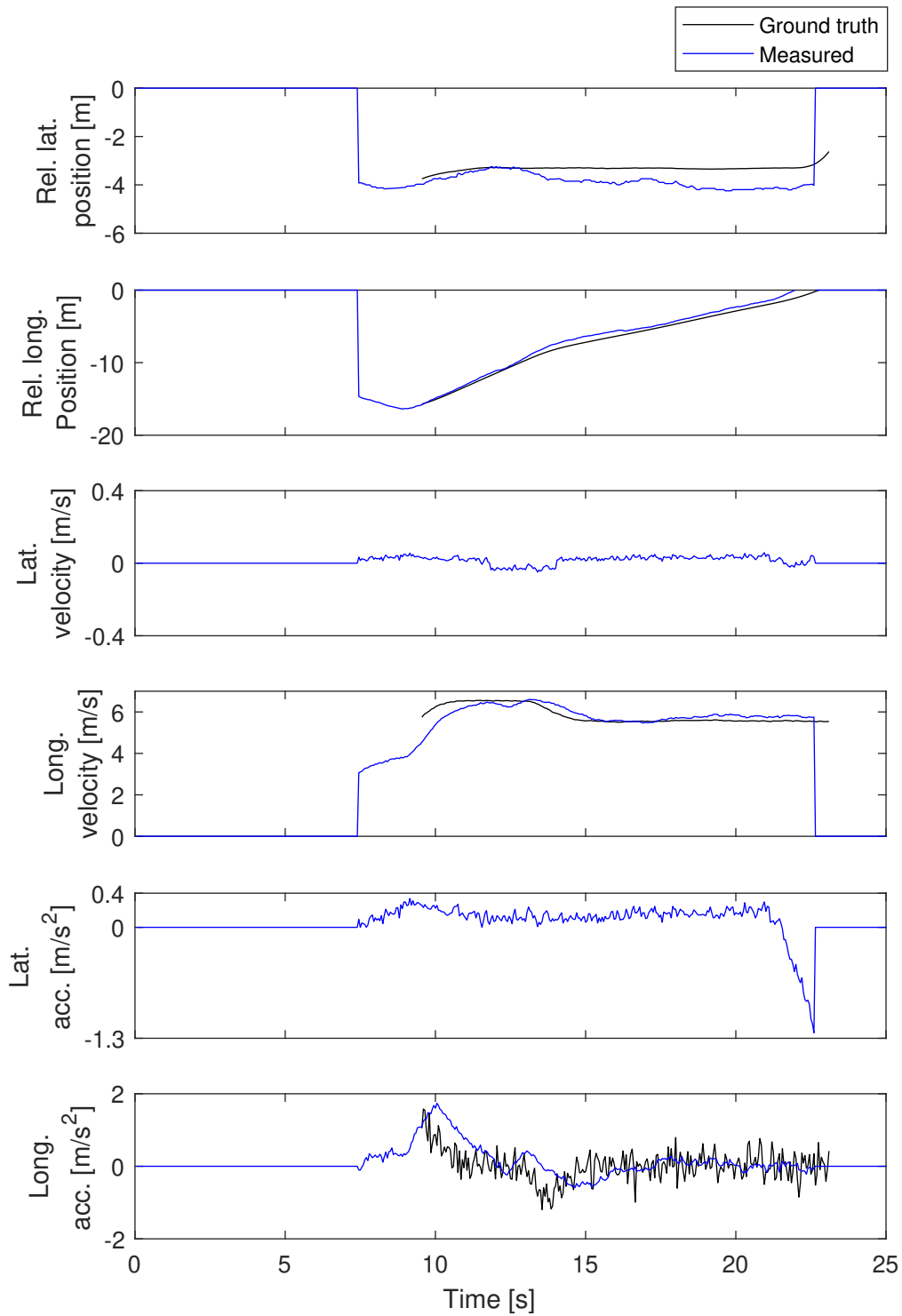


Figure A.4: Curve radius 9 m, host vehicle velocity 17 kph, object velocity 20 kph, lateral distance 3.3 m.

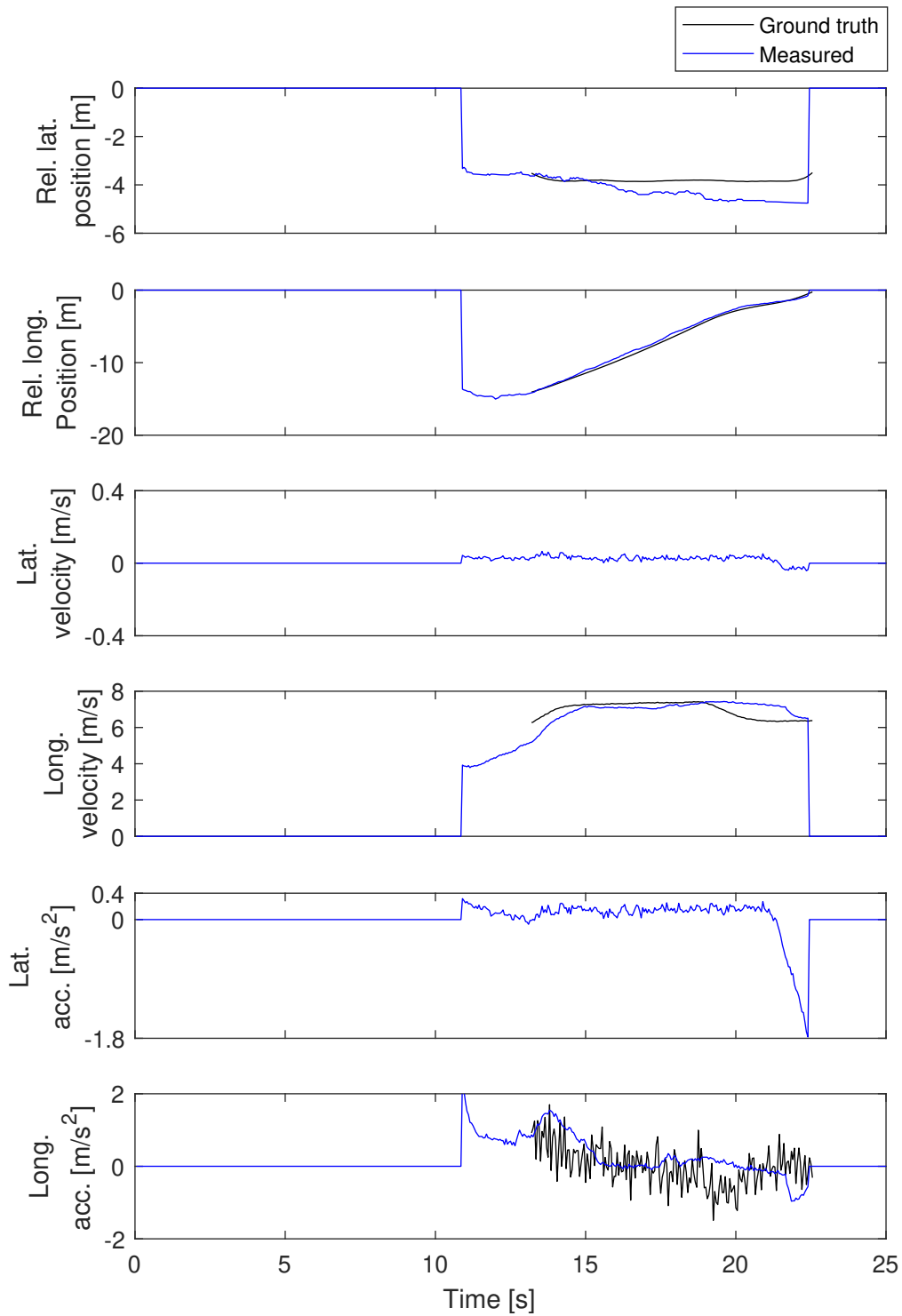


Figure A.5: Curve radius 9 m, host vehicle velocity 20 kph, object velocity 23 kph, lateral distance 3.8 m.

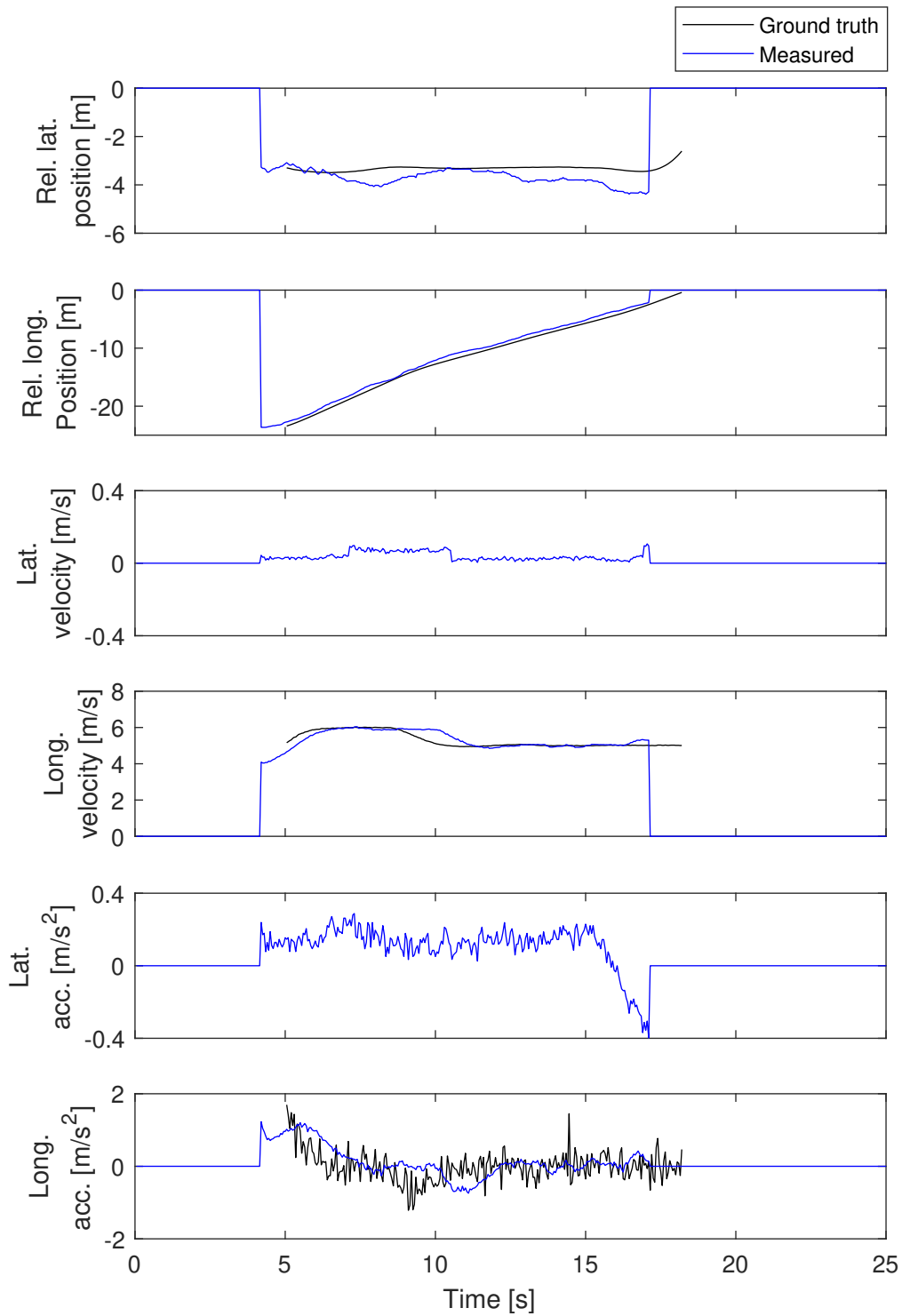


Figure A.6: Curve radius 12 m, host vehicle velocity 13 kph, object velocity 18 kph, lateral distance 3.3 m.

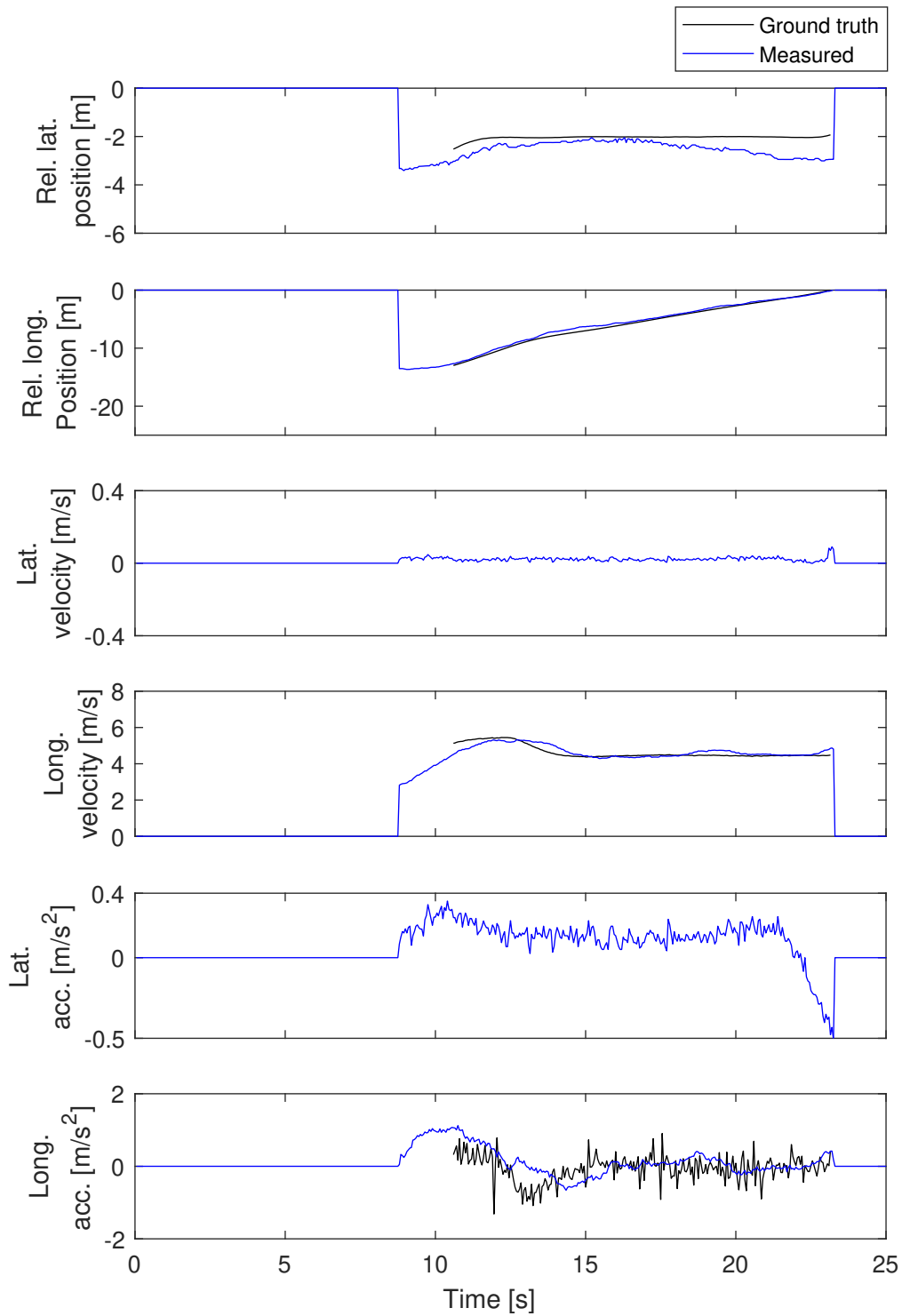


Figure A.7: Curve radius 9 m, host vehicle velocity 13 kph, object velocity 16 kph, lateral distance 2.0 m.

B

Predicted TTI, simulation results

Section 4.5.4 presents the predicted TTI between the host vehicle and the object in a test scenario based on simulation data. This appendix provides additional graphs of the same kind for different scenarios. The parameters used in each scenario are listed in the caption of each figure. Note that the object generally disappears outside the radar's FOV shortly before the collision occurs. This is why the TTI is generally predicted to the default, 3 seconds, at the time of the collision.

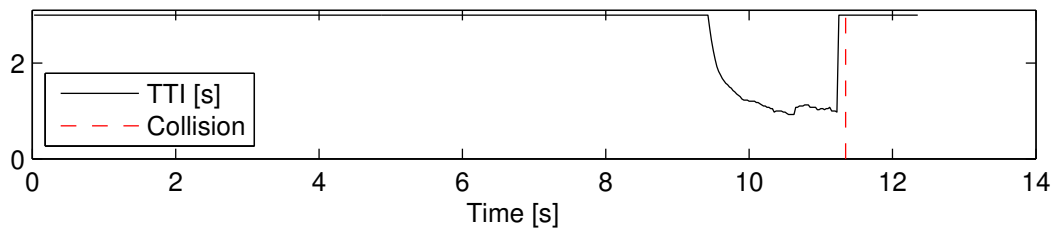


Figure B.1: Curve radius 6 m, host vehicle velocity 10 kph, object velocity 18 kph, lateral distance 2.3 m.

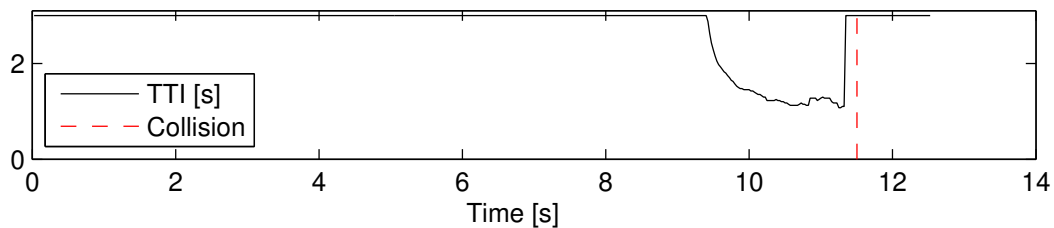


Figure B.2: Curve radius 6 m, host vehicle velocity 10 kph, object velocity 18 kph, lateral distance 2.8 m.

B. Predicted TTI, simulation results

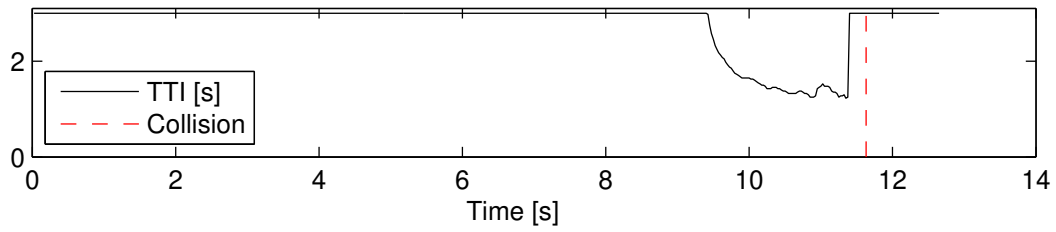


Figure B.3: Curve radius 6 m, host vehicle velocity 10 kph, object velocity 18 kph, lateral distance 3.3 m.

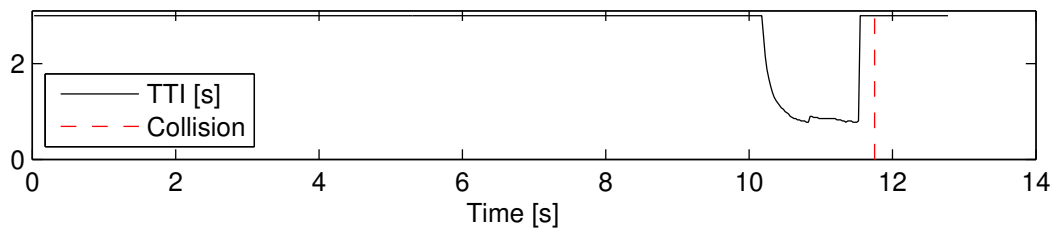


Figure B.4: Curve radius 9 m, host vehicle velocity 15 kph, object velocity 23 kph, lateral distance 1.8 m.

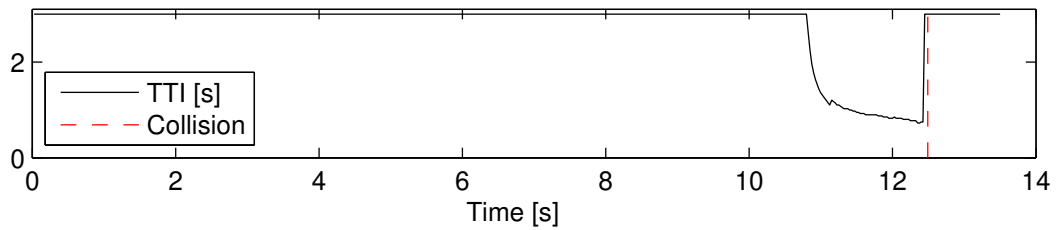


Figure B.5: Curve radius 9 m, host vehicle velocity 15 kph, object velocity 18 kph, lateral distance 2.3 m.

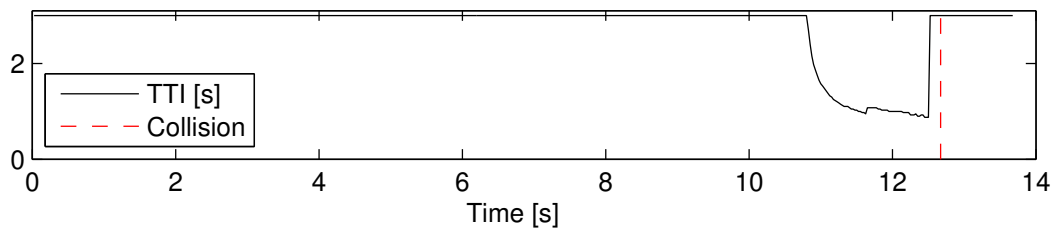


Figure B.6: Curve radius 9 m, host vehicle velocity 15 kph, object velocity 18 kph, lateral distance 2.8 m.

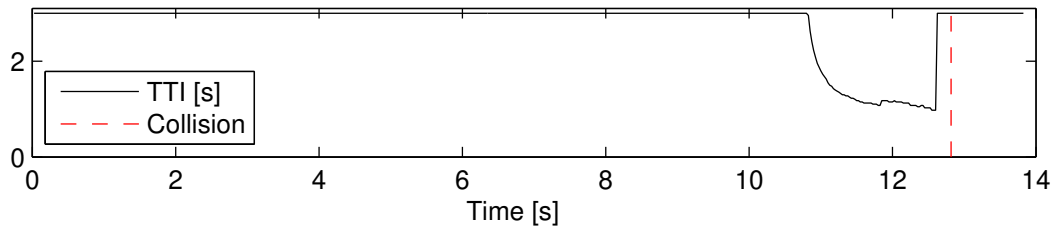


Figure B.7: Curve radius 9 m, host vehicle velocity 15 kph, object velocity 18 kph, lateral distance 3.3 m.

The phenomenon seen in Figure B.8 and B.9, where the graph changes drastically after the time of collision can be ignored. This is a result of the properties of the simulation data. In the simulation environment it is possible for the host vehicle and the object to continue along their paths despite that a collision have occurred. Hence, strange values may occur as the bounding boxes overlap etc.

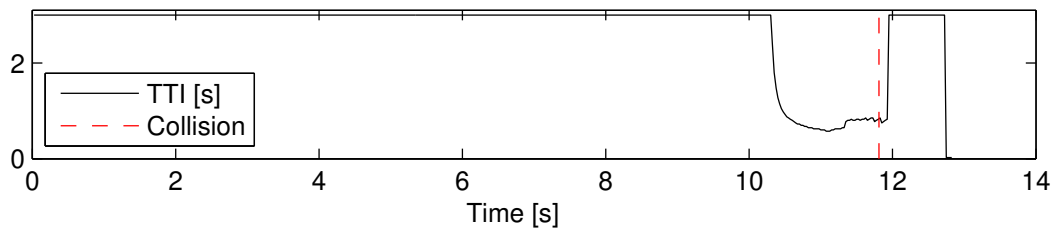


Figure B.8: Curve radius 12 m, host vehicle velocity 25 kph, object velocity 23 kph, lateral distance 2.8 m.

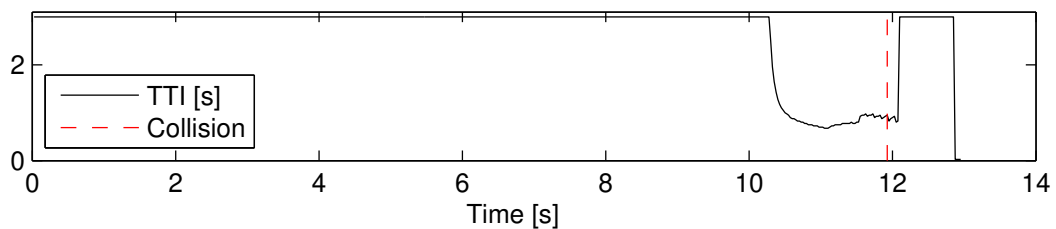


Figure B.9: Curve radius 12 m, host vehicle velocity 25 kph, object velocity 23 kph, lateral distance 3.3 m.

C

Required braking/acceleration, simulation results

Section 5.4 of the report presents the required braking/acceleration to avoid the collision in a test based on simulation data. The value at each time instant is the maximal braking/acceleration required to avoid all edges of the object throughout the entire prediction horizon. This appendix provides similar graphs from additional test cases. The parameters used in each scenario are listed in the caption of each figure. Note that the object generally disappears outside the radar's FOV shortly before the collision occurs. This is why the required braking and acceleration drops to zero before the time of collision.

The phenomenon seen in Figure C.8 and C.9, where the graph changes drastically after the time of collision can be ignored. This is a result of the properties of the simulation data. In the simulation environment it is possible for the host vehicle and the object to continue along their paths despite that a collision have occurred. Hence, strange values may occur as the bounding boxes overlap etc.

C. Required braking/acceleration, simulation results

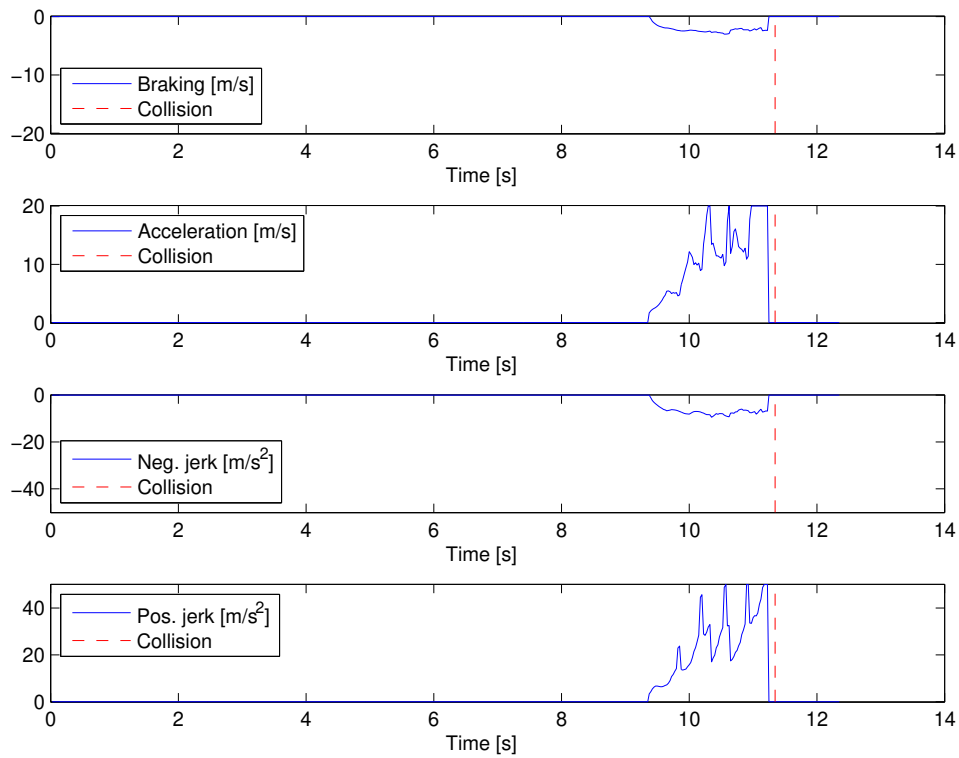


Figure C.1: Curve radius 6 m, host vehicle velocity 10 kph, object velocity 18 kph, lateral distance 2.3 m.

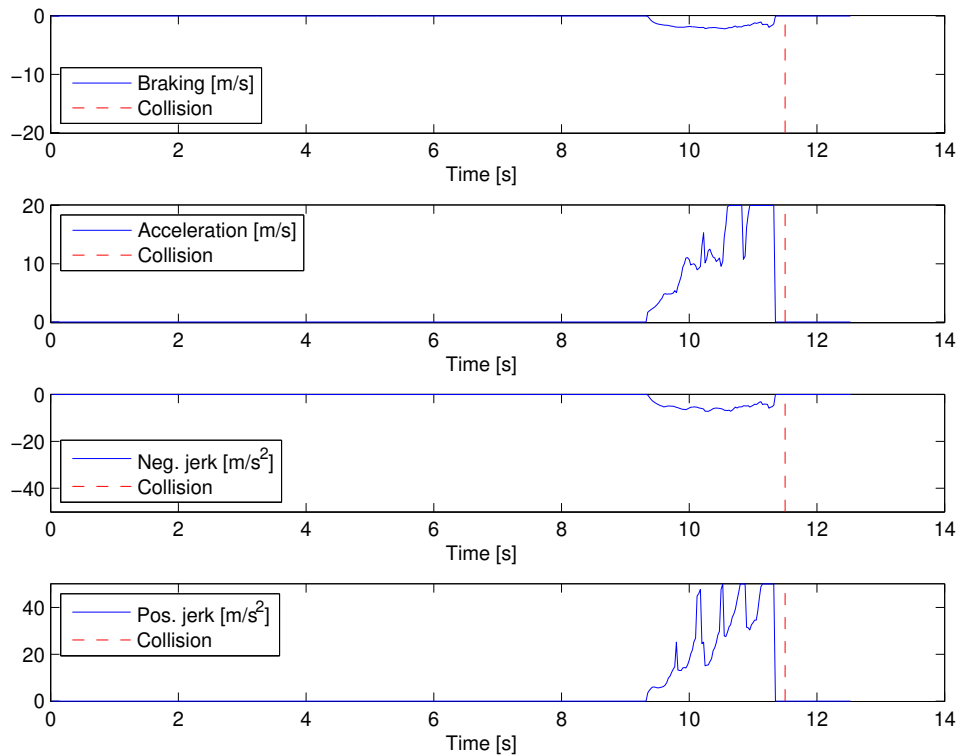


Figure C.2: Curve radius 6 m, host vehicle velocity 10 kph, object velocity 18 kph, lateral distance 2.8 m.

C. Required braking/acceleration, simulation results

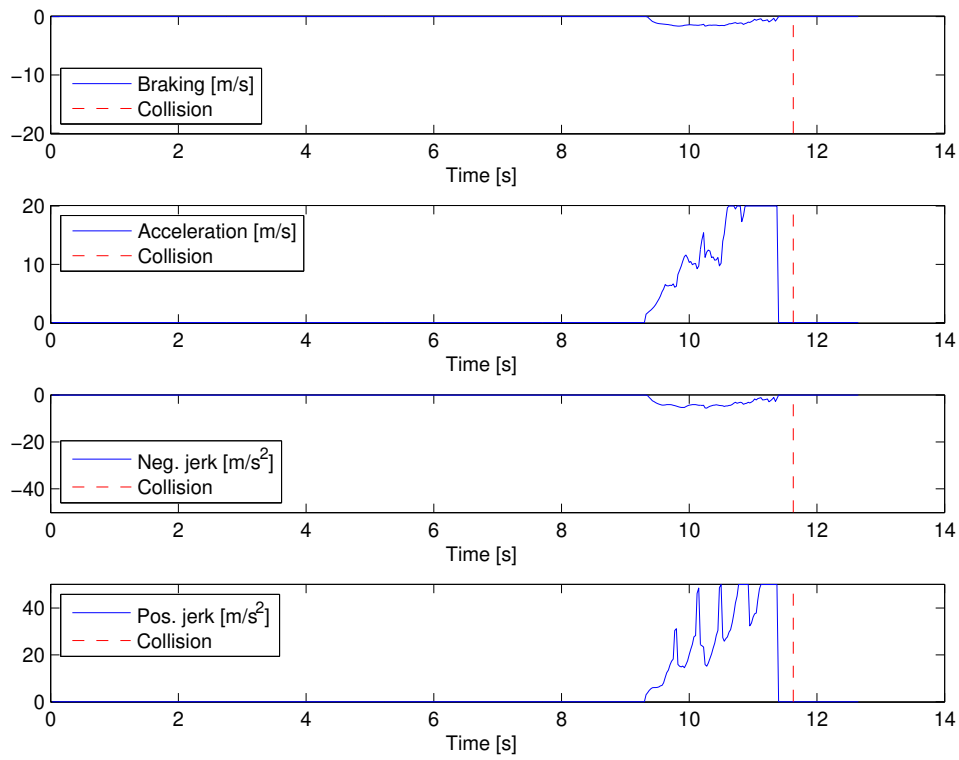


Figure C.3: Curve radius 6 m, host vehicle velocity 10 kph, object velocity 18 kph, lateral distance 3.3 m.

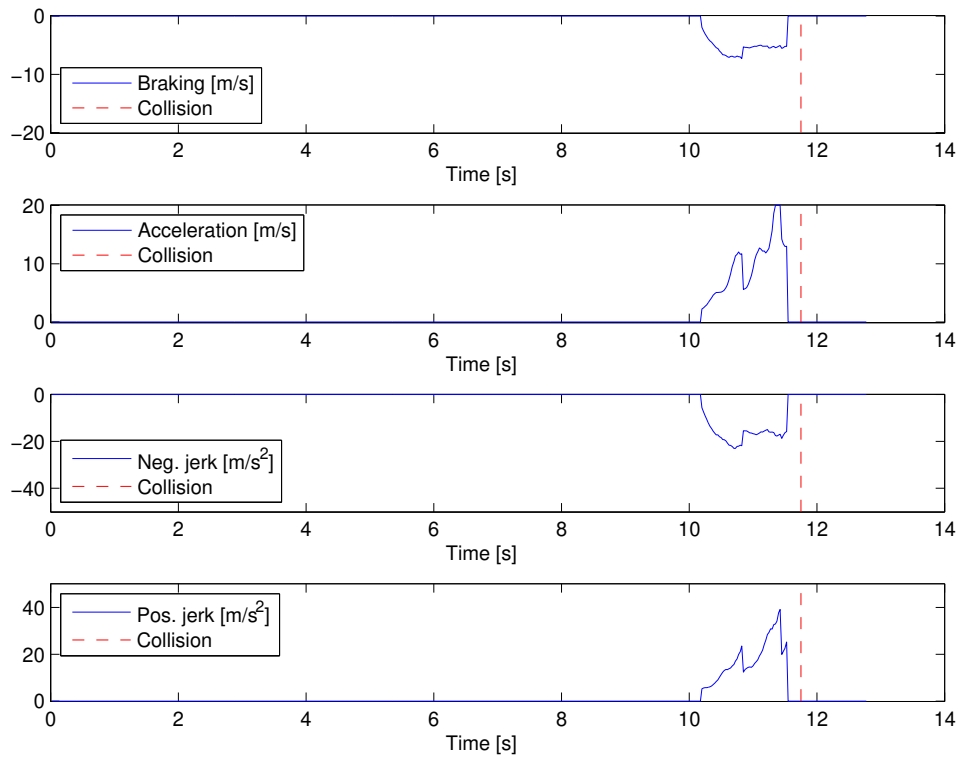


Figure C.4: Curve radius 9 m, host vehicle velocity 15 kph, object velocity 23 kph, lateral distance 1.8 m.

C. Required braking/acceleration, simulation results

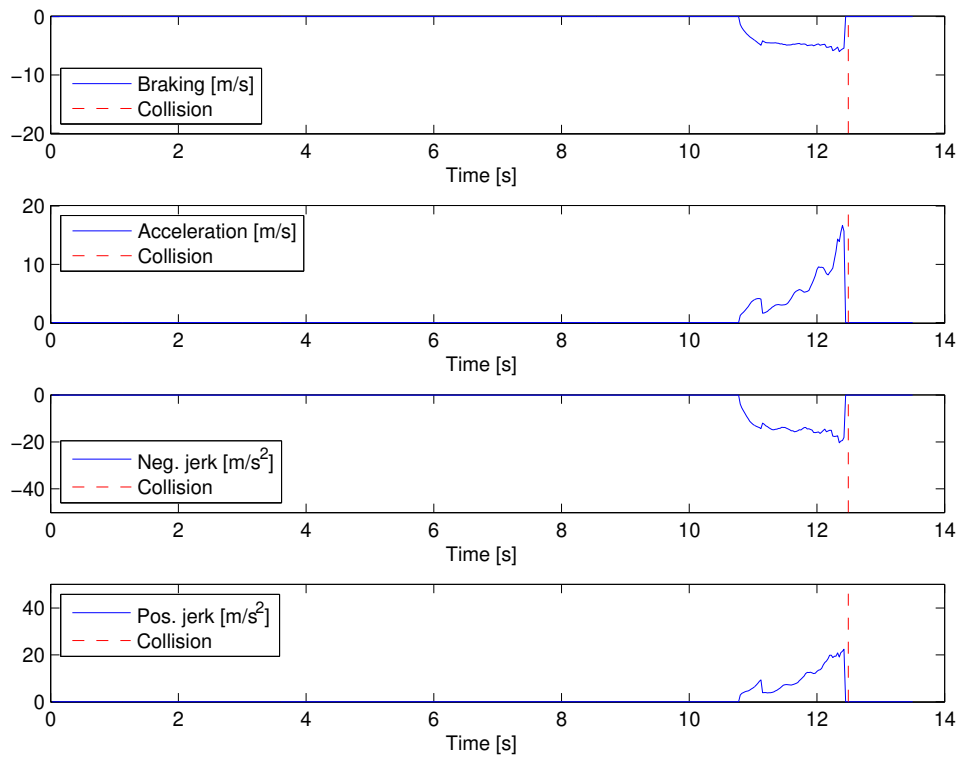


Figure C.5: Curve radius 9 m, host vehicle velocity 15 kph, object velocity 18 kph, lateral distance 2.3 m.

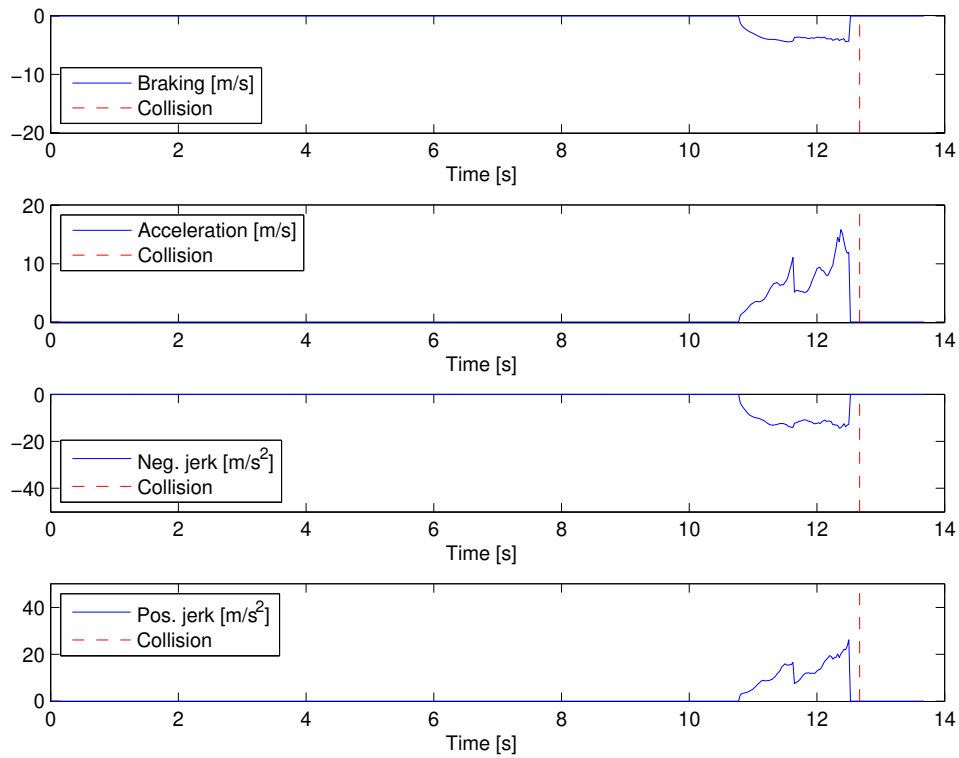


Figure C.6: Curve radius 9 m, host vehicle velocity 15 kph, object velocity 18 kph, lateral distance 2.8 m.

C. Required braking/acceleration, simulation results

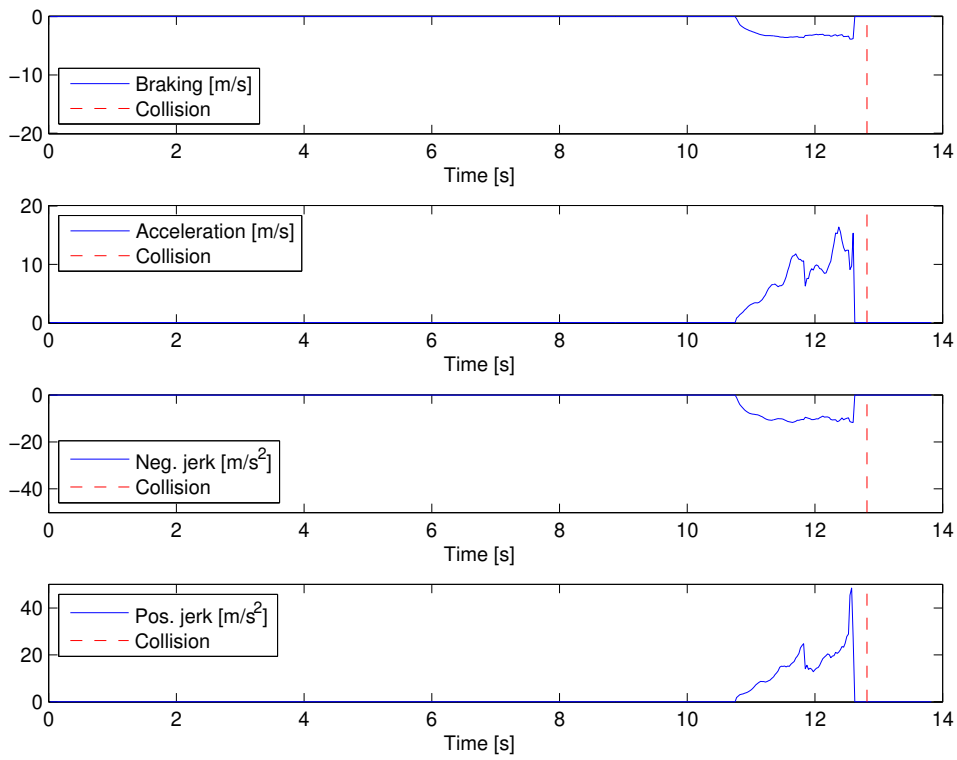


Figure C.7: Curve radius 9 m, host vehicle velocity 15 kph, object velocity 18 kph, lateral distance 3.3 m.

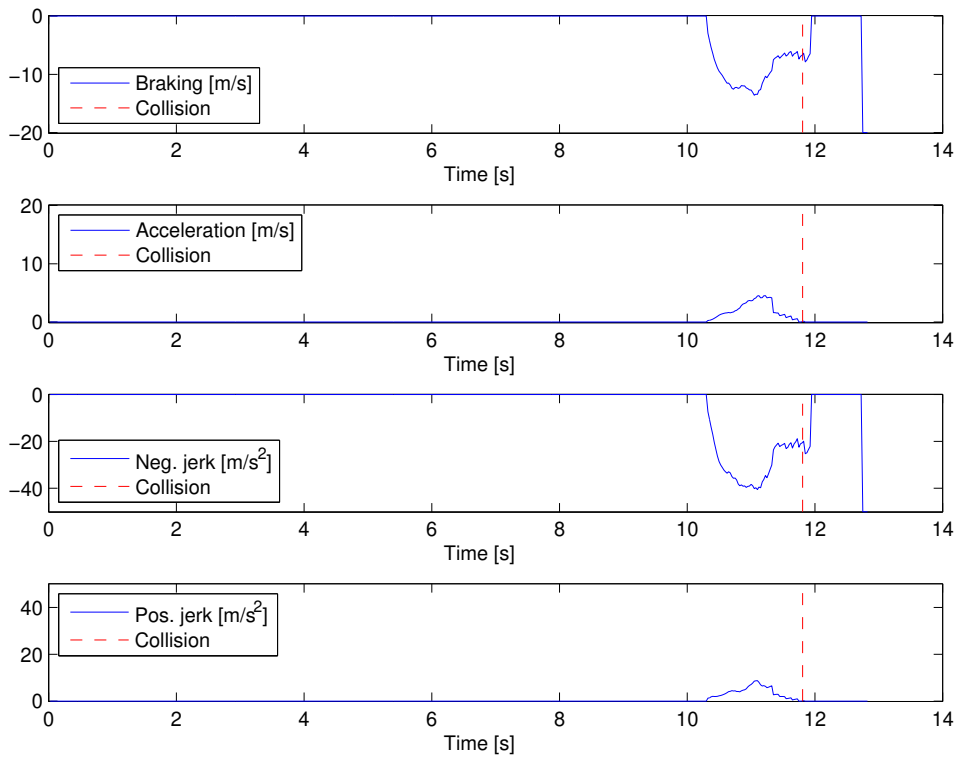


Figure C.8: Curve radius 12 m, host vehicle velocity 25 kph, object velocity 23 kph, lateral distance 2.8 m.

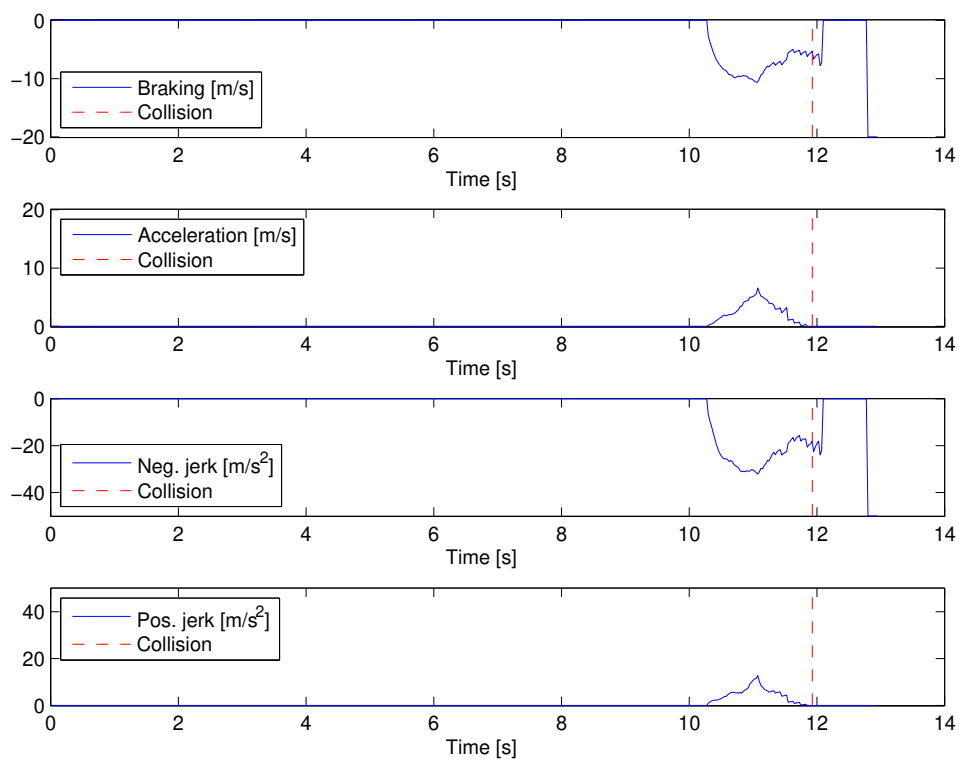


Figure C.9: Curve radius 12 m, host vehicle velocity 25 kph, object velocity 23 kph, lateral distance 3.3 m.

D

Required steering, simulation results

Section 5.4 of the report presents the required steering to avoid the collision in a test based on simulation data. The value at each time instant is the maximal steering required to avoid all edges of the object throughout the entire prediction horizon. This appendix provides similar graphs from additional test cases. The parameters used in each scenario are listed in the caption of each figure. Note that the object generally disappears outside the radar's FOV shortly before the collision occurs. This is why the required steering drops to zero before the time of collision.

The first of the two drastic drops in the curvature required to pass the object on the right side appears because the objects are predicted to be side by side as further discussed in Section 5.4.

D. Required steering, simulation results

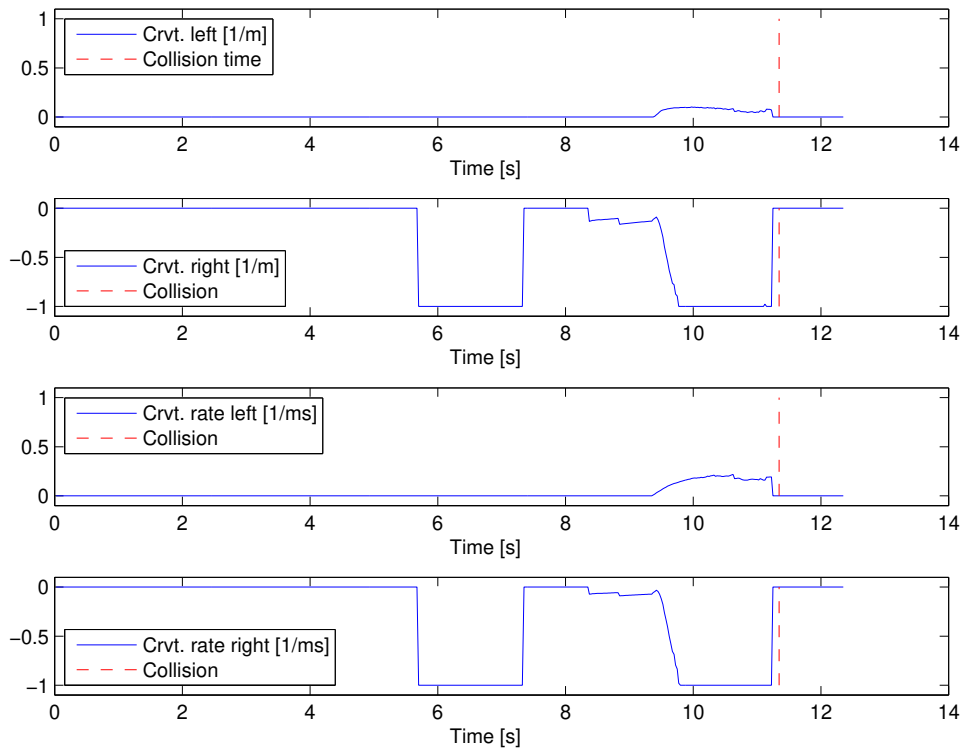


Figure D.1: Curve radius 6 m, host vehicle velocity 10 kph, object velocity 18 kph, lateral distance 2.3 m.

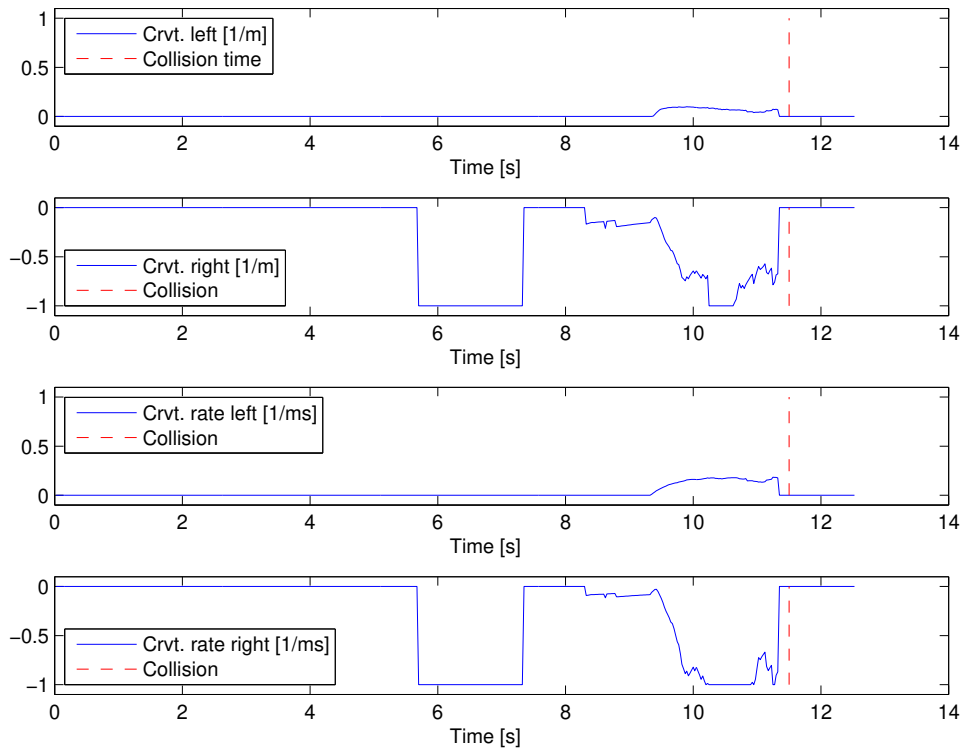


Figure D.2: Curve radius 6 m, host vehicle velocity 10 kph, object velocity 18 kph, lateral distance 2.8 m.

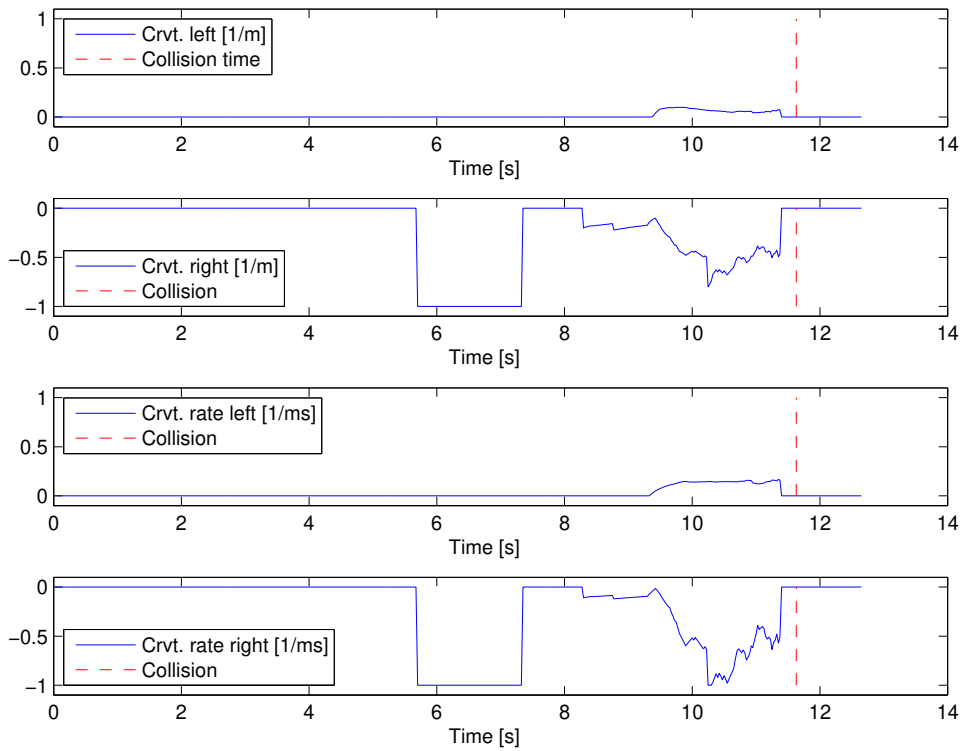


Figure D.3: Curve radius 6 m, host vehicle velocity 10 kph, object velocity 18 kph, lateral distance 3.3 m.

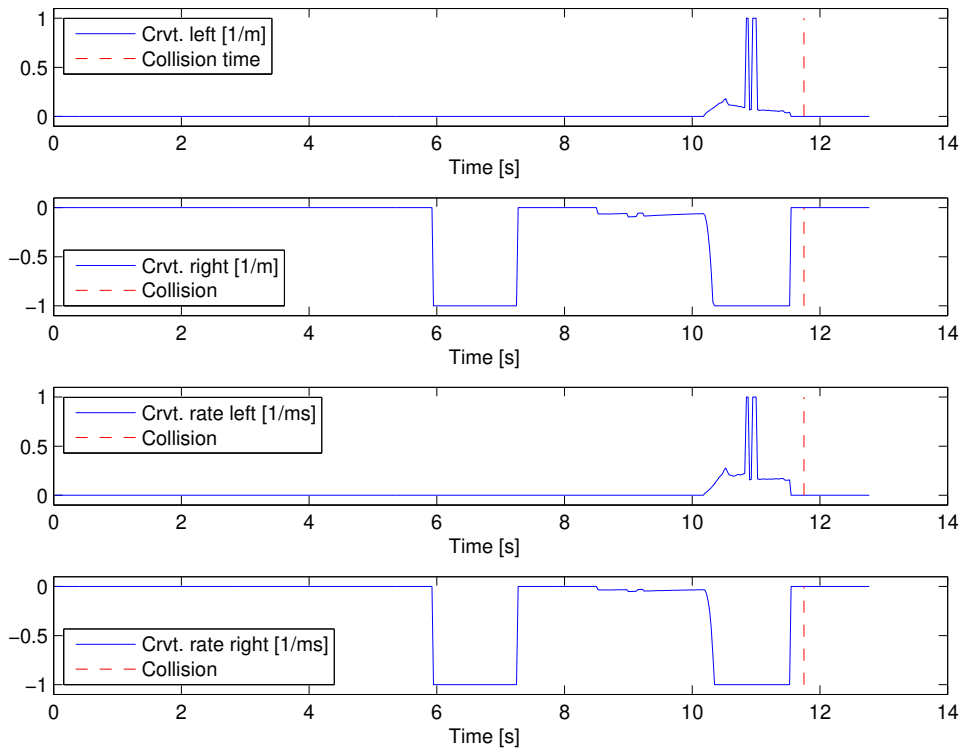


Figure D.4: Curve radius 9 m, host vehicle velocity 15 kph, object velocity 18 kph, lateral distance 1.8 m.

D. Required steering, simulation results

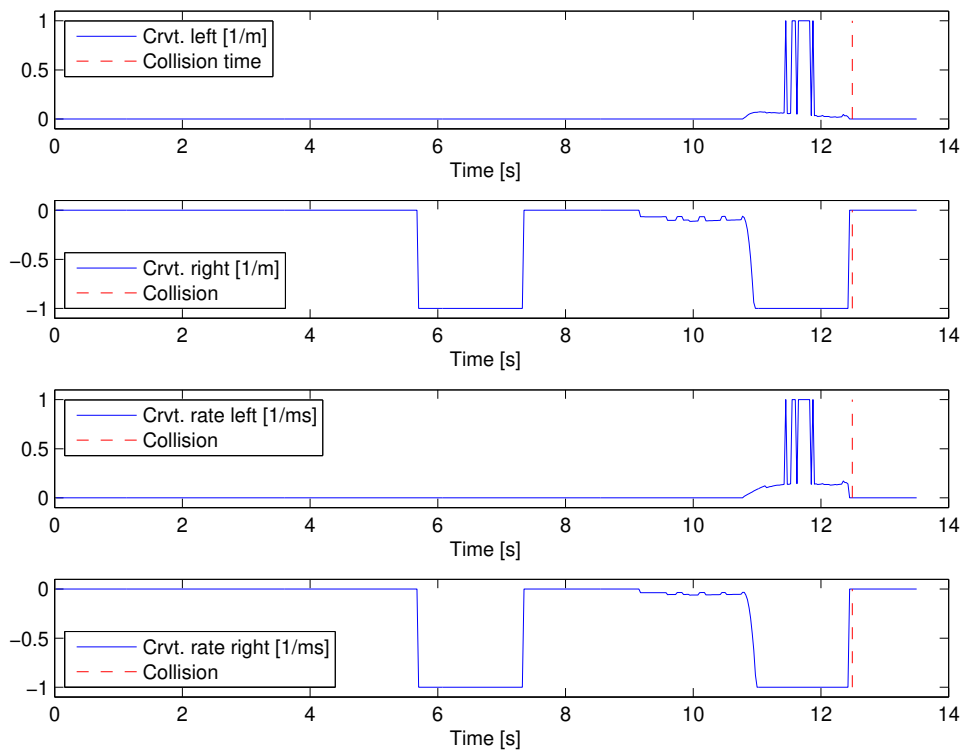


Figure D.5: Curve radius 9 m, host vehicle velocity 15 kph, object velocity 18 kph, lateral distance 2.3 m.

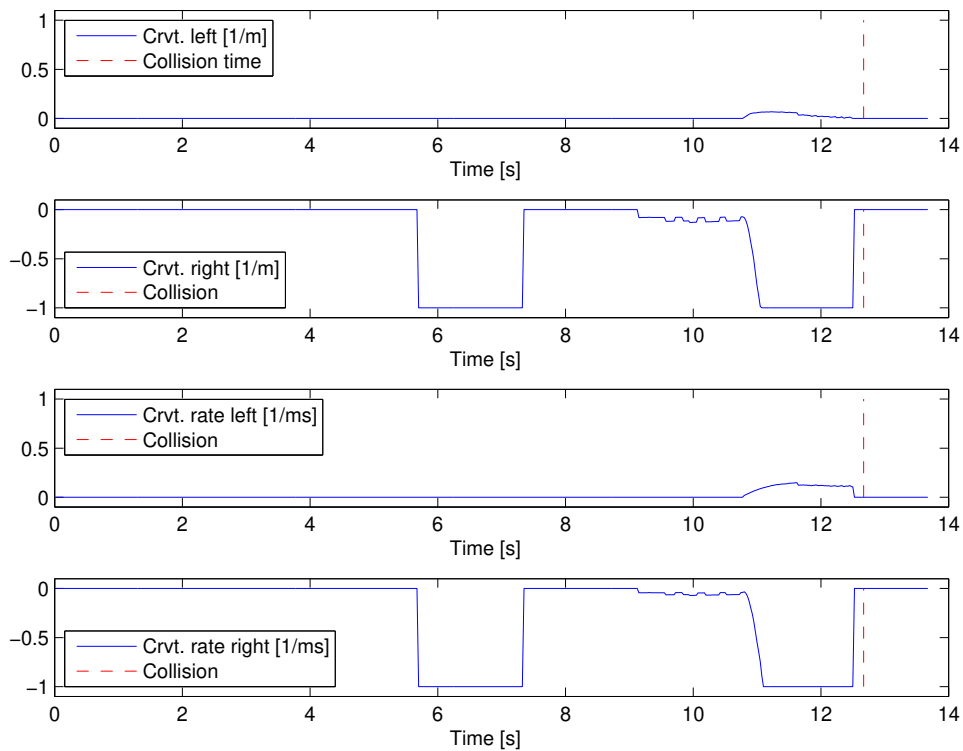


Figure D.6: Curve radius 9 m, host vehicle velocity 15 kph, object velocity 18 kph, lateral distance 2.8 m.

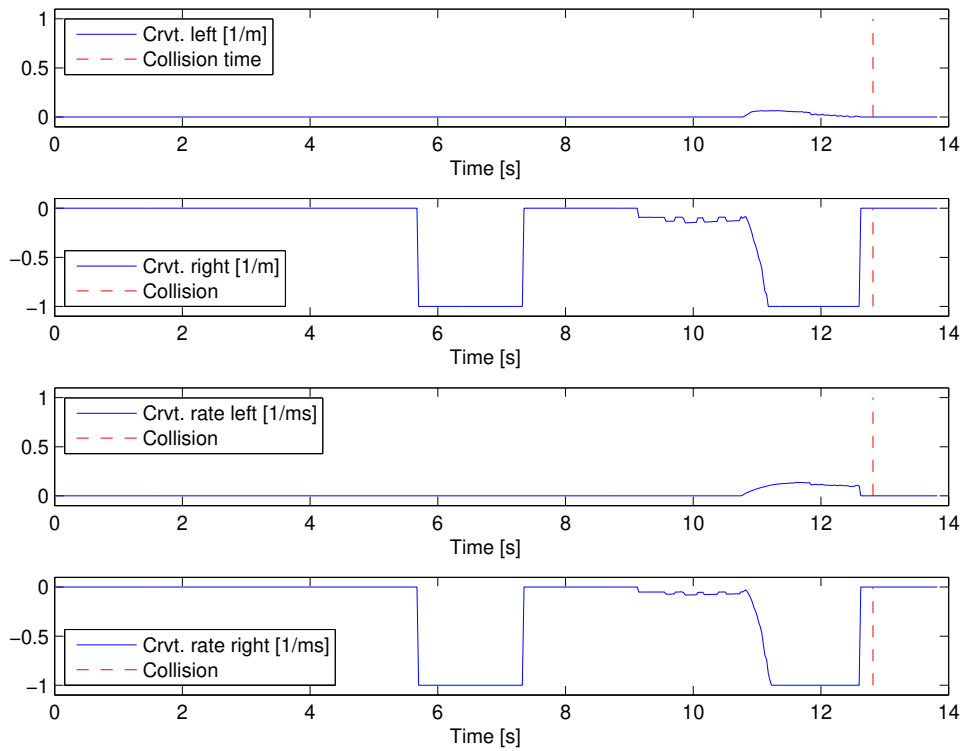


Figure D.7: Curve radius 9 m, host vehicle velocity 15 kph, object velocity 18 kph, lateral distance 3.3 m.

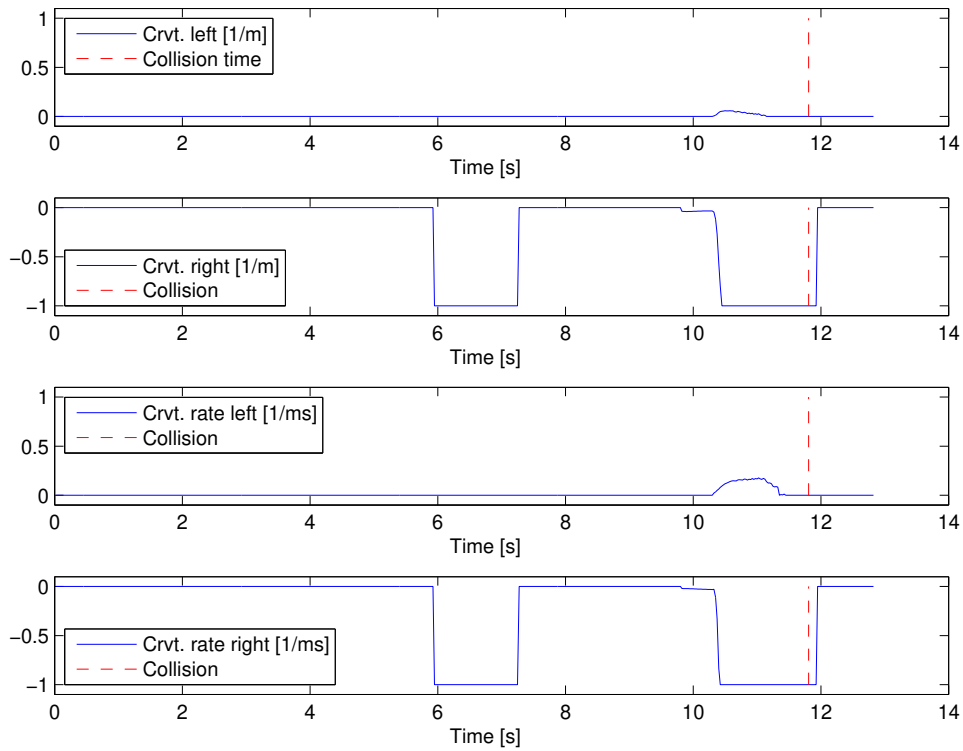


Figure D.8: Curve radius 12 m, host vehicle velocity 25 kph, object velocity 23 kph, lateral distance 2.8 m.

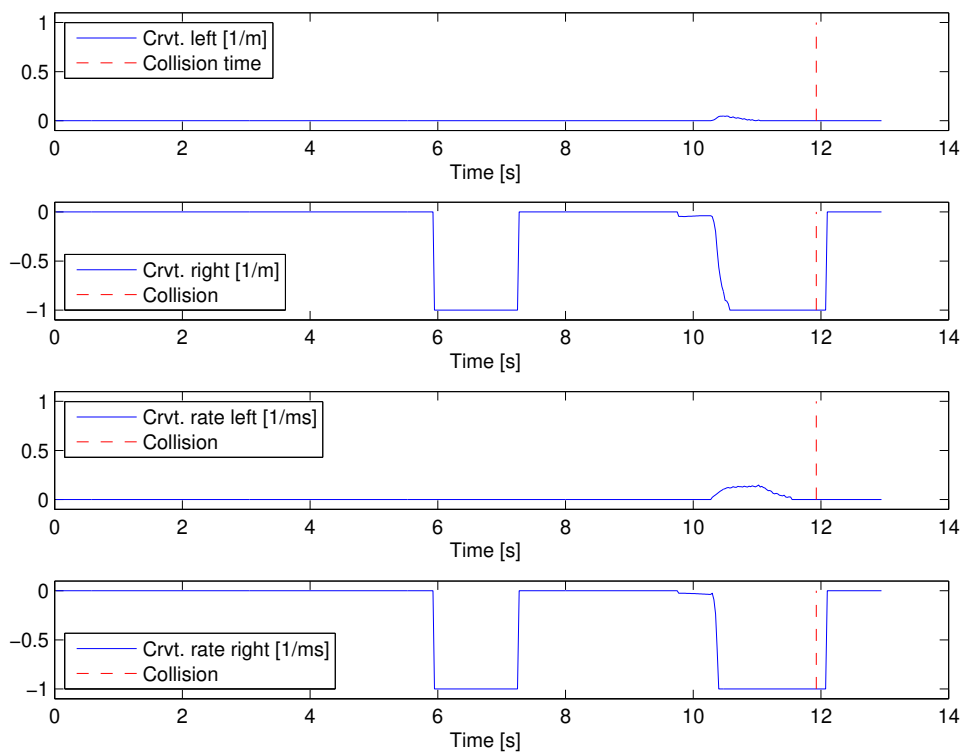


Figure D.9: Curve radius 12 m, host vehicle velocity 25 kph, object velocity 23 kph, lateral distance 3.3 m.

E

Predicted TTI, proving ground results

Section 6.3 of the report presents the estimated TTI in a test run based on proving ground data. This appendix provides similar graphs from additional test cases. The parameters used in each scenario are listed in the caption of each figure. Note that the green dashed line is an approximation of the time of collision if the test runs were not terminated early. Hence, it is only an indication of at which time the TTI should reach zero.

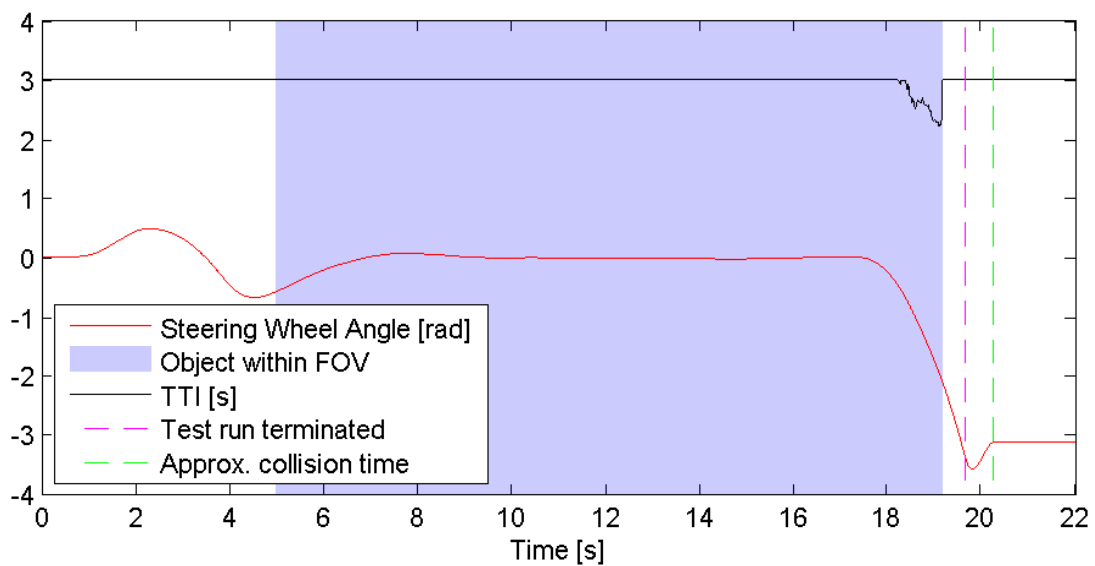


Figure E.1: Curve radius 6 m, host vehicle velocity 10 kph, object velocity 13 kph, lateral distance 2.8 m.

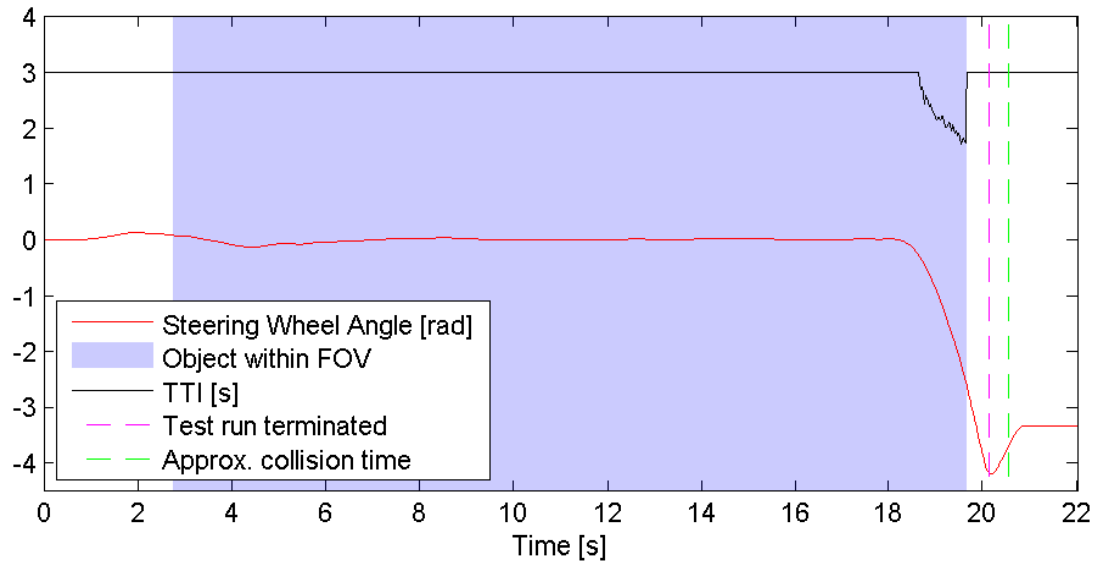


Figure E.2: Curve radius 6 m, host vehicle velocity 15 kph, object velocity 18 kph, lateral distance 3.3 m.

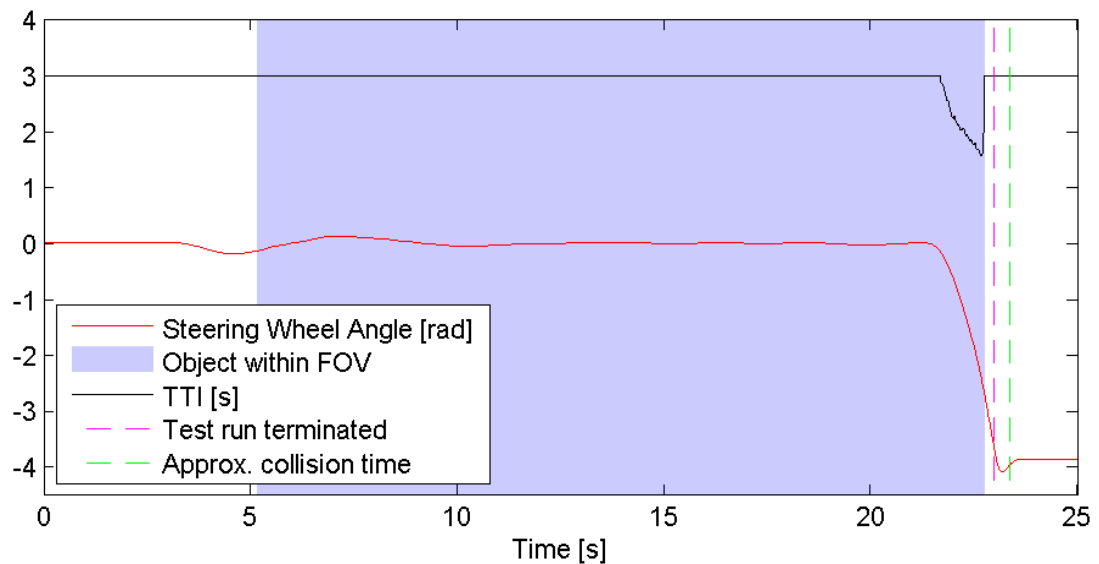


Figure E.3: Curve radius 6 m, host vehicle velocity 17 kph, object velocity 20 kph, lateral distance 3.3 m.

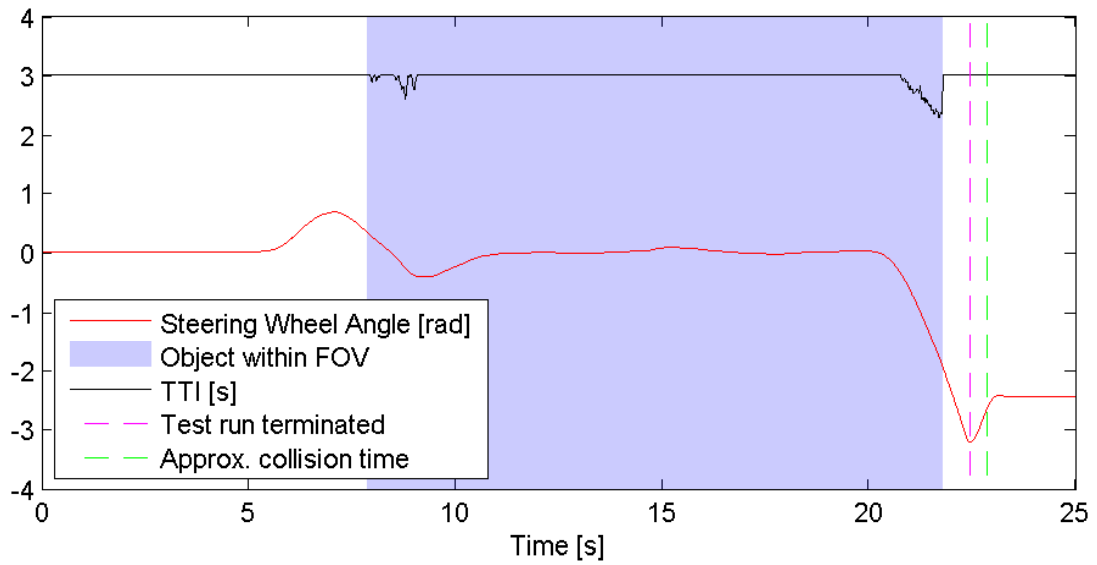


Figure E.4: Curve radius 9 m, host vehicle velocity 13 kph, object velocity 16 kph, lateral distance 3.3 m.

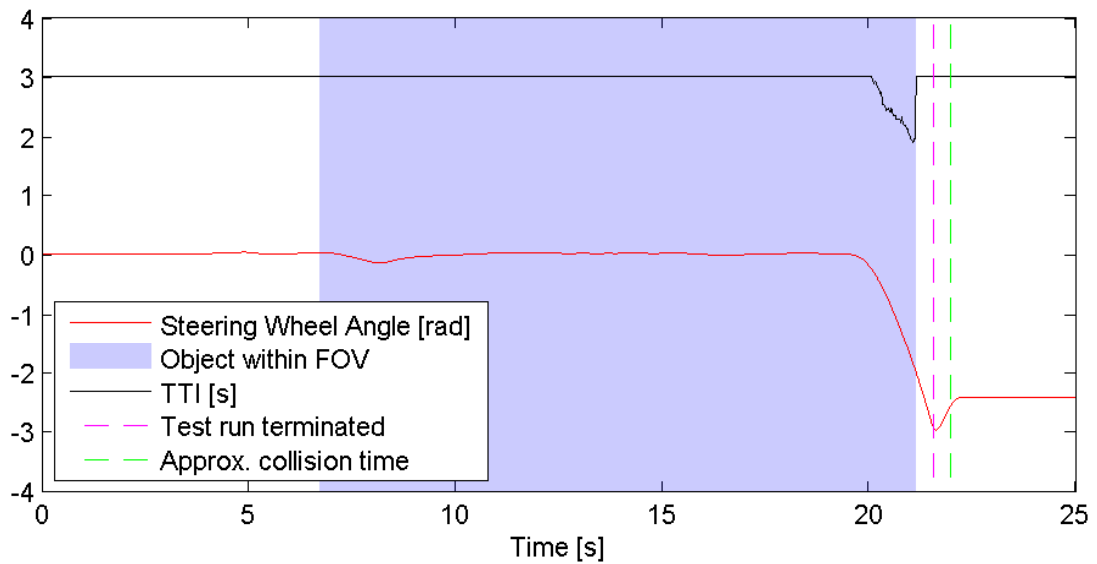


Figure E.5: Curve radius 9 m, host vehicle velocity 15 kph, object velocity 18 kph, lateral distance 3.3 m.

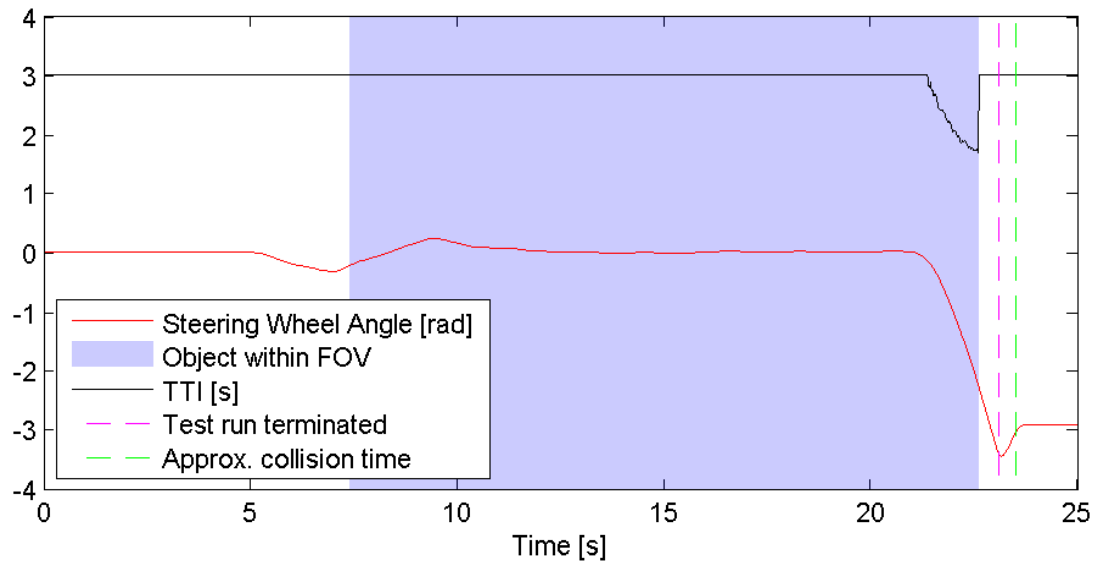


Figure E.6: Curve radius 9 m, host vehicle velocity 17 kph, object velocity 20 kph, lateral distance 3.3 m.

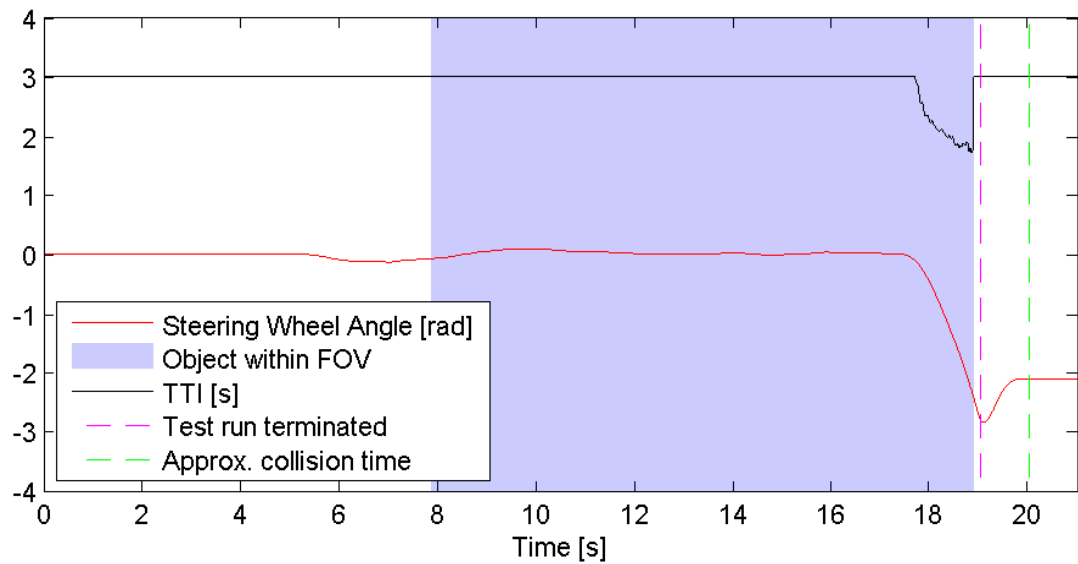


Figure E.7: Curve radius 9 m, host vehicle velocity 20 kph, object velocity 23 kph, lateral distance 3.8 m.

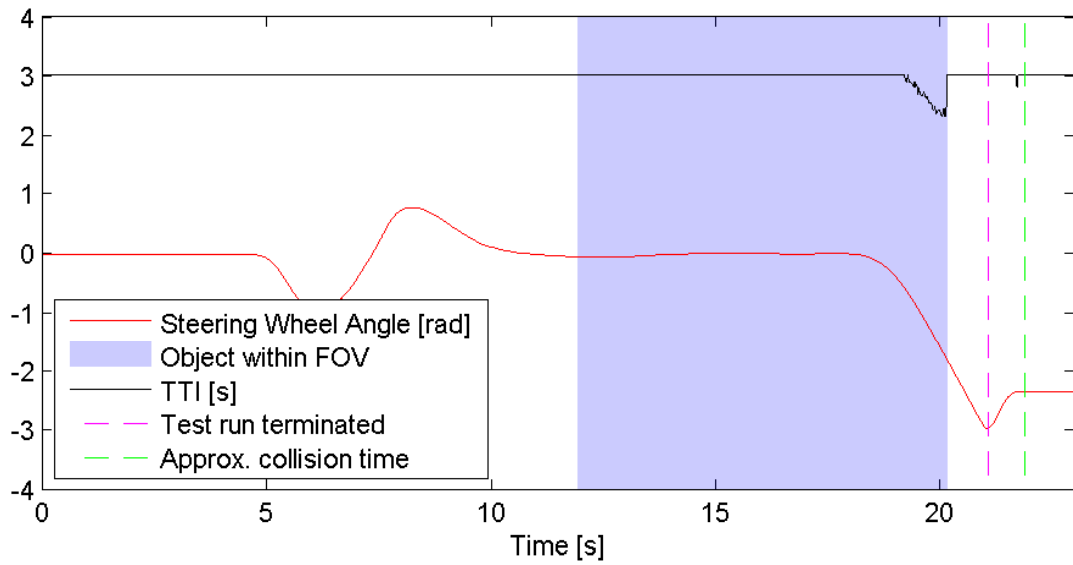


Figure E.8: Curve radius 12 m, host vehicle velocity 13 kph, object velocity 18 kph, lateral distance 3.3 m.

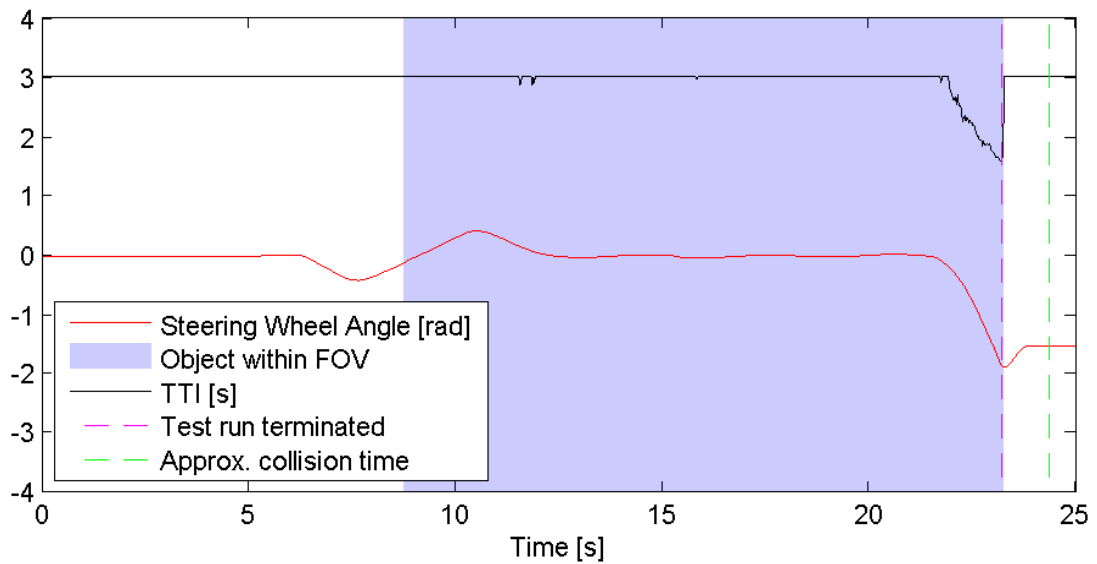


Figure E.9: Curve radius 9 m, host vehicle velocity 13 kph, object velocity 16 kph, lateral distance 2.0 m.

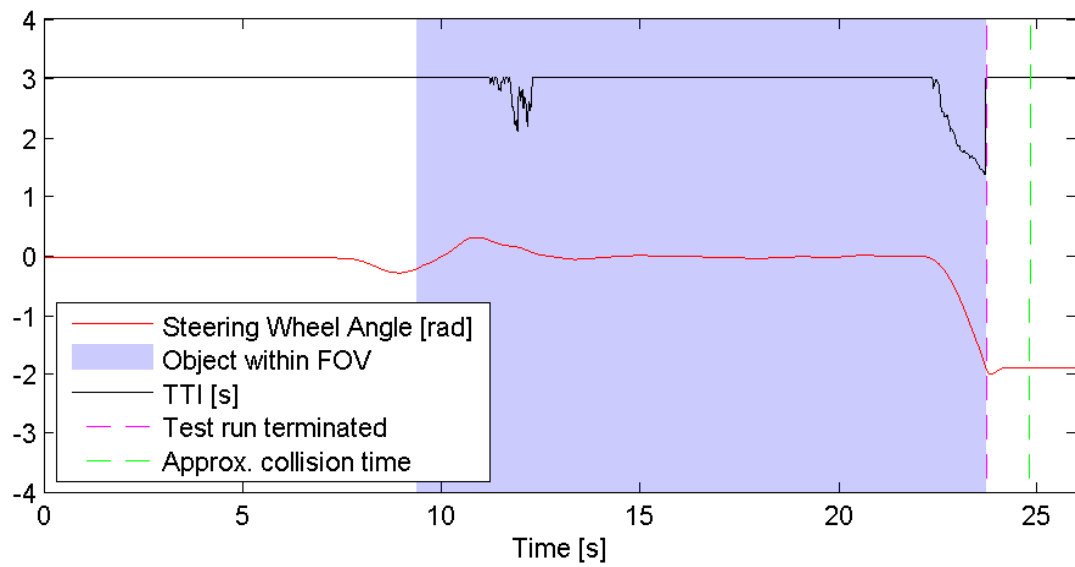


Figure E.10: Curve radius 9 m, host vehicle velocity 15 kph, object velocity 18 kph, lateral distance 2.0 m.

F

Required braking/acceleration, proving ground results

Section 6.3 of the report presents the required braking/acceleration to avoid a collision in a test run based on proving ground data. The value at each time instant is the required braking/acceleration to avoid all edges of the object throughout the entire prediction horizon. This appendix provides similar graphs from additional test cases. The parameters used in each scenario are listed in the caption of each figure. Note that the green dashed line is an approximation of the time of collision if the test runs were not terminated early.

The rapidly fluctuating values seen in Figure F.9 and F.10 is a result of the very small lateral distance between the host vehicle and the object. As they travel very close to each other the measurement noise in the radar sensor is enough to cause object predictions that bends into the path of the host vehicle. Hence, causing the algorithm to believe that an intersection is to happen very soon.

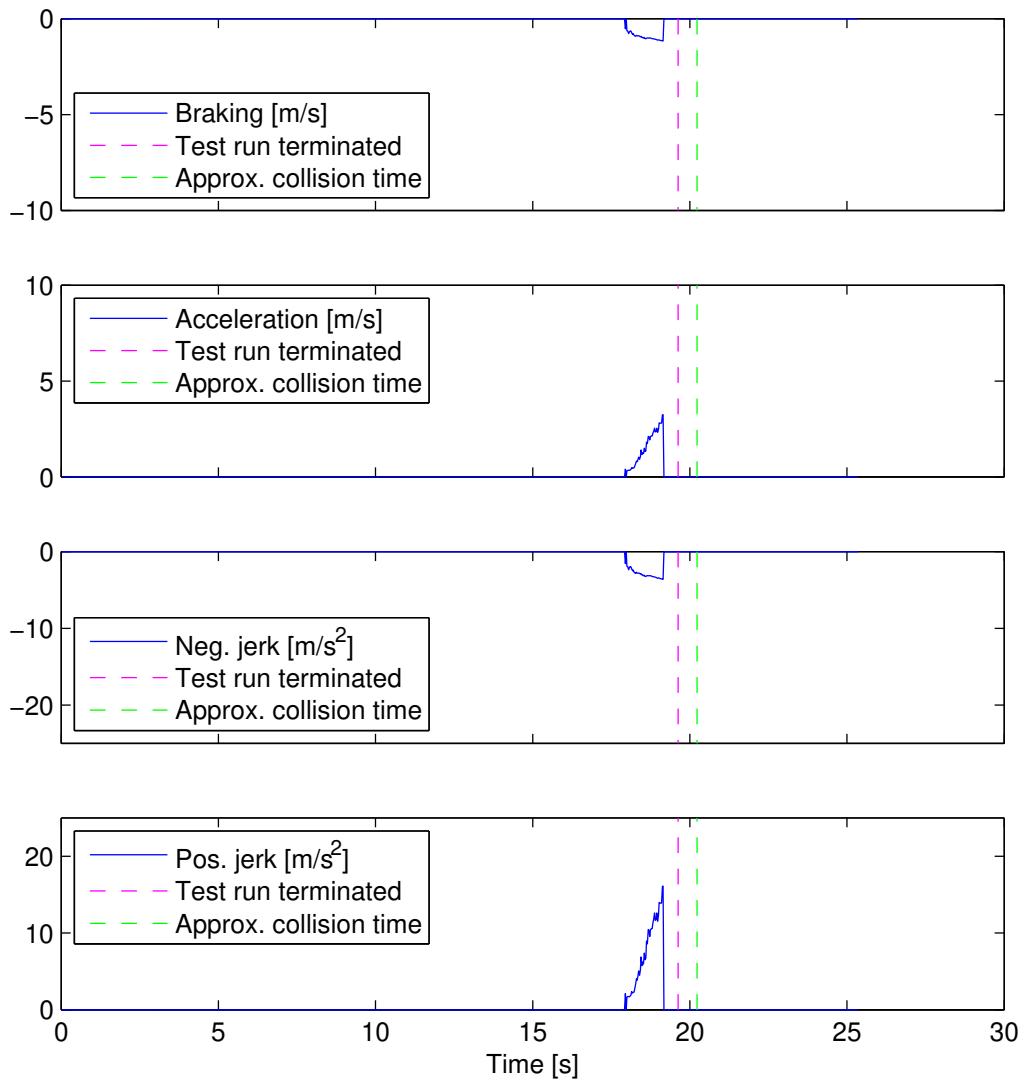


Figure F.1: Curve radius 6 m, host vehicle velocity 10 kph, object velocity 13 kph, lateral distance 2.8 m.

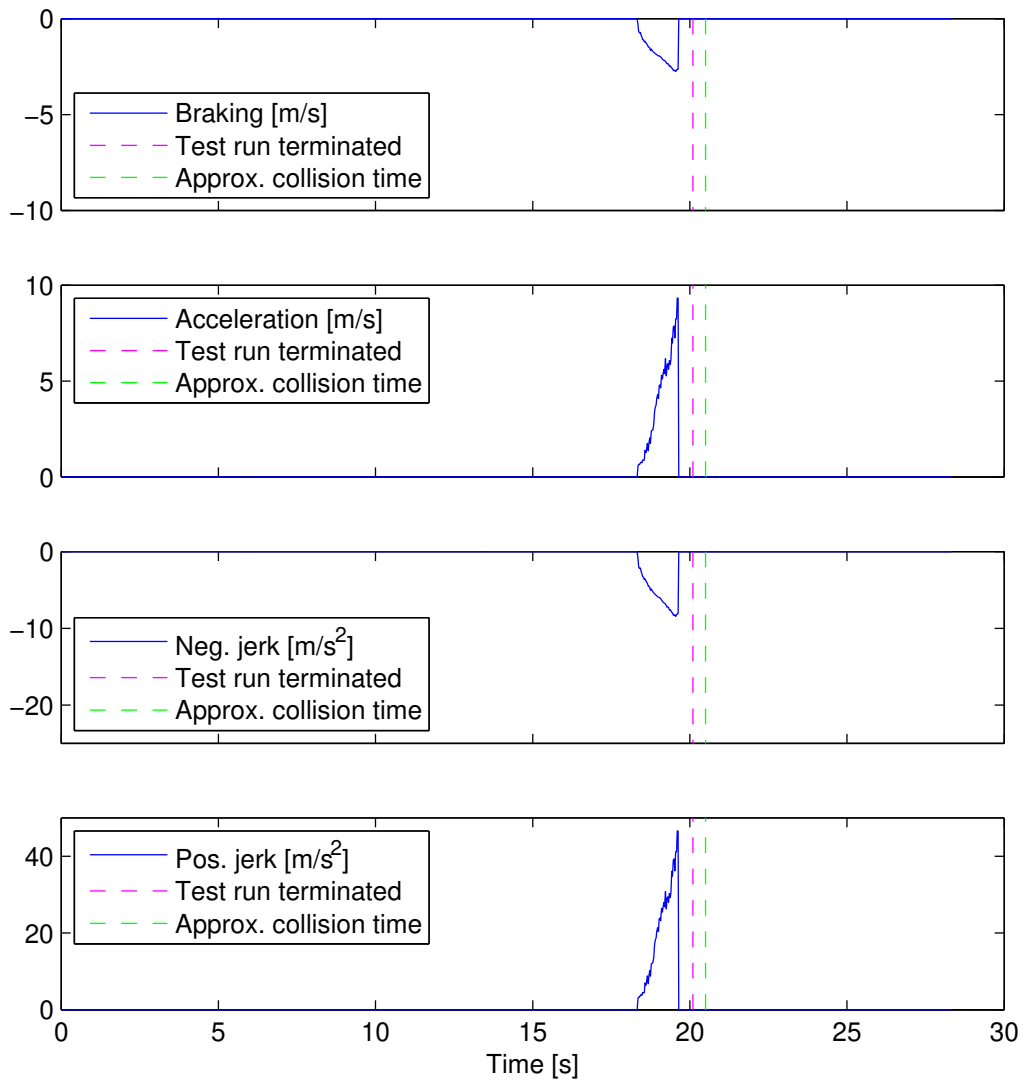


Figure F.2: Curve radius 6 m, host vehicle velocity 15 kph, object velocity 18 kph, lateral distance 3.3 m.

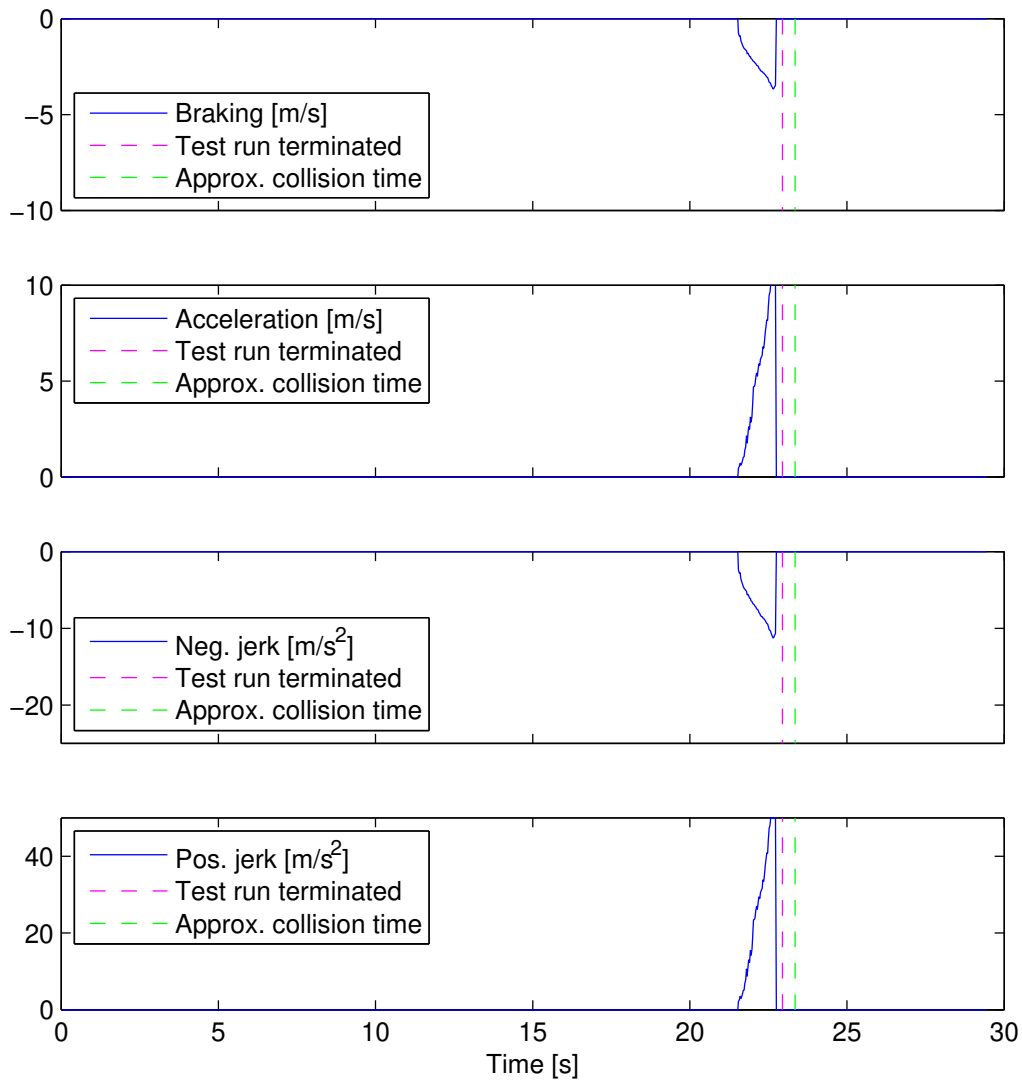


Figure F.3: Curve radius 6 m, host vehicle velocity 17 kph, object velocity 20 kph, lateral distance 3.3 m.

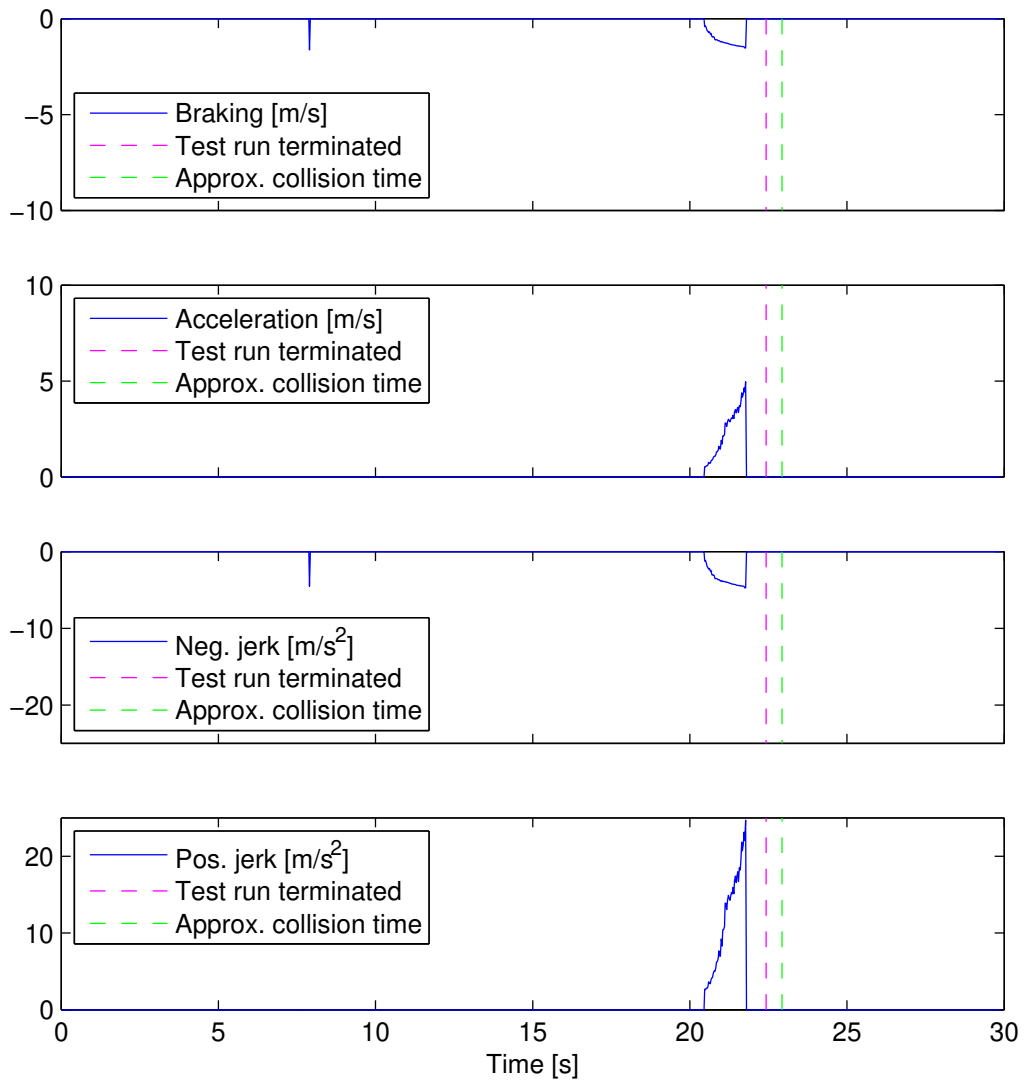


Figure F.4: Curve radius 9 m, host vehicle velocity 13 kph, object velocity 16 kph, lateral distance 3.3 m.

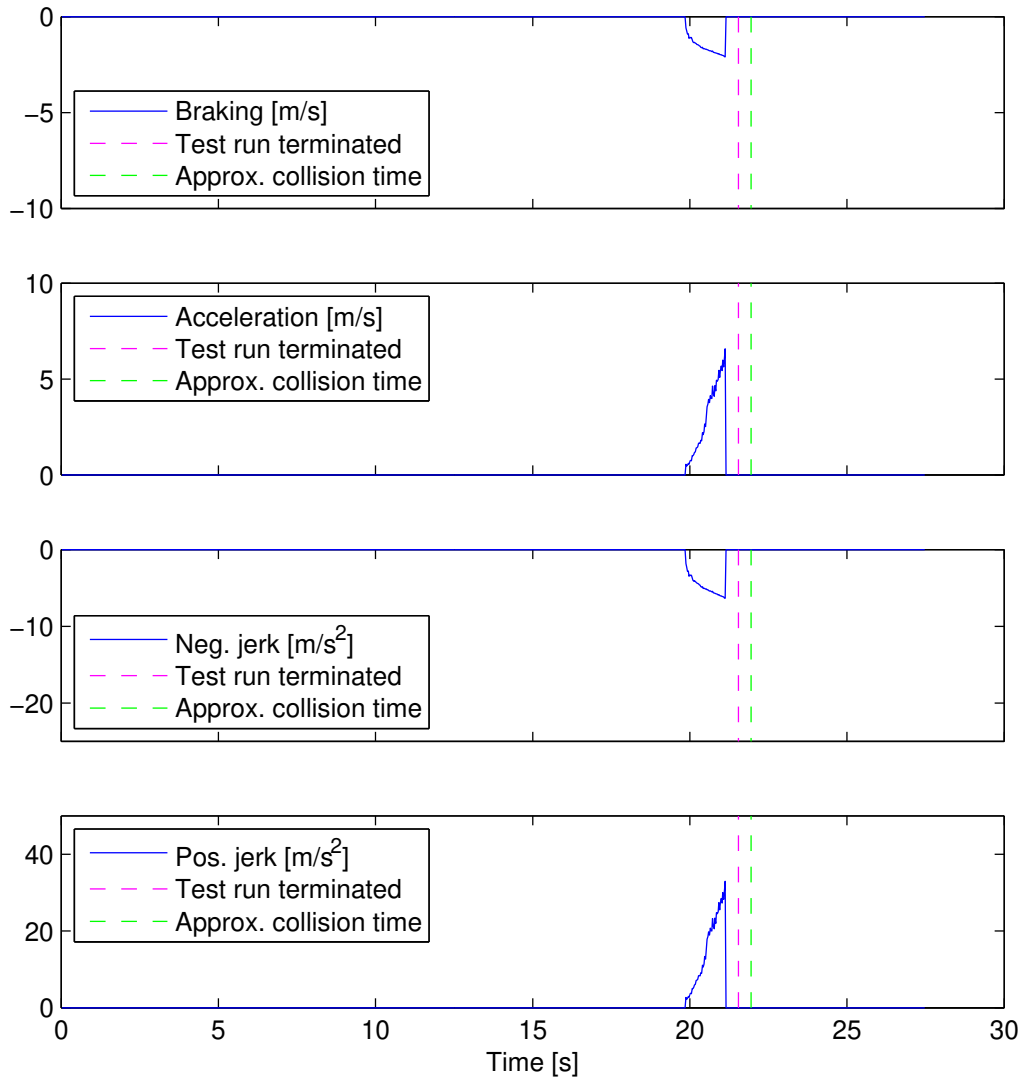


Figure F.5: Curve radius 9 m, host vehicle velocity 15 kph, object velocity 18 kph, lateral distance 3.3 m.

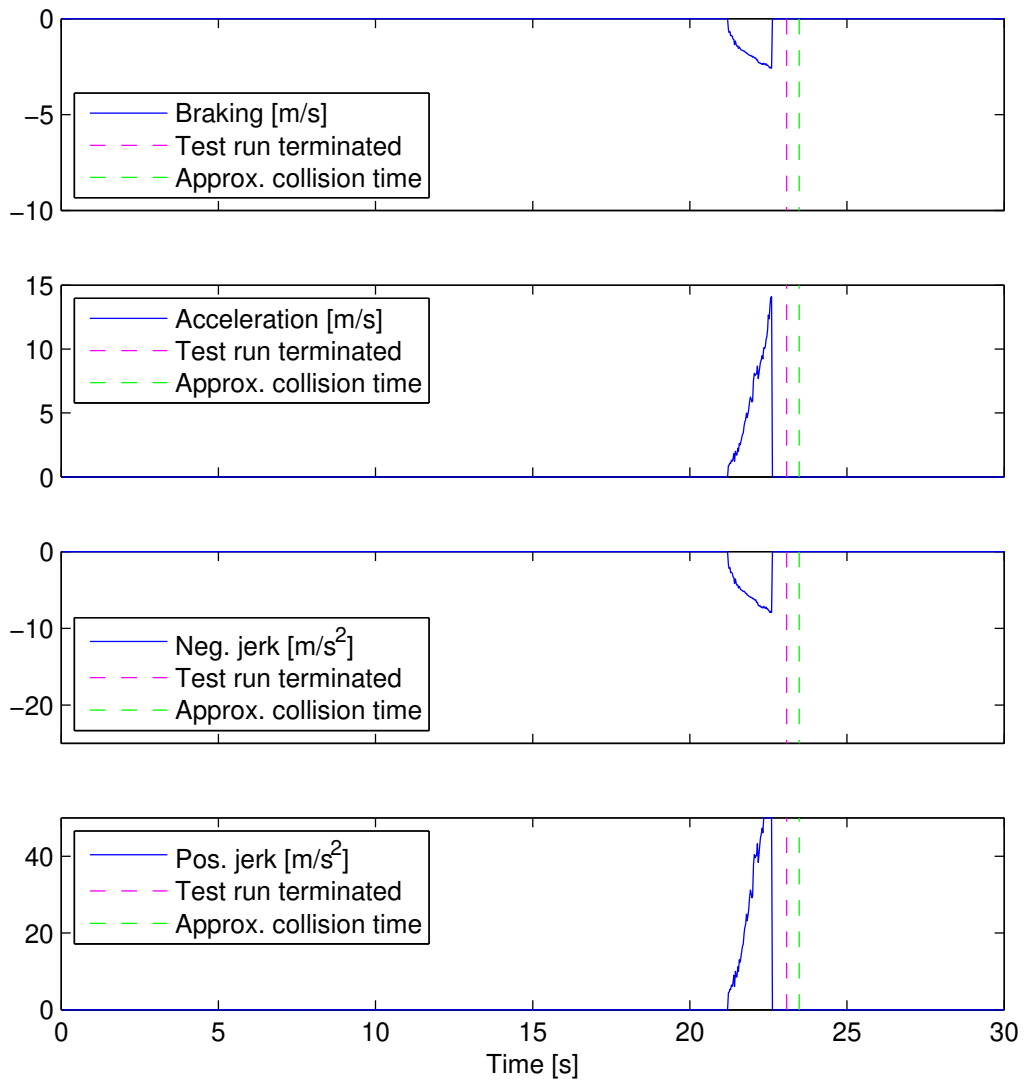


Figure F.6: Curve radius 9 m, host vehicle velocity 17 kph, object velocity 20 kph, lateral distance 3.3 m.

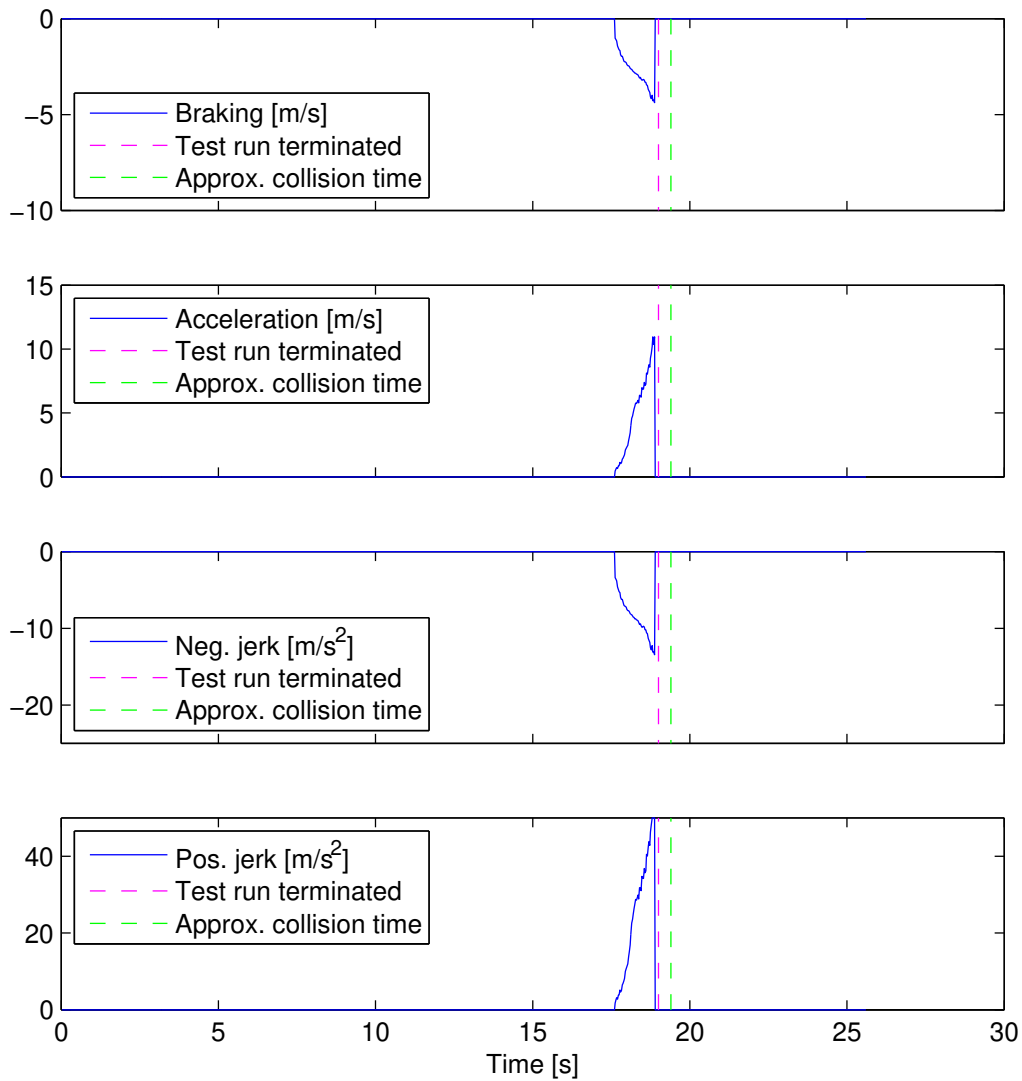


Figure F.7: Curve radius 9 m, host vehicle velocity 20 kph, object velocity 23 kph, lateral distance 3.8 m.

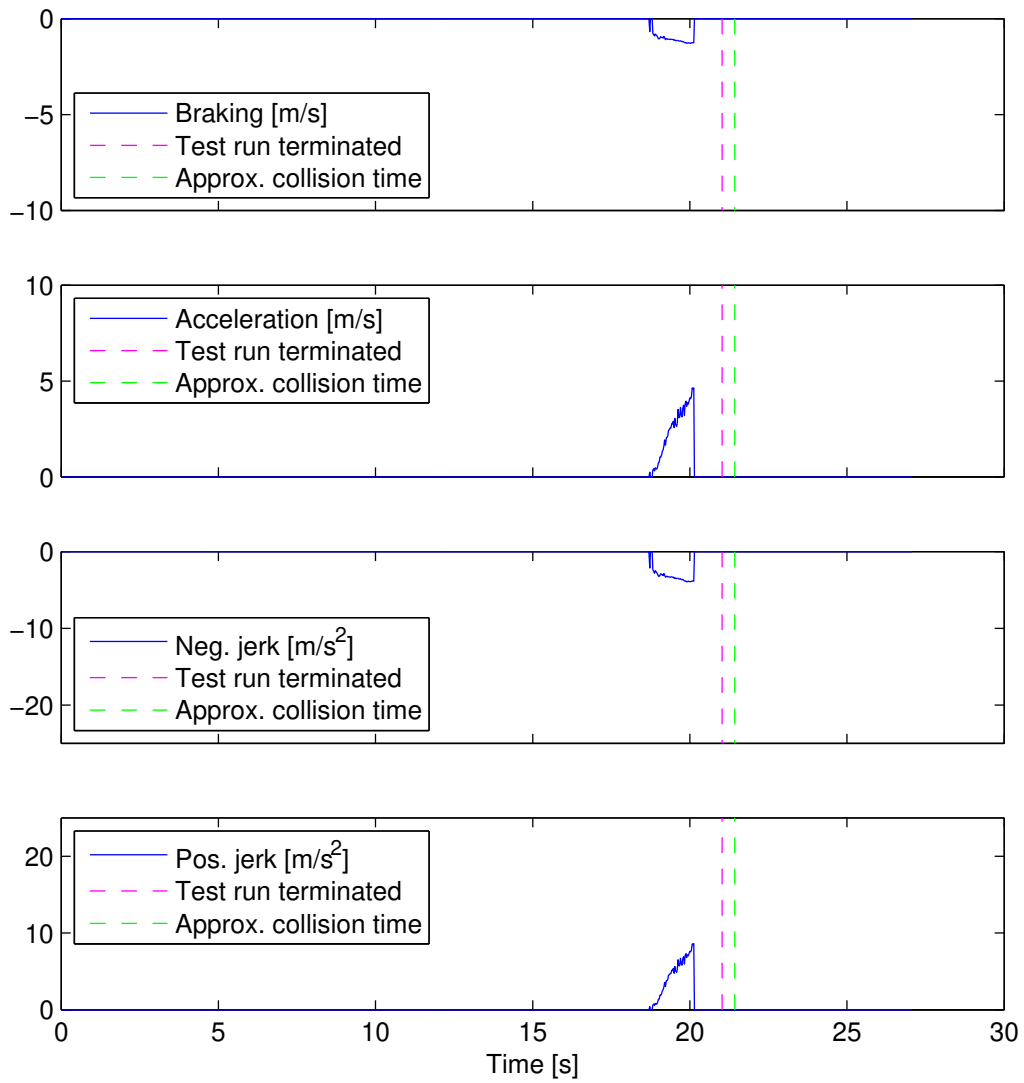


Figure F.8: Curve radius 12 m, host vehicle velocity 13 kph, object velocity 18 kph, lateral distance 3.3 m.

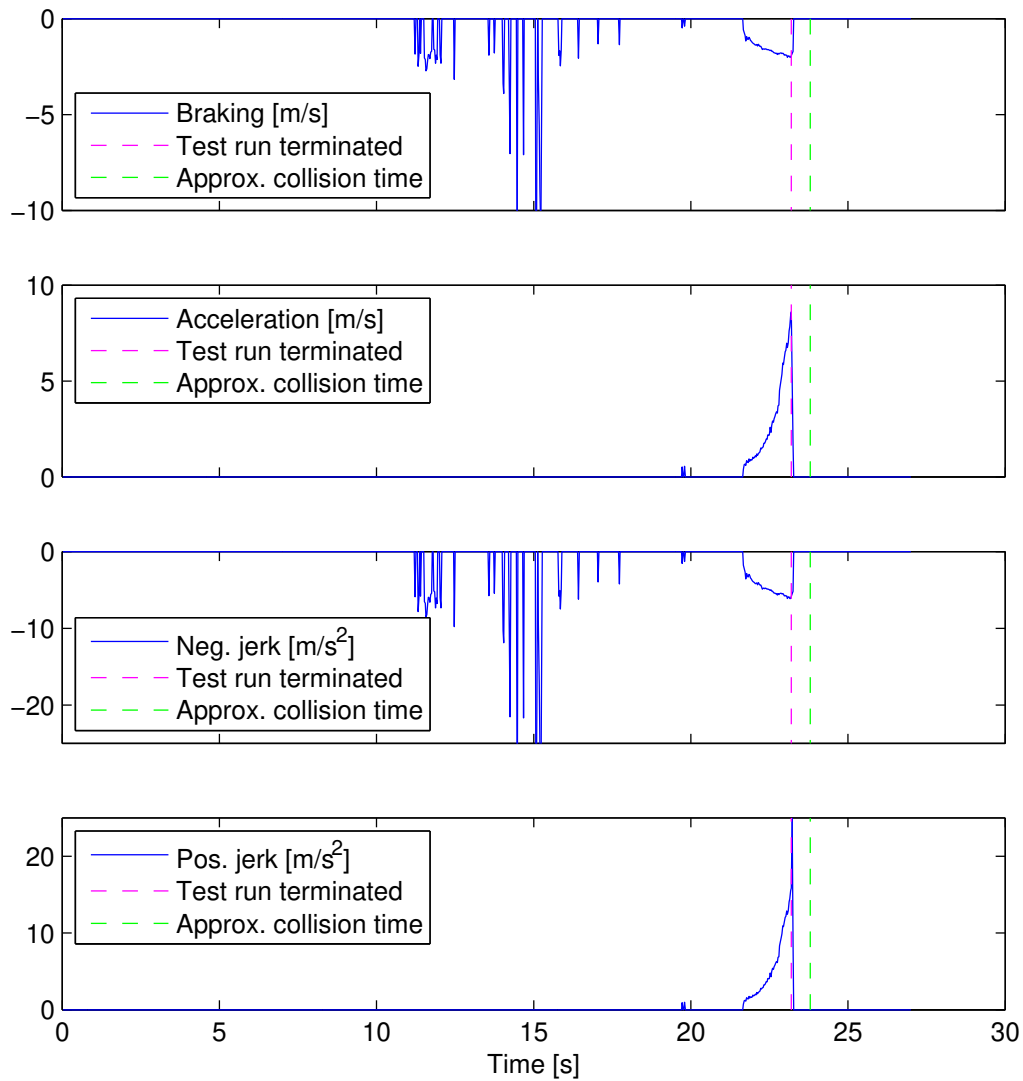


Figure F.9: Curve radius 9 m, host vehicle velocity 13 kph, object velocity 16 kph, lateral distance 2.0 m.

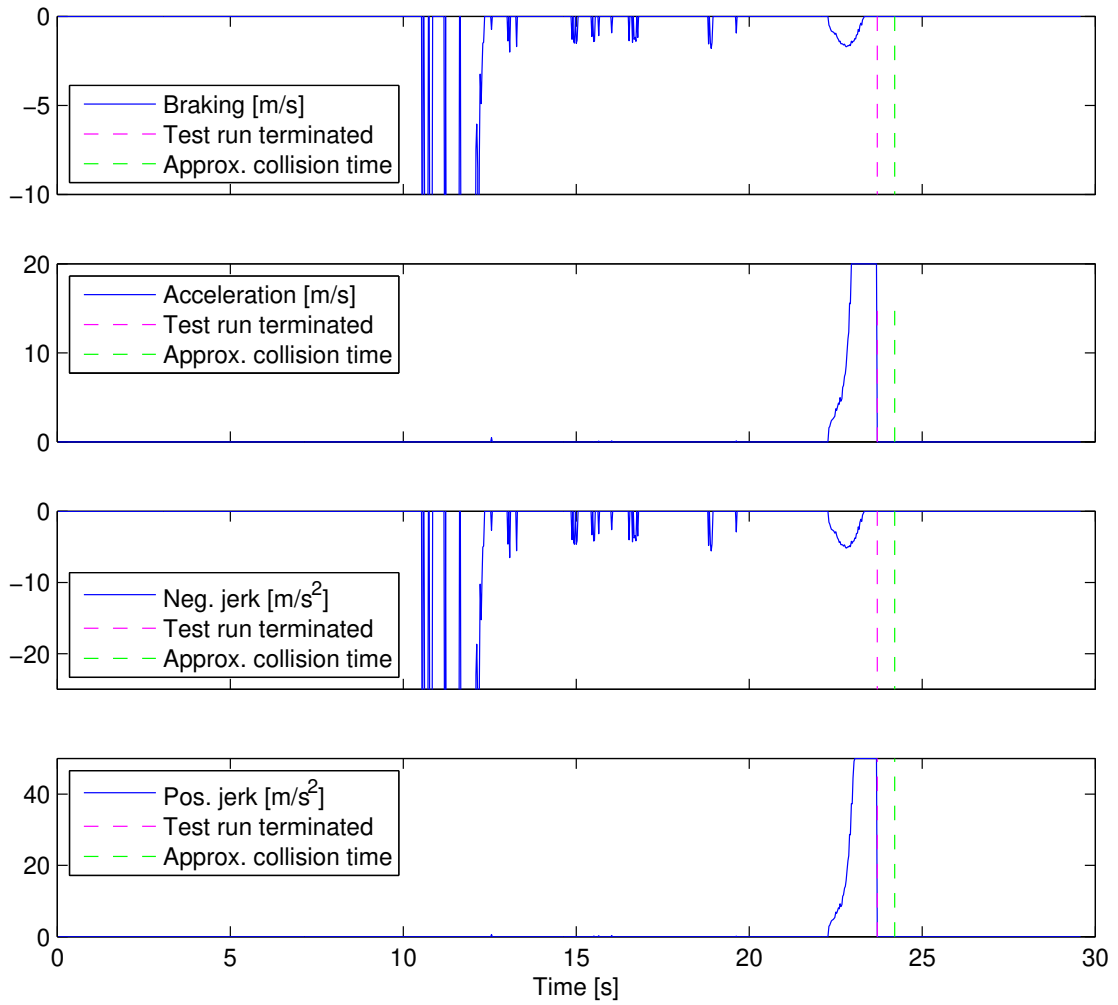


Figure F.10: Curve radius 9 m, host vehicle velocity 15 kph, object velocity 18 kph, lateral distance 2.0 m.

G

Required steering, proving ground results

Section 6.3 of the report presents the required steering to avoid a collision in a test run based on proving ground data. The value at each time instant is the required steering to avoid all edges of the object throughout the entire prediction horizon. This appendix provides similar graphs from additional test cases. The parameters used in each scenario are listed in the caption of each figure. Note that the green dashed line is an approximation of the time of collision if the test runs were not terminated early.

The wide drop in the curvature required to pass the object on the right side appears because the objects are predicted to be side by side during this time as further discussed in Section 5.4.

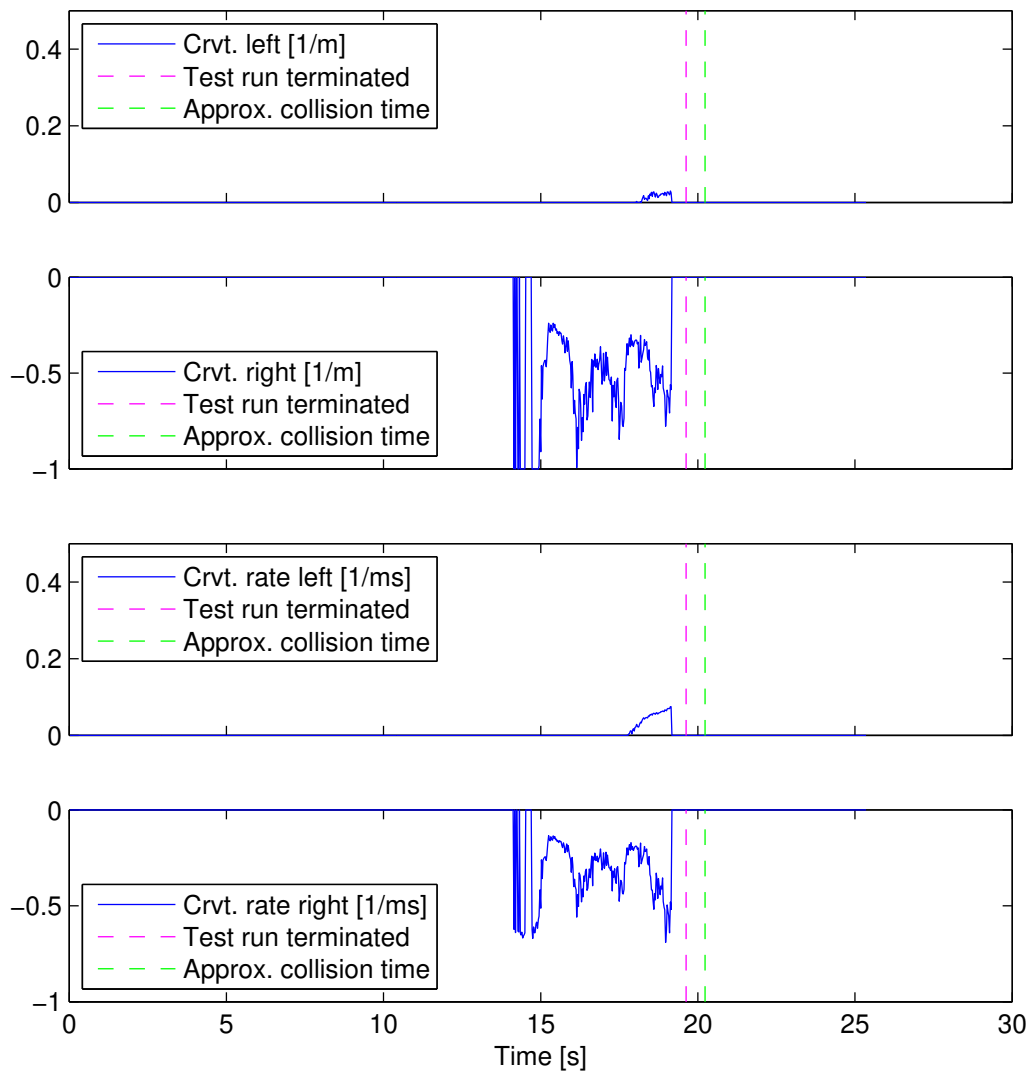


Figure G.1: Curve radius 6 m, host vehicle velocity 10 kph, object velocity 13 kph, lateral distance 2.8 m.

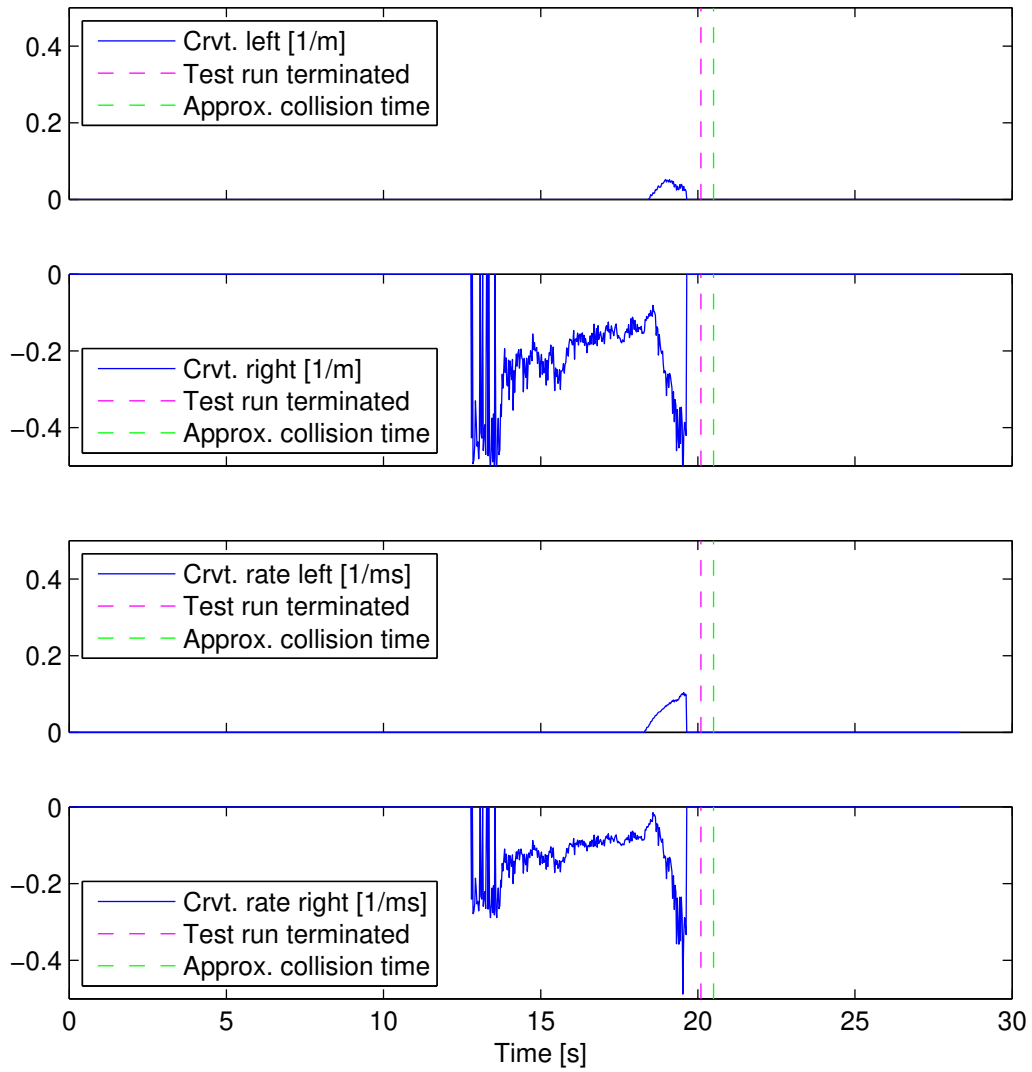


Figure G.2: Curve radius 6 m, host vehicle velocity 15 kph, object velocity 18 kph, lateral distance 3.3 m.

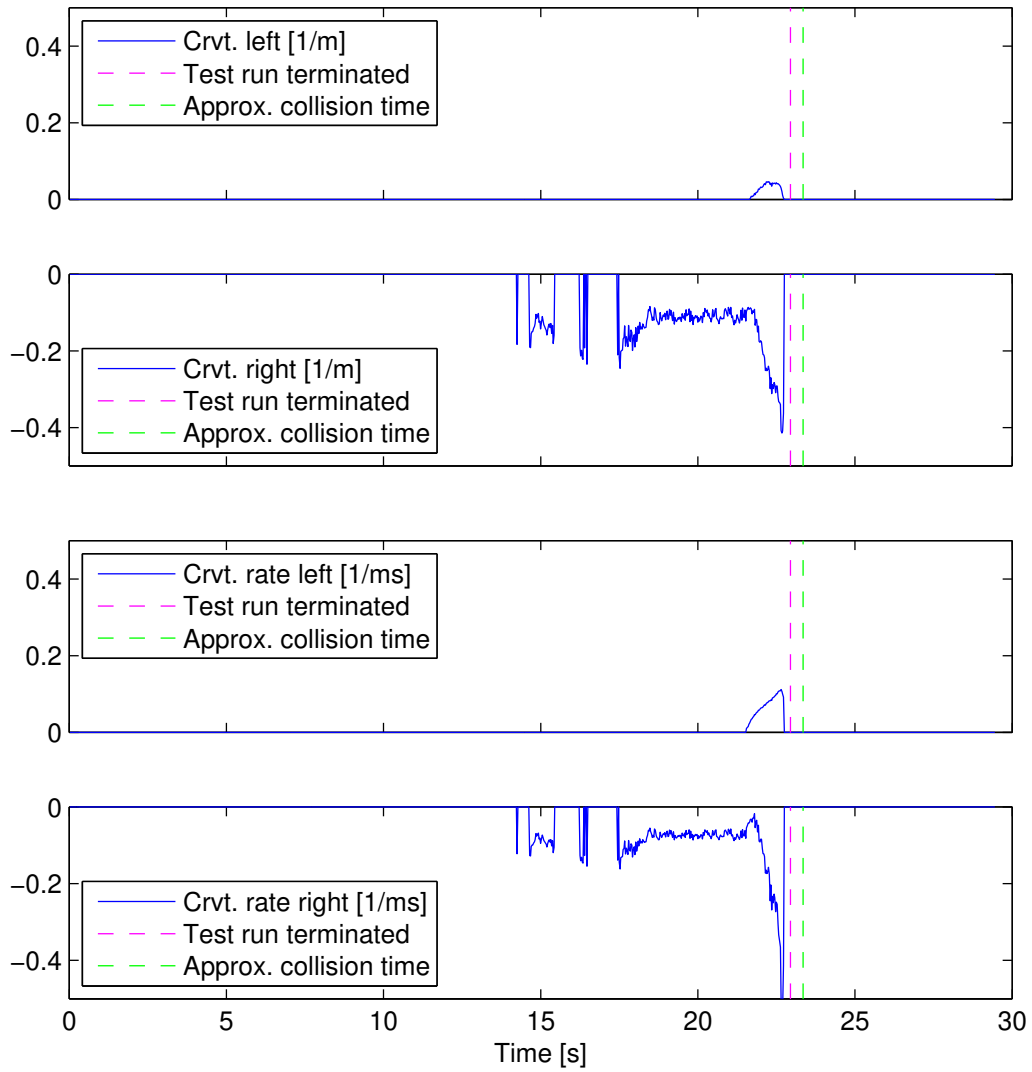


Figure G.3: Curve radius 6 m, host vehicle velocity 17 kph, object velocity 20 kph, lateral distance 3.3 m.

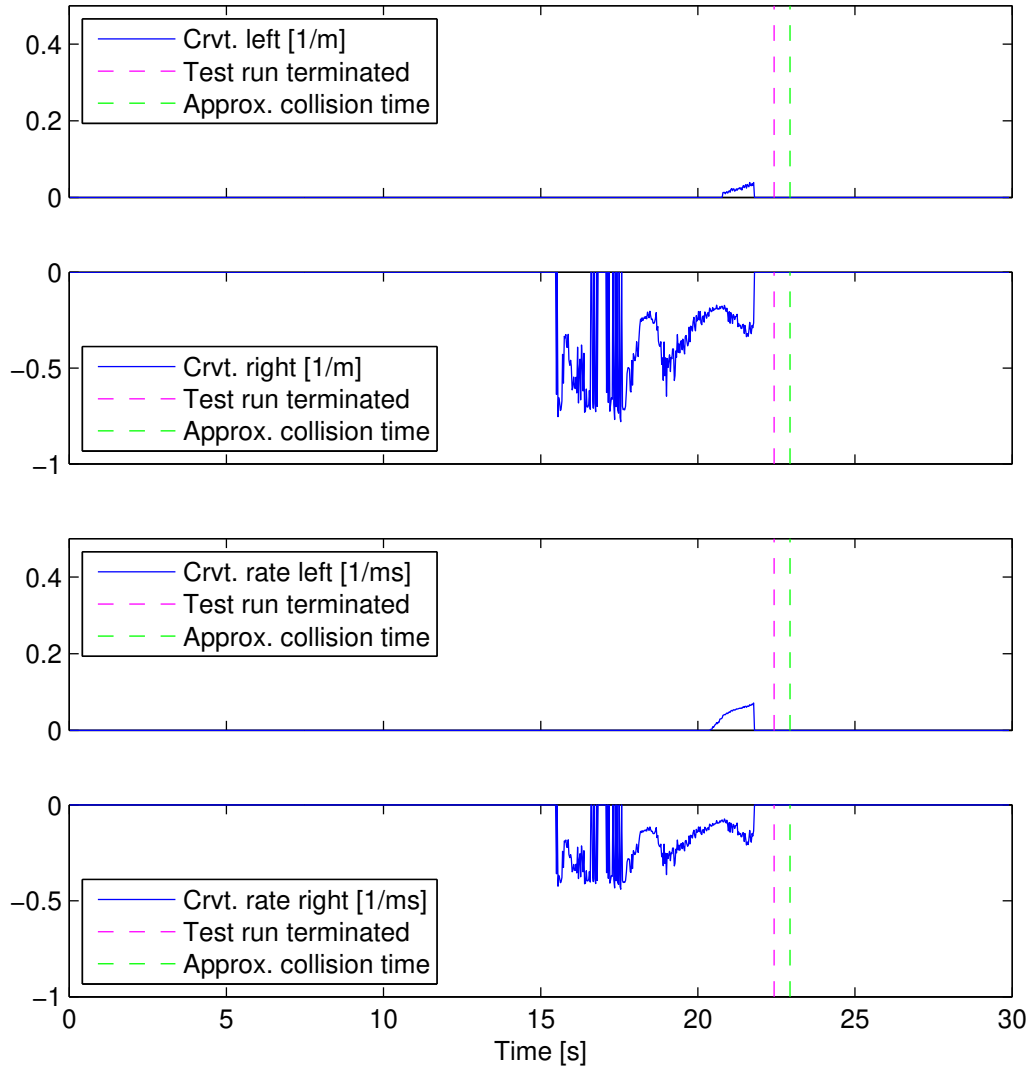


Figure G.4: Curve radius 9 m, host vehicle velocity 13 kph, object velocity 16 kph, lateral distance 3.3 m.

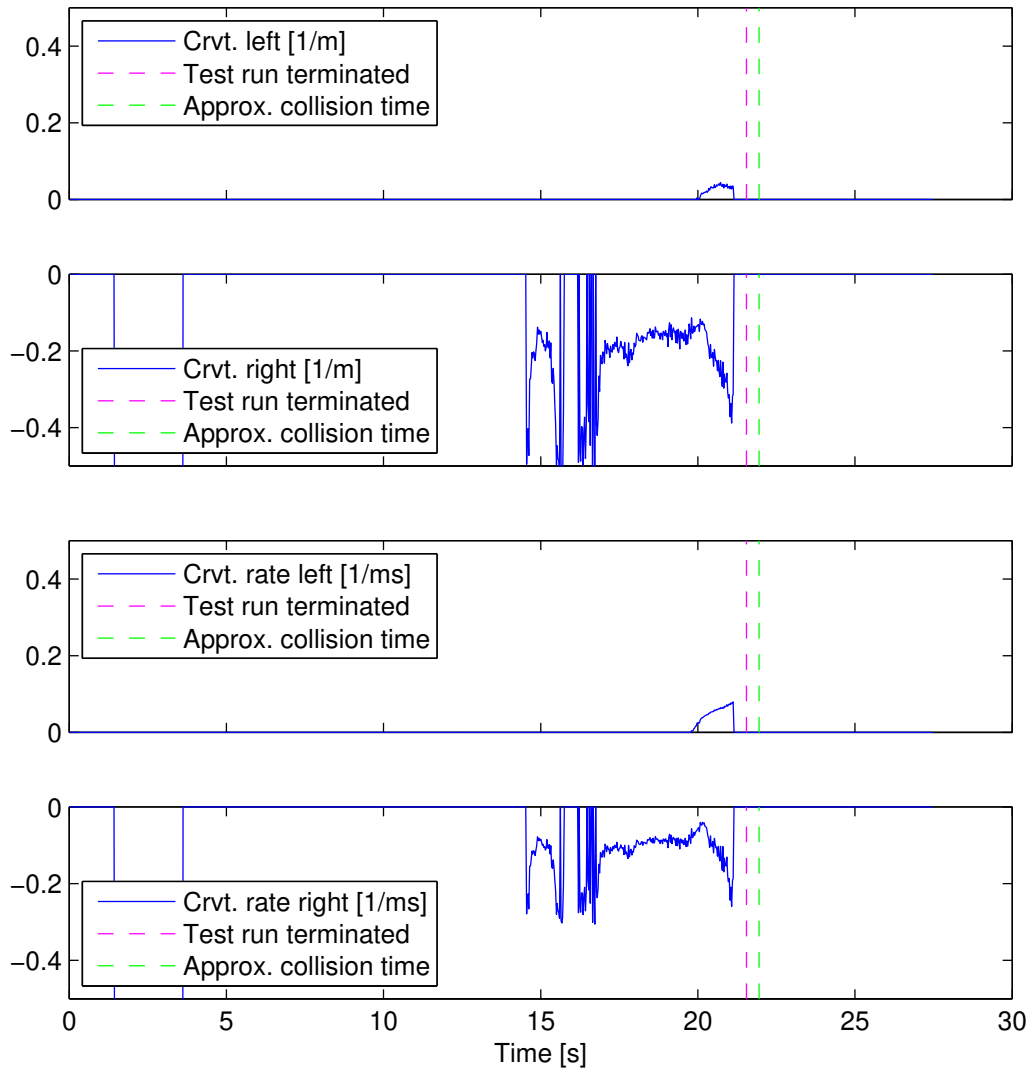


Figure G.5: Curve radius 9 m, host vehicle velocity 15 kph, object velocity 18 kph, lateral distance 3.3 m.

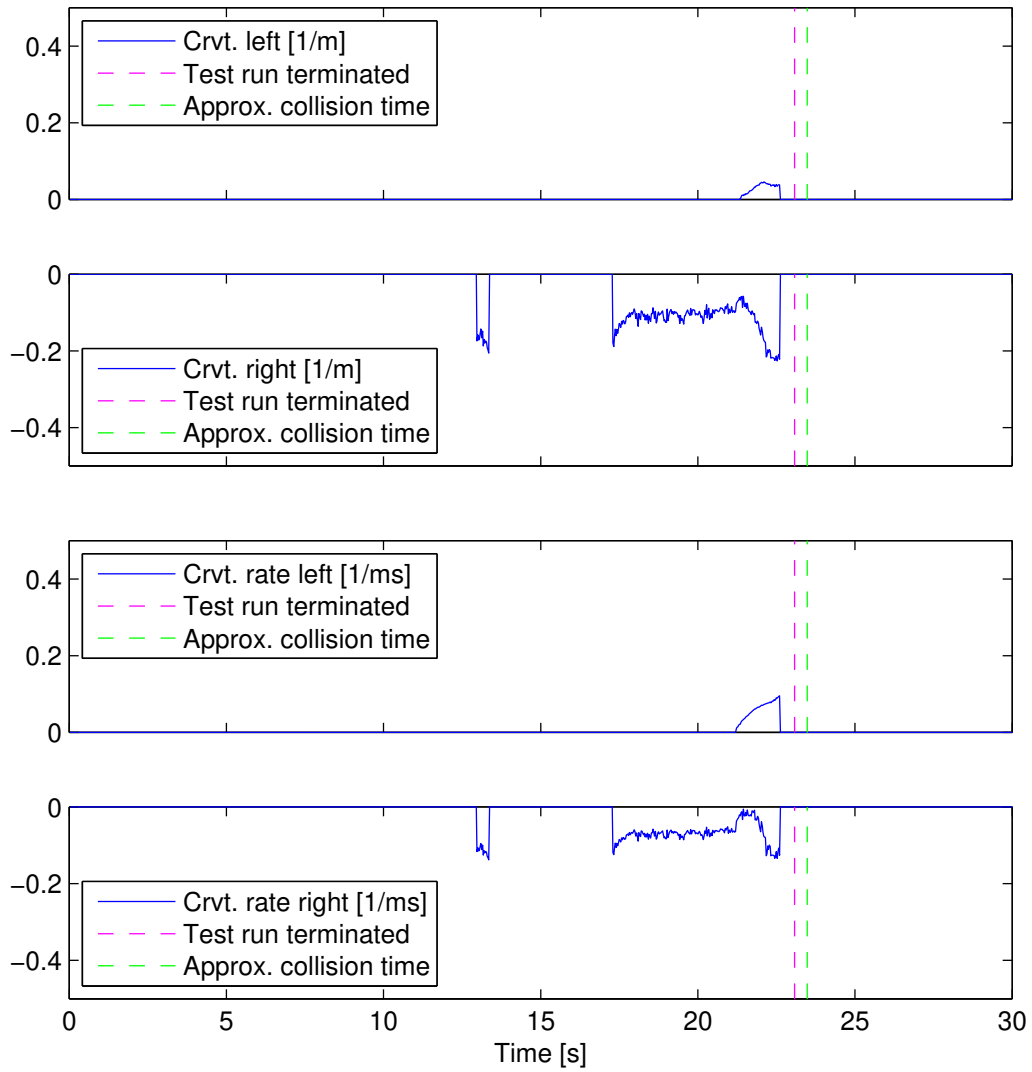


Figure G.6: Curve radius 9 m, host vehicle velocity 17 kph, object velocity 20 kph, lateral distance 3.3 m.

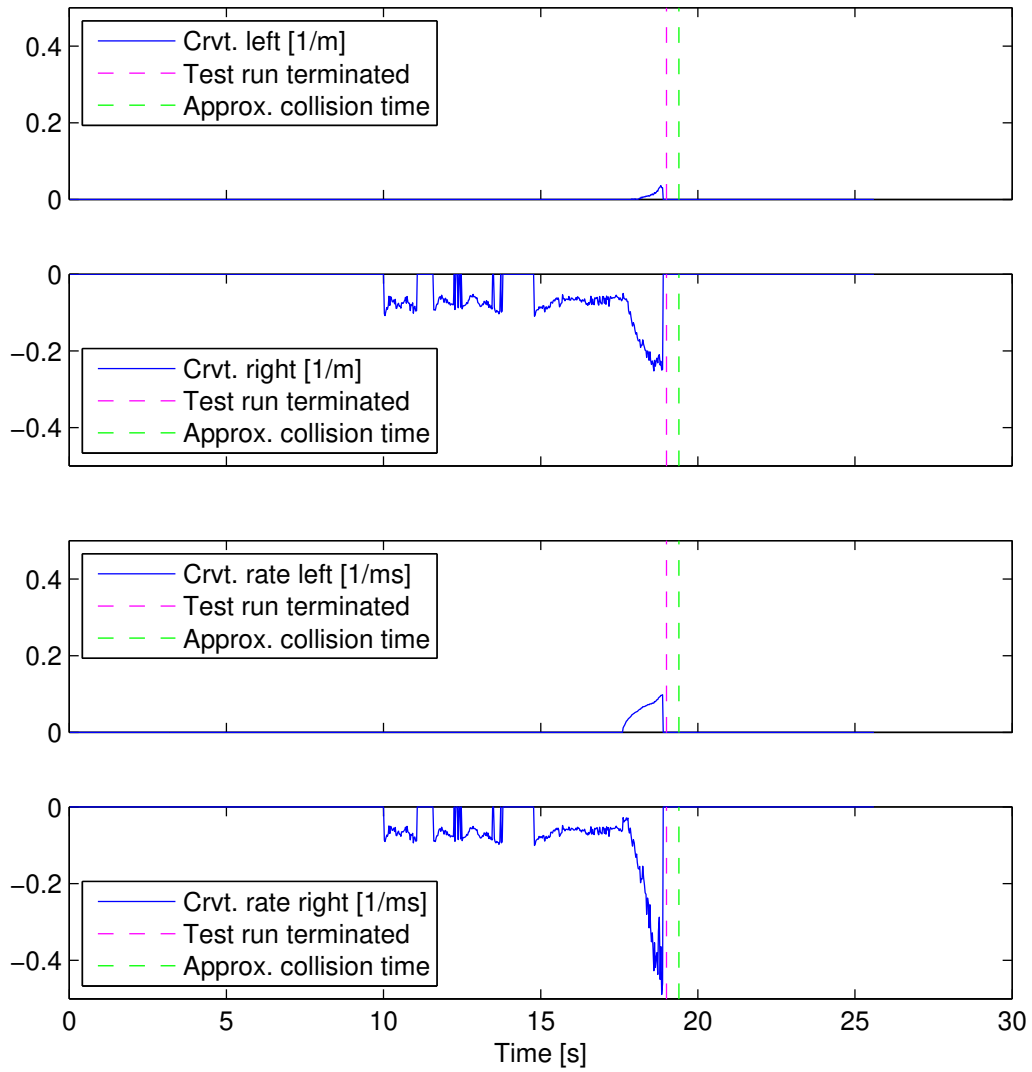


Figure G.7: Curve radius 9 m, host vehicle velocity 20 kph, object velocity 23 kph, lateral distance 3.8 m.

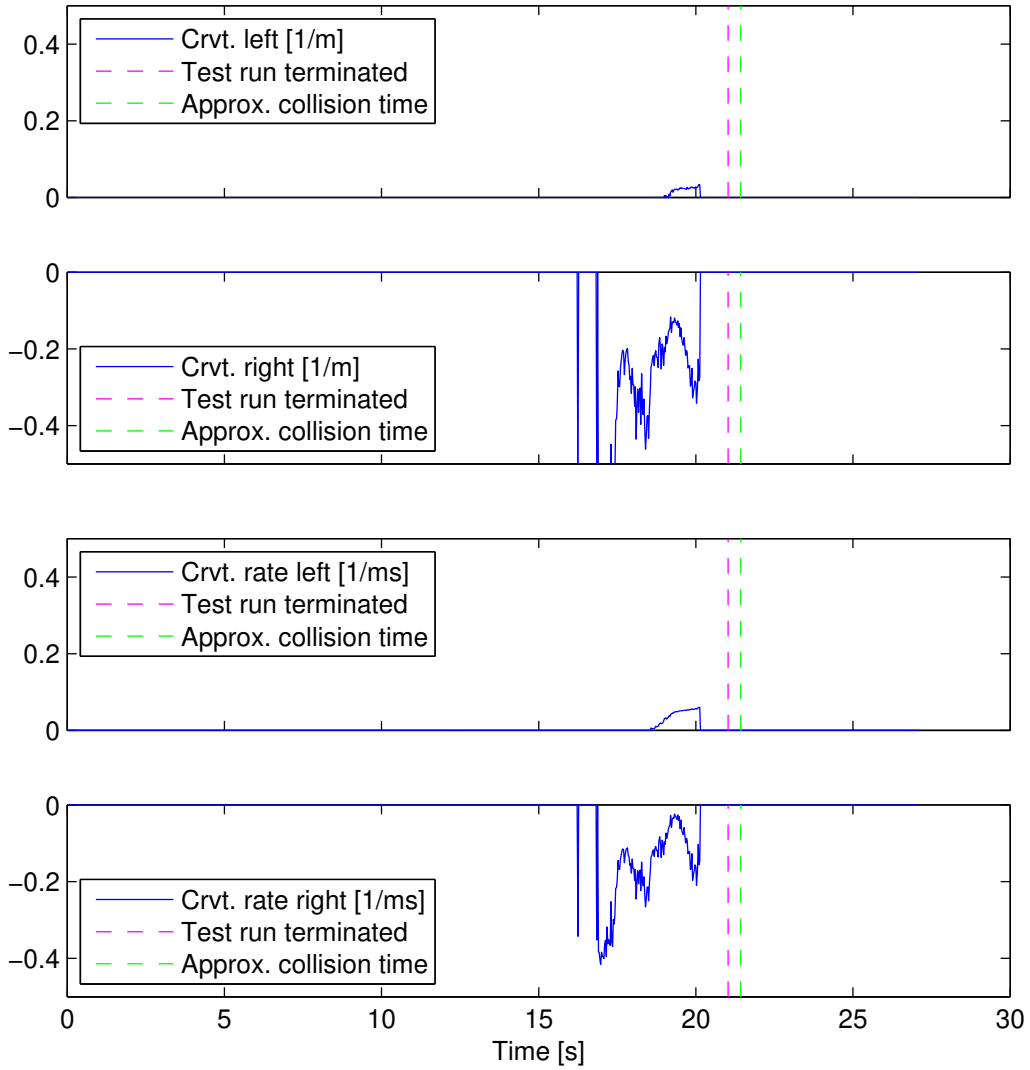


Figure G.8: Curve radius 12 m, host vehicle velocity 13 kph, object velocity 18 kph, lateral distance 3.3 m.

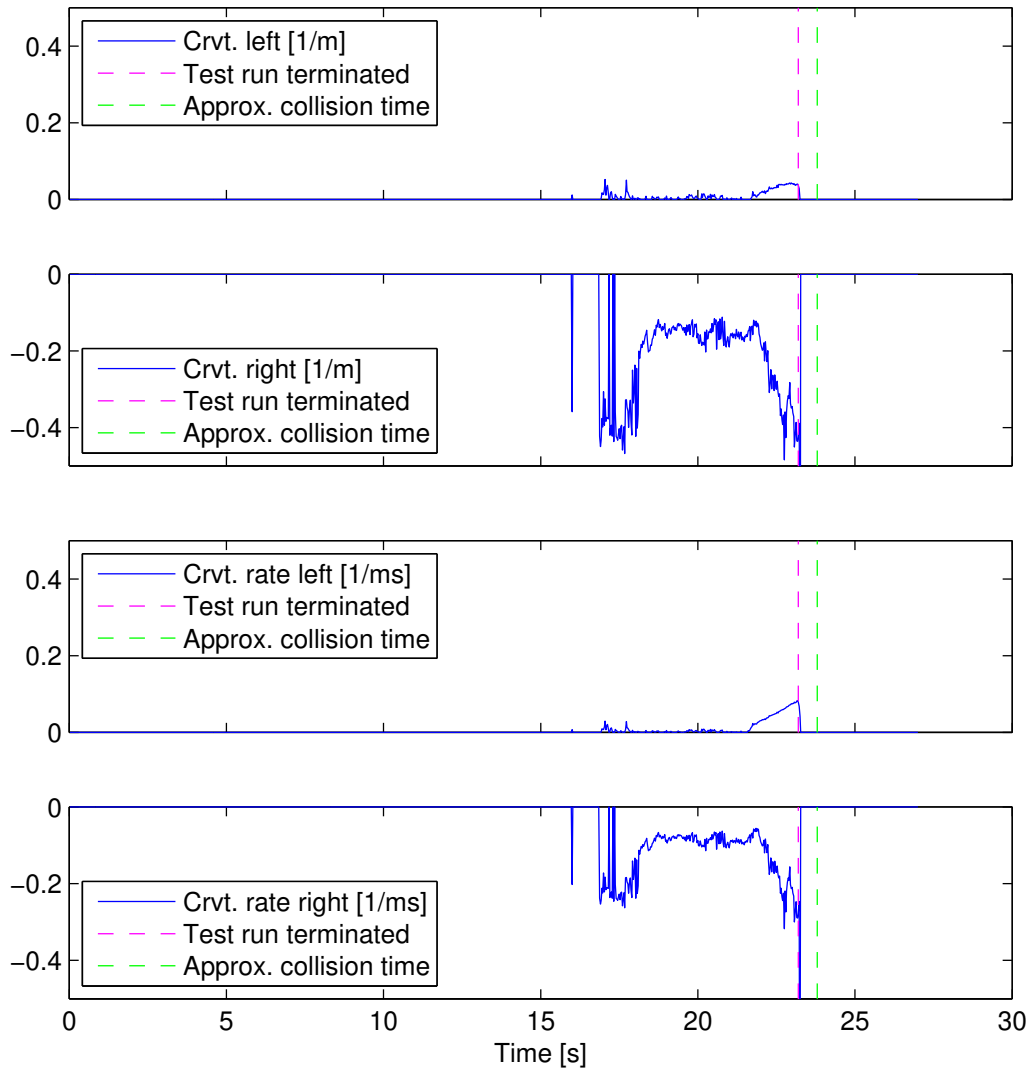


Figure G.9: Curve radius 9 m, host vehicle velocity 13 kph, object velocity 16 kph, lateral distance 2.0 m.

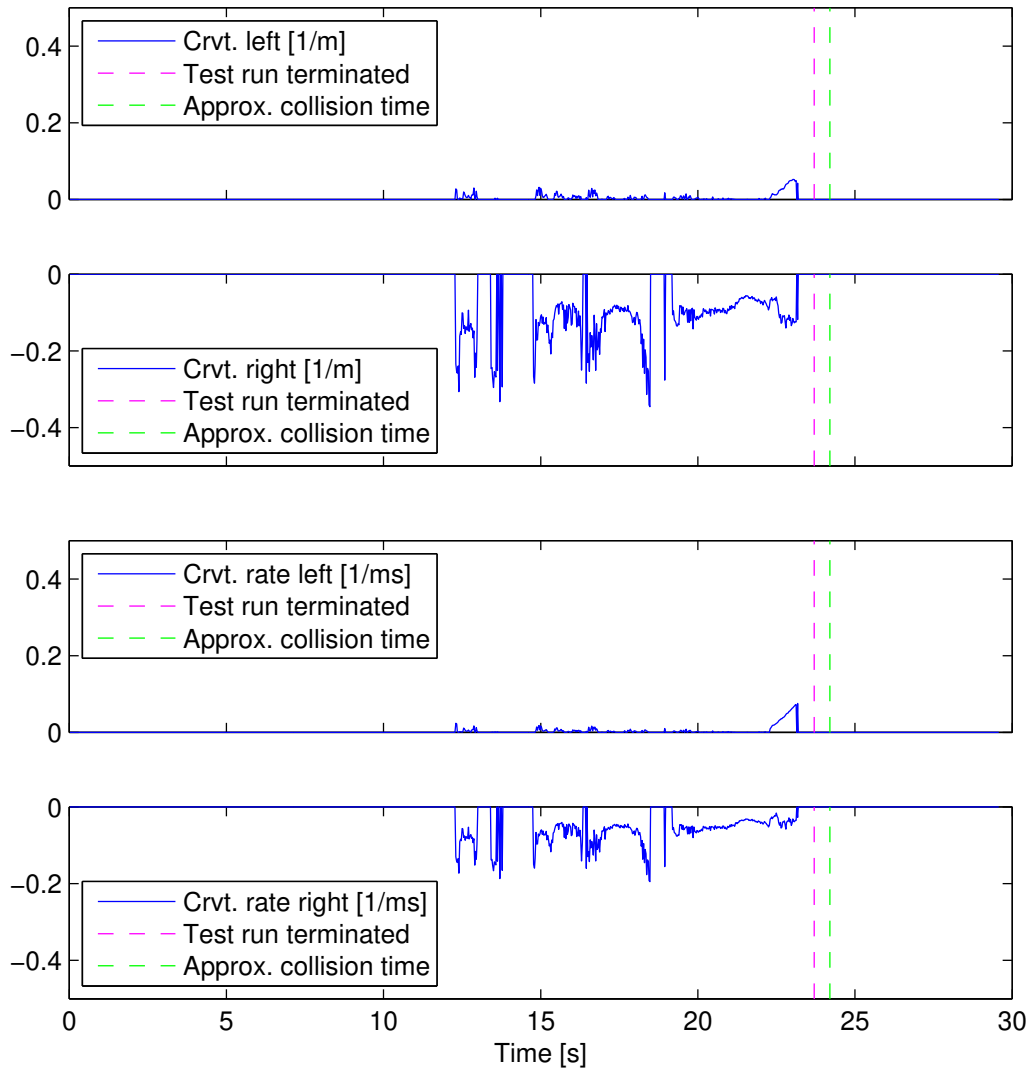


Figure G.10: Curve radius 9 m, host vehicle velocity 15 kph, object velocity 18 kph, lateral distance 2.0 m.